ELECTRON MICROSCOPY OF ORGANIC THIN FILMS

BY

CIARAN EWINS

Thesis submitted for the degree of Doctor of Philosophy

Department of Chemistry, Glasgow University

APRIL 1992

ACKNOWLEDGEMENTS

I would like to thank all those who have assisted me over the course of my research and the production of this thesis.

Special thanks are due to my supervisors Dr John Fryer and Dr David Morris for their guidance, advice and helpful criticism.

The project was a SERC sponsored CASE award in conjunction with ICI plc. I would therefore like to thank those at ICI Wilton who were of great assistance, Dr Tim Ryan, Dr Simon Allen and Dr Andrew Thorne.

Davi Thom is due a great deal of thanks for among other things, continually fixing the electron microscopes after I had broken them.

I would also like to thank Tony Ritchie for mass spectra, George M^{c}Culloch for Infra Red spectra and Kim Wilson for micro analyses.

I would like thank my father Dr Robert Ewins for helpful advice and for drawing the chemical structures.

Finally, and perhaps most importantly, thanks to my mother for babysitting Patrick and also to my wife AnnaMaria for being patient.

TO ANNAMARIA AND PATRICK

TABLE OF CONTENTS

SUMMARY

Thin films of organic materials are increasingly being used for technological applications. In this study two methods of thin film production, Physical Vapour Deposition (PVD) and Solution Casting on a water surface, have been used to prepare thin films of organic materials for investigation by Transmission Electron Microscopy.

The polycyclic aromatic compounds perylene and quaterrylene were evaporated under high vacuum onto the (001) face of a freshly cleaved crystal of KCl. Substrate temperature was shown to play a important role in determining the crystallinity and morphology of the thin film produced. An optimum substrate temperature was found at which deposited crystals were smooth, formed large domains and did not undergo re-evaporation from the substrate.
Lattice images were obtained for the quaterrylene and some image processing was attempted.

The second class of compounds studied were a range of octasubstituted phthalocyanines that were synthesised. These compounds are potential one dimensional conductors since they stack in a "face to face" manner allowing good π-orbital overlap. The compounds prepared were all based on the octa-dodecyloxy-phthalocyanine unit and were the metal free, copper, silicon-dihydroxy and polysiloxane derivatives.

Films of these compounds could be prepared by allowing a chloroform solution of these compound to evaporate on a water surface. Information was obtained by electron diffraction and by lattice imaging. The most common packing arrangement was for a stack of molecules to lie parallel to the water surface. The molecules in the stack could be either tilted or perpendicular to the stack. Only the copper derivative showed any evidence of lying flat on the water surface. The unusual packing of these molecules was explained in terms of the strong hydrophobic interaction between the paraffin side chains and the water surface.

CHAPTER 1: MOLECULAR ELECTRONIC MATERIALS

1.1 Organic Materials and Molecular Electronics

Scientists from many disciplines are now working together in the study of organic materials and their uses in optics and electronics. A broad range of disciplnes are involved, organic chemistry, crystallography, material science and electronic engineering. The compounds involved have potential for such applications as data storage, semiconductors, optical switches and even superconductors. It is believed that these new compounds can be used to produce components that will be smaller and faster than todays silicon based devices (Carter 1982).

Organic compounds exist in many different forms, as gases, liquids, liquid crystals and solids. Each phase possesses different properties, and with polymers materials can be adapted to many different shapes and sizes. Organic molecules are very versatile and it is possible to fine tune their properties by small structural changes. Molecules can even be designed and theoretical models used to predict properties before an attempt to synthesise the compound is made (Pugh 1988). The large number of known organic compounds, about six million, provides a huge selection of possible materials. The human body itself can be studied and used as a model for the design of electrical devices, for example the brain itself could be described as the greatest computer ever built.

Few organic materials have yet been utilised, two notable exceptions being alkylcyanobiphenyls for liquid crystal displays, and triglycine sulphate as a piezo-electric sensor (Fig. 1). However it is likely that as these and other materials become better understood and the ability to incorporate them into devices increases they will find many new uses.

1.2 Electrical Properties of Organic Materials

Organic materials have long been thought of as insulators, but in 1953 a crystal of perylene doped with bromine was shown to have metallic conductivity. In 1973 a charge transfer complex with a conductance comparable to metals was prepared from TTF and TCNQ (Fig. 1). This has led to the synthesis of many conducting charge transfer complexes containing sulphur and selenium as electron donors (Ferraris 1973).

Polymers have also been shown to have conductivities comparable to metals. Doped polyacetylene and doped polythiophene are two examples (Fig. 1).

To date, organic conductors have required dopants to achieve metallic conductivities. Most dopants such as molecular bromine or uranium hexafluoride act as oxidising agents and create charge carriers in the crystal. This has meant that many of these conductors are not stable.

The phenomenon of organic superconductivity was observed in 1980 at 1°K and at 1200 atm pressure with

FIG. 1

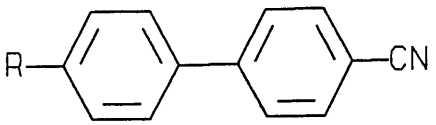

Alkylcyanobiphenyl

(R = alkyl)

$(NH_2CH_2COOH)_3 . H_2SO_4$

Triglycine sulphate

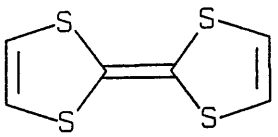

Tetrathiafulvalene
(TTF)

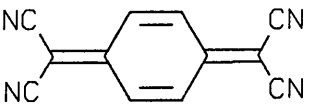

Tetracyanoquino-
dimethane (TCNQ)

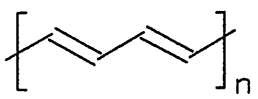

Polyacetylene

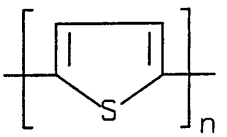

Polythiophene

$(TMTSF)_2PF_6$ (Fig. 2), (Wudl 1984). The highest temperature for the onset of superconductivity yet observed is 10.4°K for the copper thiocyanate salt (BEDT-TTF)-$Cu(SCN)_2$ (Fig. 2), (Urayama 1988).

1.3 Optical Properties of Organic Materials

Optical properties such as the rotation of plane polarised light and birefringence have long been known for organic compounds. Recently however nonlinear optical (NLO) properties have been observed (Chemla 1988). These properties are caused by the oscillating electric field of incident radiation interacting with a polarisable molecule and setting up an oscillating electric dipole. The induced dipole per unit volume is called the polarisation, P, and is linearly proportional to the applied field E. The susceptability / is a sum of the hyperpolarisabilities of the individual molecules in the crystal.

$$P = \epsilon_o \chi_1 E$$

ϵ_o is a universal constant.

χ_1 is the linear electric susceptibility.

This induced dipole combines with the original radiation to produce a new wave. To identify the NLO properties of the wave we must consider small corrections to the above equation. These corrections are contributions to P which depend on higher powers of E.

$$P = \epsilon_o(\chi_1 E + \chi_2 E^2 + \chi_3 E^3 + \ldots)$$

The odd terms (χ_1 etc) in this expression contribute to the polarisation of all materials, but the even coeffi-

cients only amount to a non zero sum if the material lacks a centre of symmetry.

Second order effects are controlled by χ_2. Two of the most common manifestations of second order nonlinearity are the electro-optic effect, where an electric field can be used to alter the refractive index of a solid, and frequency doubling where the new wave has double the frequency of the incident wave. These can be used to make optical switches, to amplify signals or to modulate a wave carrying information.

Nitroaniline (Fig. 2) is an example of a compound with excellent NLO properties. However it crystallises in a centrosymmetric space group. This would result in the resultant oscillating dipole of all the molecules in the crystal summing to zero. However 2-methyl-4-nitroaniline (Fig. 2) was then produced and could be crystallised in a non-centrosymmetric space group. This is a good example of the tailoring of properties that is possible with organic compounds and is a major advantage over inorganic optical crystals.

1.4 Polycyclic Aromatic Compounds

Polycyclic aromatics have been studied extensively, because of their electronic properties. They possess large delocalised clouds of electrons which can conduct electricity, and in that respect they have been compared to small fragments of graphite (Bredas 1985). They are also a very common atmospheric pollutant since they are

FIG. 2

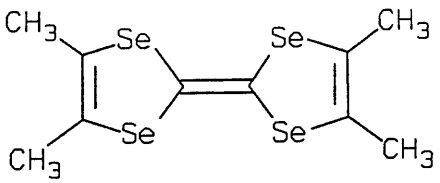

Tetramethyltetraselena-fulvalene (TMTSF)

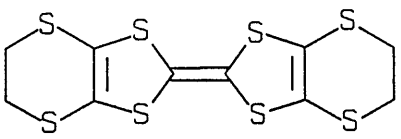

Bis(ethylenedithiolo)tetra-thiafulvalene (BEDT TTF)

Nitroaniline

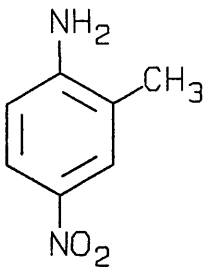

2-Methyl-4-nitroaniline

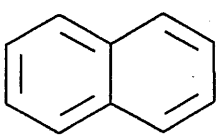

Naphthalene

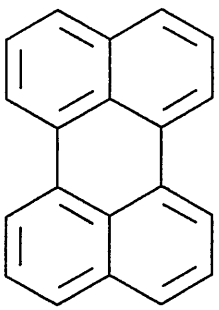

Perylene

formed during the combustion of hydrocarbons and coals. Many polycyclic aromatic compounds are carcinogens (Jones 1979). This is because they are able to intercalate with the helices of DNA and have been reported to cause genetic mutations.

1.5 The Perinaphthalenes

The perinaphthalenes are a series of polycyclic aromatic compounds consisting of naphthalene units linked together by peri bonds. Perylene consists of two naphthalenes and is followed in the series by terrylene and quaterrylene (Fig. 3), (Shrivastava 1960). No higher analogues have been isolated. The largest member of the perinaphthalenes is polyperinaphthalene (Fig. 3) which has been made in small quantities. It has been postulated that polyperinaphthalene would be an intrinsic conductor and may conduct in a fashion similar to graphite without the need for doping. However investigations of polyperinaphthalene's conducting properties are inconclusive because of difficulties obtaining a pure sample. Polyperinaphthalene is made by pyrolysis of 3,4,9,10-perylene-tetracarboxylic dianhydride (Fig. 3), (Murakami 1984). Theoretical studies (Bredas 1985) suggest that polyperinaphthalene would not be an intrinsic conductor though it may have a band gap as low as 0.29 eV depending on the crystal structure.

Perylene is collected by the extraction of the heavier fractions of crude oil. It has been much studied because

FIG. 3

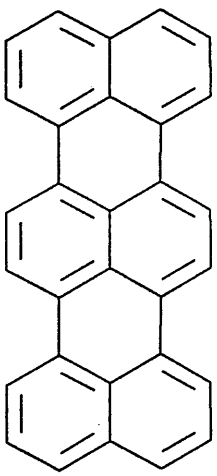

Terrylene

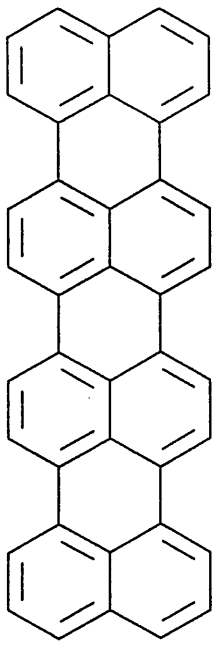

Quaterrylene

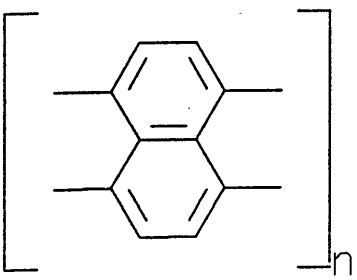

Polyperinaphthalene

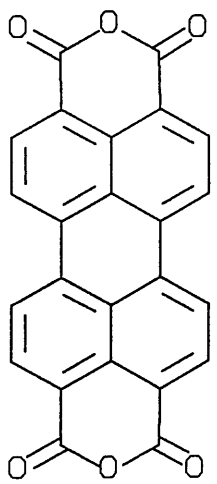

3,4,9,10-Perylenetetra-carboxylic dianhydride

of its conductive properties. Metallic conductance was first observed in an organic system in a perylene bromine complex. Room temperature conductivities for polycrystalline samples of pure perylene are of the order of 10^{-1} Scm^{-1} and about two orders of magnitude higher for single crystals. Raman and Mossbauer measurements indicate that the perylene-iodine complex, which is a conductor, is not a molecular complex but rather a partially oxidised mixed valence compound (Teitelbaum et al 1979).

The bonding in perylene and other perinaphthalenes is of interest because of the nature of the peri-bonds which link the naphthalene units. The conventional value for a the length of a single C-C bond which is sp^3 hybridised is 0.154 nm. When sp^2 hybridisation occurs the bond length shortens to 0.148 nm and delocalisation shortens it even further. Any conjugation would shorten the peri C-C bonds. However their length in perylene and the other perinaphthalenes of 0.152 nm suggests almost no double bond character, and the benzenoid character in such molecules is therefore localised (Shrivastava 1960).

There exist two different packing modes for perylene (figure 4), one in which the molecules are arranged in dimer pairs, α-perylene, and one where the common herringbone structure is found, β-perylene. Both are monoclinic and have the space group $P2_1/a$ (Fig. 4), (Tanaka 1963). Terrylene and quaterrylene have been found to isostructural to the dimeric form of perylene. The intermolecular spacings in these dimeric structures are

FIG. 4

Crystal Structures of Perylene

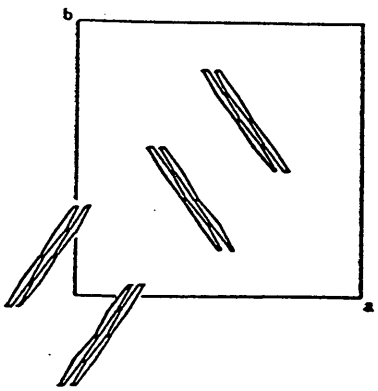

α-perylene

a = 1.135 nm
b = 1.087 nm
c = 1.031 nm
ß = 100.8°
$P2_1/a$

4 molecules per unit cell

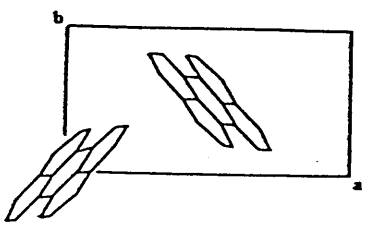

ß-perylene

a = 1.127 nm
b = 0.588 nm
c = 0.965 nm
ß = 92.1°
$P2_1/a$

2 moloecules per unit cell

important for the overlap of π orbitals, in perylene the spacing is 0.346 nm, in quaterrylene it is 0.341 nm, while in graphite it is 0.335 nm.

Terrylene can be made by condensing 1-bromo-naphthalene with perylene. Quaterrylene can be made by condensing perylene in a AlCl/NaCl melt (Clar et al 1956). Since quaterrylene is insoluble in all solvents it must be purified by fractional sublimation. The crystals used in the X ray structure analysis were grown from the vapour phase.

Quaterrylene shows large increases in conductivity upon exposure to strong Lewis acids such as AsF_5 (Naarmann et al 1982). Quaterrylene with an ionisation potential of 6.11 eV is expected to form a broader range of charge transfer complexes than perylene (I.P. = 6.97 eV).

1.6 Phthalocyanines

Phthalocyanines are an extremely important class of compounds with over 4000 papers published about them. They were discovered in the 1930's and quickly found use as pigments. They are now also used in lasers, as lubricants, in medicine and as semiconductors and conductors (Moser and Thomas 1983a).

The X ray crystal structure analysis of copper phthalocyanine (Fig. 5) was carried out by J.M. Robertson at Glasgow University in 1935 (Robertson 1935). It was the first full structure determination of a large organic molecule. Many different phases can exist in phthalocyanine crystals (Fig. 5). Two of the most common arrange-

FIG. 5

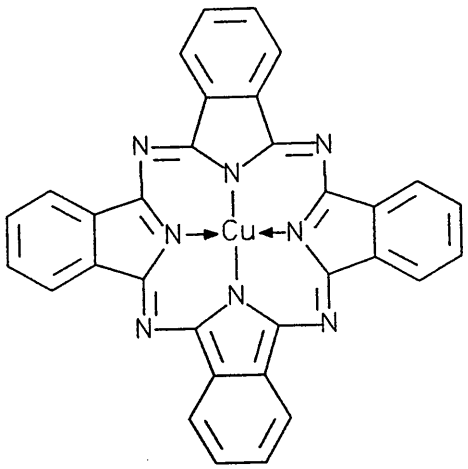

Copper Phthalocyanine

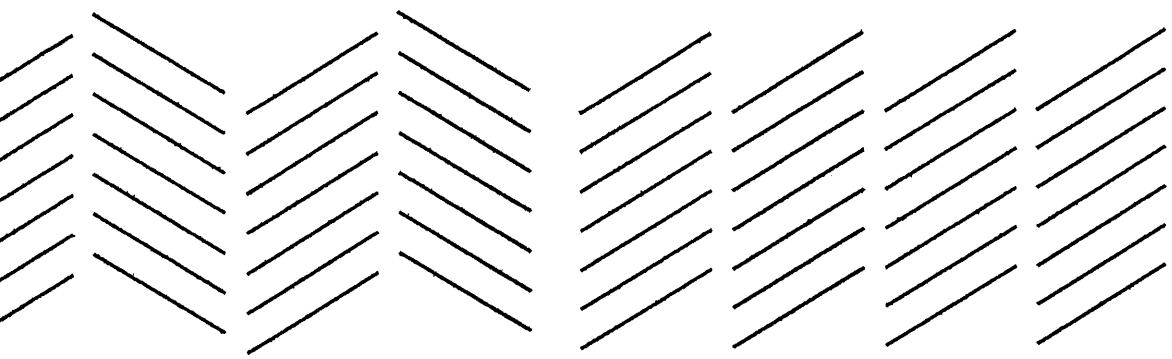

Packing in Phthalocyanines

FIG. 6

Main methods of synthesis of metal phthalocyanines

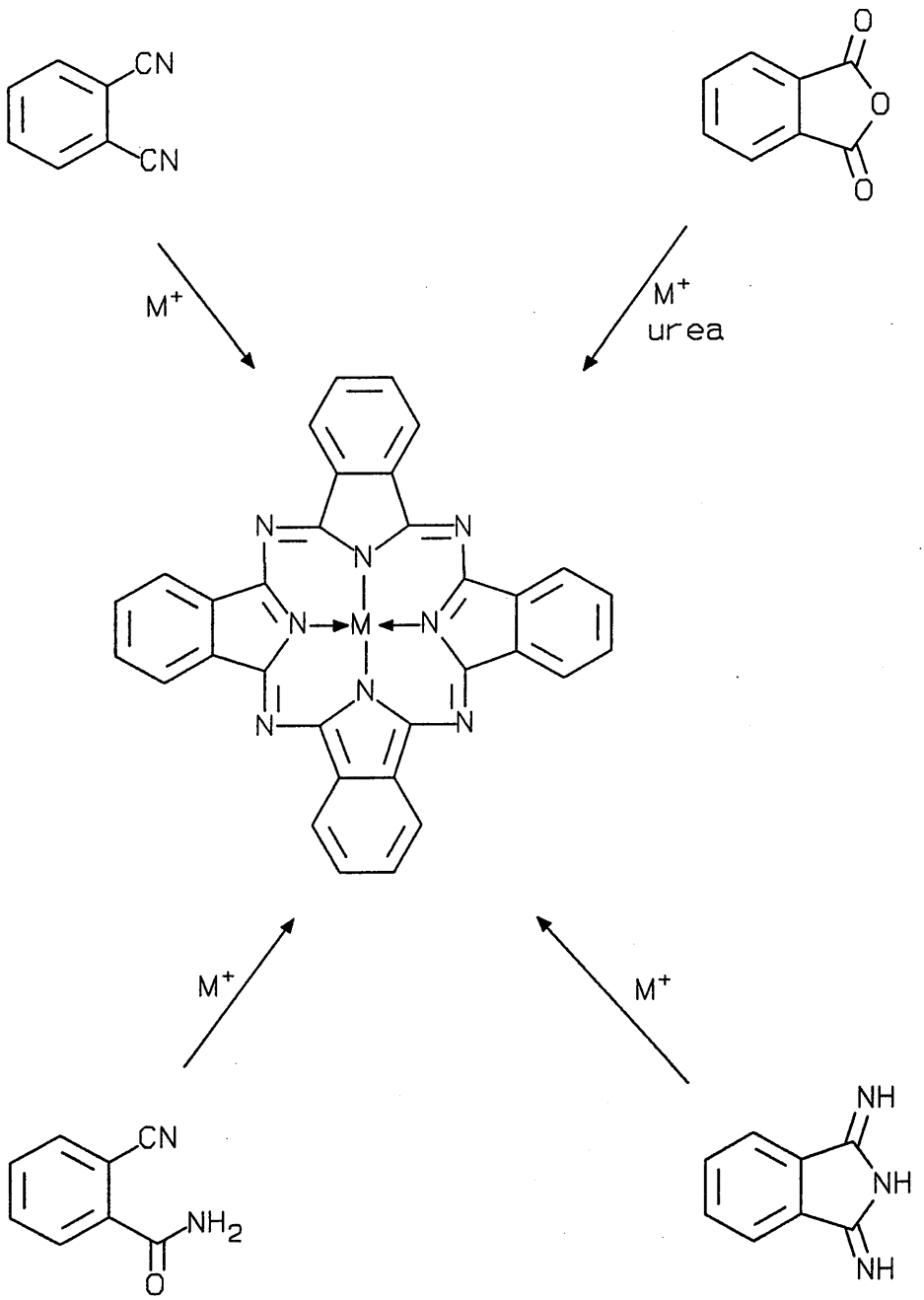

ments are a "herringbone" structure where there is an alternate stacking sequence and "tile" where the sequence is parallel. The energy differences between phases is small and phase transitions can be brought about by heating or by solvents.

The main methods used to synthesise phthalocyanines are summarised in figure 6 (Moser and Thomas 1983b).

The conducting properties of phthalocyanines have been widely studied and in an undoped state they are generally semiconductors. They can be co-crystallised with molecular iodine to yield a mixed valence low dimensional conductor (Schramm et al 1980). Molecular iodine acts as an oxidising agent and creates charge carriers. The conduction is generally explained in terms of conduction down the stack of molecules. Replacing a central metal atom with two hydrogens does not greatly affect the conductivity. Conduction between parallel molecules will be improved by increasing the overlap between the π-electron systems on adjacent molecules, therefore the closer the molecules the greater the conductance. This led Kenney to synthesise a stacked system (Fig. 7). In this cofacial assembly the phthalocyanine units are held close together (Kenney and Joyner 1960). When doped this system is a metallic conductor. Another approach to improve the π-electron was the preparation of phthalocyanine based liquid crystals such as the octadodecyloxy methyl phthalocyanine (Fig. 7).

FIG. 7

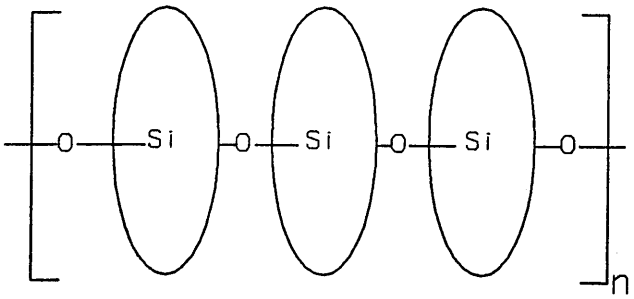

 = phthalocyanine

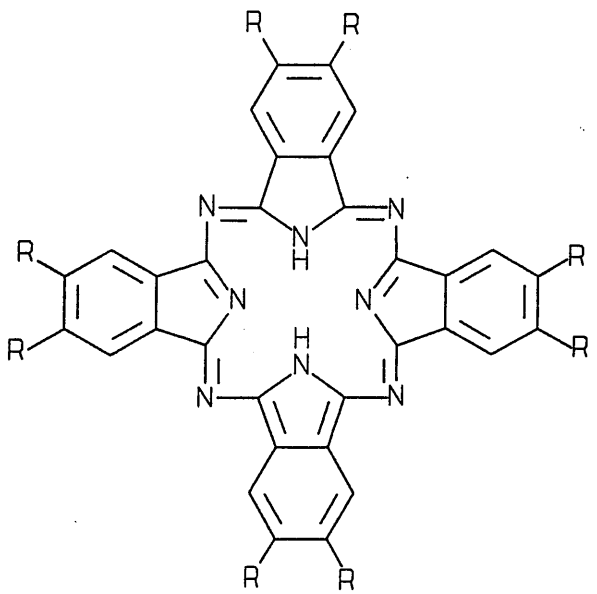

R = $CH_2OC_{12}H_{25}$

Octakis(dodecyloxymethyl)phthalocyanine

1.7 Liquid Crystals

It has been estimated that approximately five percent of all organic compounds are liquid crystals (Streinrasser and Pohl 1973). The liquid crystalline state lies between the solid and liquid phases and is often called the fourth state of matter. In a liquid crystal the molecules are in a semi ordered state with long range orientational order. They are however viscous liquids with the molecules undergoing a good deal of motion while maintaining the overall ordering.

The liquid crystalline phase was discovered in 1888 by Reinitzer, an Austrian botanist (Reinitzer 1888). He noticed that cholesterol benzoate (Fig. 8) appeared to have two melting points, the solid undergoing a transition to a cloudy liquid, which on further heating became a clear liquid. Reinitzer showed his discovery to Lehnmann, a German physicist, who then set about investigating this phenomenon. He found that above the first melting point the cholesterol benzoate had the physical properties of a liquid and the optical properties of a solid, in particular it was birefringent. Lehnmann proposed the term "liquid crystal". The term "mesophase" is now often used and means the same as "liquid crystal".

In 1922 Friedel recognised the existence of different molecular orderings within mesophases and he proposed the terms "nematic" and "smectic" mesophases. Friedel also recognised that liquid crystallinity was important for the organisation of biological compounds in living

systems (Friedel 1922).

For the next forty years very little research was carried out into liquid crystals and they were regarded as a curiosity of little practical use. That changed dramatically in the 1960's when George Gray at Hull University prepared a new stable liquid crystal for use in visual displays (Howells 1984). His alkylcyanobiphenyls could be switched between visible and invisible states by the application of a tiny electrical potential.

Liquid crystals can be divided into two classes, Thermotropic and Lyotropic. Thermotropic liquid crystals are produced by the application of heat, as in cholesterol benzoate. Lyotropic mesophases occur when more than one type of molecule is present. A common example is in a soap solution where the soap molecules will arrange themselves into micelles. Lyotropic mesophases are of vital importance in the organisation of molecules in the body (Brown and Wolken 1979). For example the phospholipid membranes that surround living cells are liquid crystalline.

1.8 Thermotropic Liquid Crystals

Thermotropic liquid crystals can be divided into three categories depending on the arrangement of the molecules. They are called nematic, smectic and cholesteric.

Nematic mesophases (Fig. 8) can be formed by non chiral molecules. Their shape is most commonly elongated or rod like. The long axes of these rods are arranged in an

FIG. 8

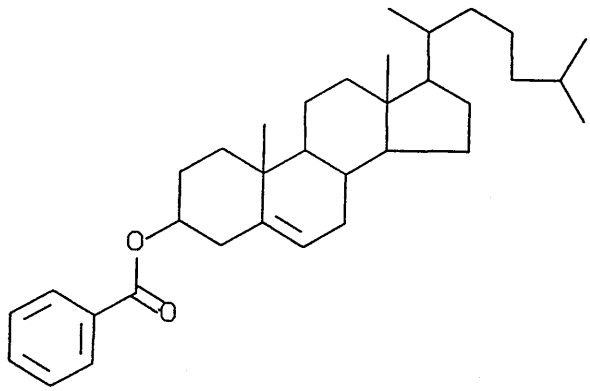

Cholesteryl benzoate

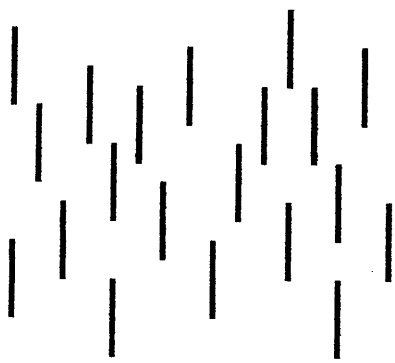

Nematic

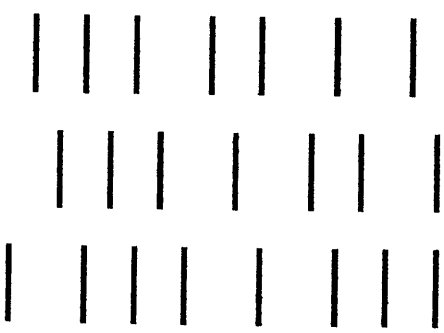

Smectic A

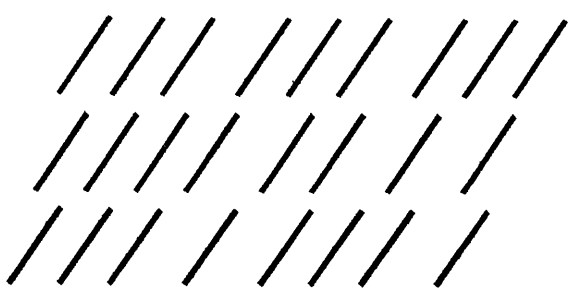

Smectic C

essentially parallel fashion, giving an orientational order. However the molecules are free to move around and therefore have no positional order.

Smectic liquid crystals have a two dimensional structure with the molecules packed in layers. Within the layers the molecules have an orientational order. There are many different types of smectic mesophase (Fig. 8). In smectic A the molecules are packed in equidistant layers. This is also the case in smectic C except that now the molecules are all tilted with respect to the plane of the layer.

Cholesteric mesophases are formed by chiral molecules. The chirality induces the long axes of the molecules to pack with a twist. This gives a helical structure to the mesophase. The distance for a 360 degree turn is called the pitch. The cholesteric mesophase is usually regarded as a modification of the nematic phase, but smectic cholesteric mesophases have been observed. Cholesteric mesophases can also be created by the addition of a chiral molecule to a non chiral mesophase (Solladie and Zimmerman 1984).

All these geometries and arrangements are sensitive to temperature changes and one compound may exhibit different mesophases at different temperatures.

The shape of a mesogen plays an important role in how molecules pack and the mesophase subsequently formed (Fig. 9). Rods and discs are two examples.

The alkylcyanobiphenyl made by Gray is a typical example

of a rod shaped mesogen. This shape encourages the molecules to pack with their long axes parallel. The large conjugated aromatic system make the molecule polarisable and again aides anisotropic packing (Luckhurst and Gray 1979).

1.9 Discotic Liquid Crystals

In 1977 a new type of mesophase was discovered by Chandrasekhar at the Raman Research Institute in Bangalore. He observed a discotic mesophase, that is, a mesophase made up of flat disc-like molecules. The hexaalkanoyloxy benzenes (the mesogens) he was looking at stacked on top of each other, rather like stacks of coins (Chandrasekhar et al 1977).

Many types of discotic mesophases exist, most have a columnar structure with the stacks organised in a two dimensional array. The most common arrangement is a hexagonal array (Emsley 1990).

Discotic mesogens usually consist of a central aromatic core surrounded by several aliphatic chains. Common core molecules include benzene, triphenylene and truxene (Fig 9). A discotic mesophase has even been observed in a substituted cyclohexane system (Sluyters et al 1989).

The columnar packing in these molecules may find applications as one dimensional conductors. Each stack of molecules is insulated from the others by the aliphatic chains, allowing the column to act like a molecular wire. The stacking of the flat molecules parallel to each

FIG. 9

Rod

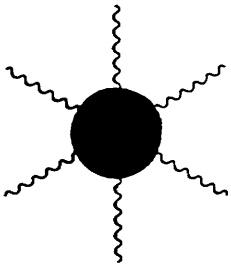

Disc

SHAPES OF MESOGENS

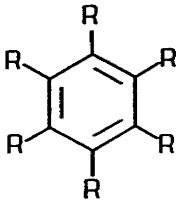

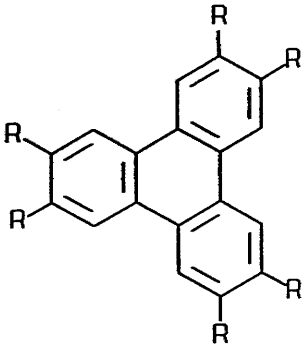

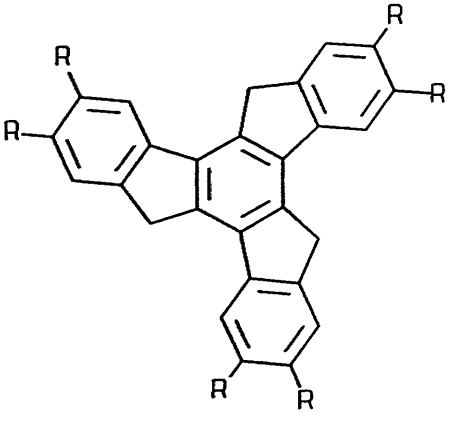

R = $-OCOC_nH_{2n+1}$

Benzene type

Triphenylene type

Truxene type

other gives good overlap of aromatic π-electrons. It is even possible that dopants could be added between the stacks without affecting the structure of the conducting cores.

1.10 Phthalocyanine Discotic Liquid Crystals

Columnar discotic mesophases were first observed in phthalocyanines by Jacques Simon in Strasbourg (Piechocki et al 1982). He observed them in the copper and metal-free derivatives of octadodecyloxymethyl phthalocyanines (Fig. 7).

Transitions were observed to a discotic mesophase at 53 and 79°C respectively. The transition temperatures were found using a polarising microscope fitted with a hot stage in the mesophase "fan like" textures were observed. X ray powder diffraction at elevated temperatures gave information about molecular packing (Fig. 10).

The distance between stacks was found to be 3.1nm and a spacing of 0.35nm was attributed to the space between the phthalocyanine rings. It is important to note that this is very close to the Van der Waal radius and is much closer than the 0.485nm observed in the beta form of copper phthalocyanine. The paraffinic side chains could be observed as a diffuse ring at 0.47nm. The apparent misfit between the aromatic core and paraffins is overcome by the formation of a periodic sequence of "pinched" regions along the stack. This was observed by X ray as being 2nm long (de Gennes 1984). The "pinched" regions are periodic defects to accomadate this defect.

Phthalocyanine has been shown to complex to over sixty different metals, and many of these have now been incorporated into discotic phthalocyanines. This can be achieved by either reacting the metal free phthalocyanine with a strong base to remove the protons and then adding appropriate metal salt, or by the tetramerization of an ortho-dinitrile around a metal ion.

Non-metals such as silicon and germanium have also been incorporated into discotic phthalocyanines. Dihydroxy silicon phthalocyanines exhibit mesophases and then when heated form siloxane oligomers which also exhibits a mesophase (Simon et al 1988). The oligomers can be seperated by size using gel permeation chromatography. It was found that only 20% of of the oligomers contained more than three phthalocyanine units.

The peripheral substituents around the phthalocyanine core have been varied extensively (Pawlowski and Hanack 1980). The most common substituent is the aliphatic chain. In the dihydroxy silicon phthalocyanine case, alkyl chains of length n=4 to n=18 all gave mesophases. In general the longer the chain the lower the transition temperature to the mesophase (Sauer and Wegner 1988). A chiral sidechain has been used to give a cholesteric mesophase (Cho and Lim 1988).

Not all octasubstituted phthalocyanines are symmetrical. Mesophases are still observed when two of the alkyl chains are replaced by nitriles. This introduces a new way of ordering these molecules (McArdle 1989). Octasub-

FIG. 10

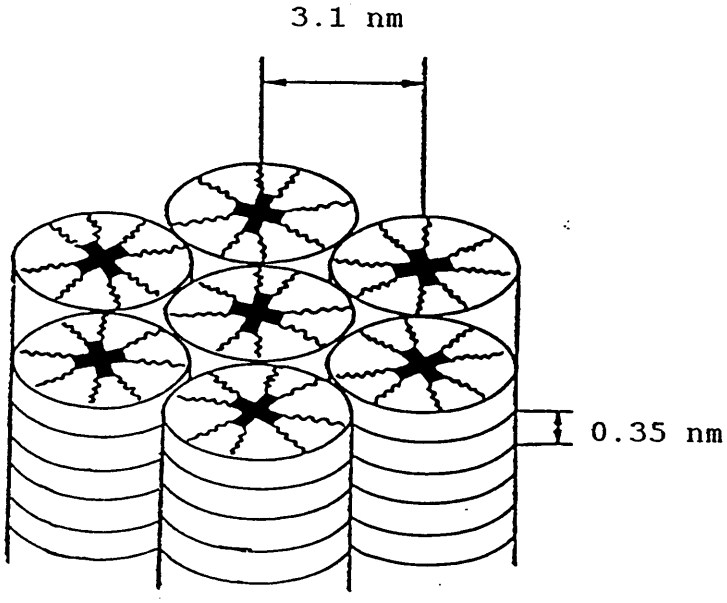

DISCOTIC MESOPHASE

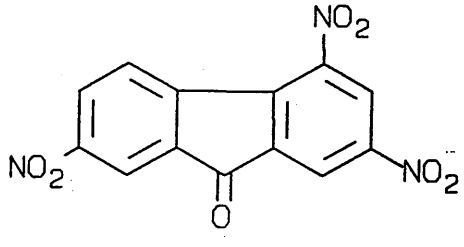

2,4,7-Trinitrofluorenone

stituted phthalocyanines, where the end carbons of two of the adjacent chains are carboxylic acid, groups have been used to form Langmuir Blodgett films (Cook et al 1987).

1.11 Polymeric Liquid Crystals

Polymeric liquid crystals have improved the prospects of making use of liquid crystals enormously. Polymers possess many properties which enhance the uses of liquid crystals. These include stability, morphological adaptability and strength (Ballauf 1987).

Polymeric liquid crystals form much like any other mesophase, but because of the long chain structure the orientation of the mesophase can be frozen in by rapid cooling. This means that properties associated with the mesophase can exist at lower temperatures, for example electro-optic properties. It also can give the polymer many unusual properties. In the aromatic polyamide Kevlar, extraordinary tensile strength is achieved by combining the highly organised structure of a liquid crystal with a polymeric structure.

There are basically two types of liquid crystal polymer. The mesogen can be part of the main polymer chain, or it can hang from the main chain as a "pendant group". Main chain polymers gives very large intramolecular forces and solvents have to be used to make the polymer processable. Those with the mesogen as a side group are more like normal polymers in their processability. Like

ordinary liquid crystals the side chain liquid crystal polymers can be aligned (poled) in an electric field, however a polymer can be cooled and the orientation will remain once the field is switched off. This has been used as a method to record and store information (Ringsdorff et al 1989).

Disc shaped groups have been incorporated into polymer chains as both main chain and side chain groups (Voigt-Martin 1989) and discotic phases have been observed. Much work has been done with the triphenylene group. This forms a discotic mesophase when hung pendant like from a polyacrylate polymer and also when incorporated into a polyester. Mesophases can be induced at lower temperatures by the addition of a flat, low molecular weight, electron acceptor. For example trinitrofluorenone (Fig. 10) forms a charge transfer complex with triphenylene polymers and as a result helps the system to align (Voigt-Martin 1989).

Phthalocyanine polymers can be made by peripheral substitution or as a chain through the complexed atom in the middle. Siloxane polymers have been shown to form discotic mesophases. Recent efforts to incorporate an octa substituted phthalocyanine as a pendant group have not yielded any mesophases (Van der Pohl 1990). No main chain phthalocyanine liquid crystal has been made either.

1.12 Techniques for the Study of Liquid Crystals

Many methods are used to study liquid crystals since they exhibit such a wide range of properties (Gray and

Windsor 1974).

The earliest studies were made using the polarised light microscope. A mesophase can be recognised by the formation of a birefringent texture. These textures are very sensitive to changes in the structure of the mesophase and can be used to identify which mesophase is present. Smectic mesophases show what is called a "fan shaped" texture, nematics a "thread like" and discotics a "focal conic" textures. The electron microscope has also been used, this is discussed later.

X ray diffraction studies were first made in the twenties, and were able to give greater information about the molecular arrangements in mesophases. For example, it was shown that the cholesteric mesophase was a variation of the nematic.

Recent advances in nuclear magnetic resonance (nmr) especially Fourier transform nmr and solid state nmr, have made this a powerful method. Magnetic resonance is used to determine the nature and strength of intramolecular forces and determine macroscopic alignments (Emsley 1990).

Thermodynamic data most commonly gathered using differential thermal analysis (DTA) and differential scanning calorimetry (DSC). These techniques give the temperatures of phase transitions and by the analysis of the amount of heat absorbed other thermodynamic data can be gathered.

CHAPTER 2: TRANSMISSION ELECTRON MICROSCOPY

2.1 Development

The transmission electron microscope is analogous to the light microscope in that it consists of a radiation source, a specimen through which the beam passes and a lens system to produce an image. The resolution of the optical microscope is limited by the wavelength of the light used:-

$$d_{min} = \lambda / 2\sin\alpha \qquad \text{(i)}$$

d_{min} is the smallest resolvable object.

λ is the wavelength of the radiation used.

α is the semi angle subtended by the object plane.

Using visible light (wavelength ≈500nm) the smallest resolvable object is about 200nm in size. Using a transmission electron microscope with a 100kV accelerating voltage, the electrons produces will have a wavelength of 0.0037 nm. Therefore a resolution of less than the length of a carbon carbon bond would be theoretically possible if wavelength was the only limitation.

The developments that led to the conception of the transmission electron microscope came in the early twentieth century. In 1924 de Broglie formulated the relationship between particle momentum and wavelength and two years later Schrodinger described the wave

properties of matter. In 1927 Davisson and Germer showed that electrons were diffracted by single crystals of nickel, and in the same year Busch demonstrated the electrons could be focussed with a magnetic lens.

With this groundwork laid, Max Knoll and Ernst Ruska were able to build the first transmission electron microscope in 1932. They were soon able to obtain a resolution of 5 nm a great improvement on the light microscope. Since then steady improvements in technology have lead to current commercial microscopes which have a resolution of greater than 0.2 nm.

The transmission electron microscope has found uses in most areas of modern science for example with biological specimens, electronic materials, plastics and catalysts, all of which are routinely examined (Fryer 1979b).

2.2 The Lens System and the Electron Gun

The transmission electron microscope consists of five main sections (Fig. 11):-

1. The electron gun
2. A condenser system
3. The specimen chamber
4. The magnification system
5. An image recording device

The electron gun is most commonly a tungsten hairpin filament. When heated electrically this will emit elec-

FIG. 11

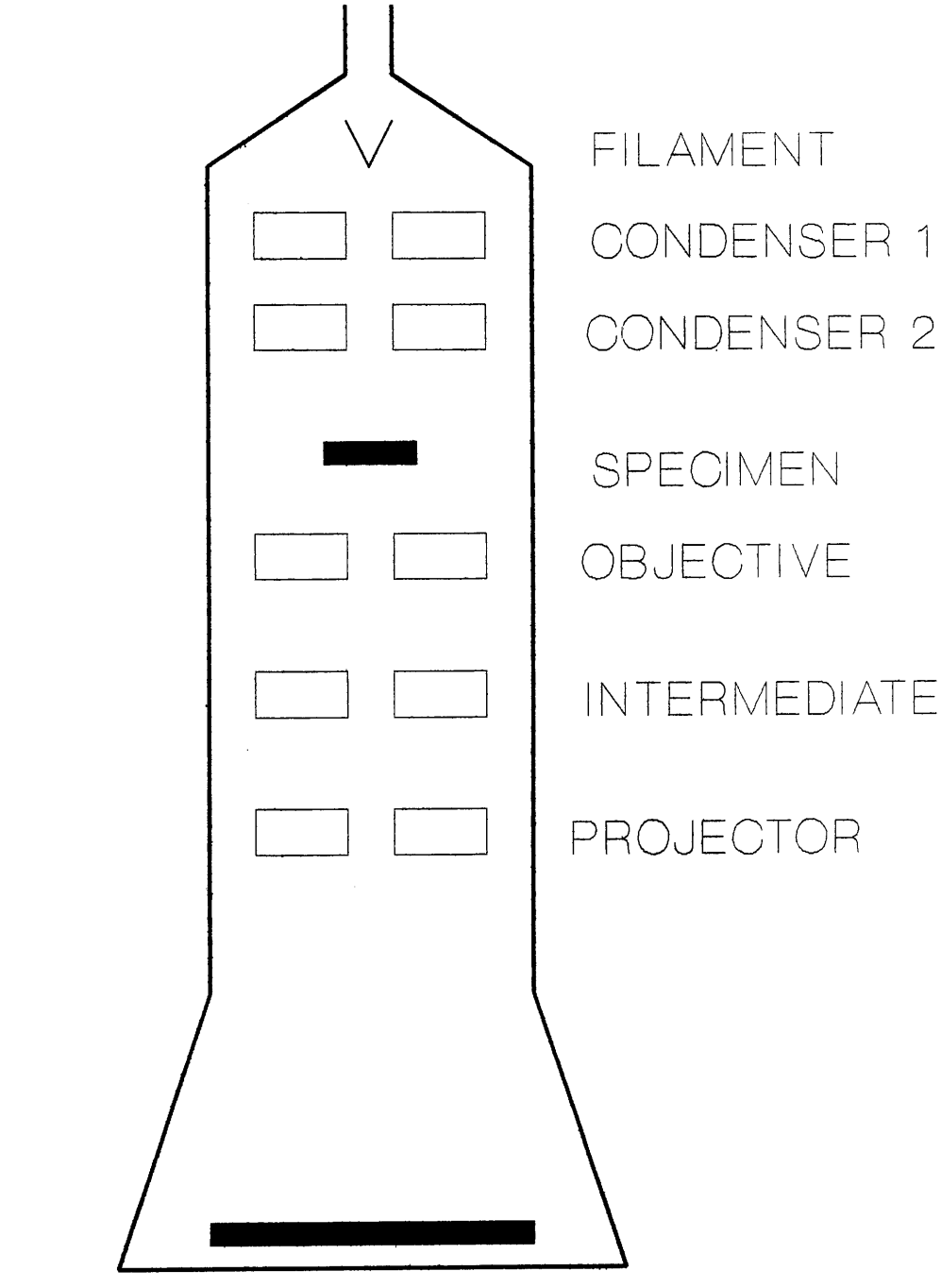
FILAMENT
CONDENSER 1
CONDENSER 2
SPECIMEN
OBJECTIVE
INTERMEDIATE
PROJECTOR
VIEWING SCREEN AND CAMERA

FIG. 12
Electron Optics

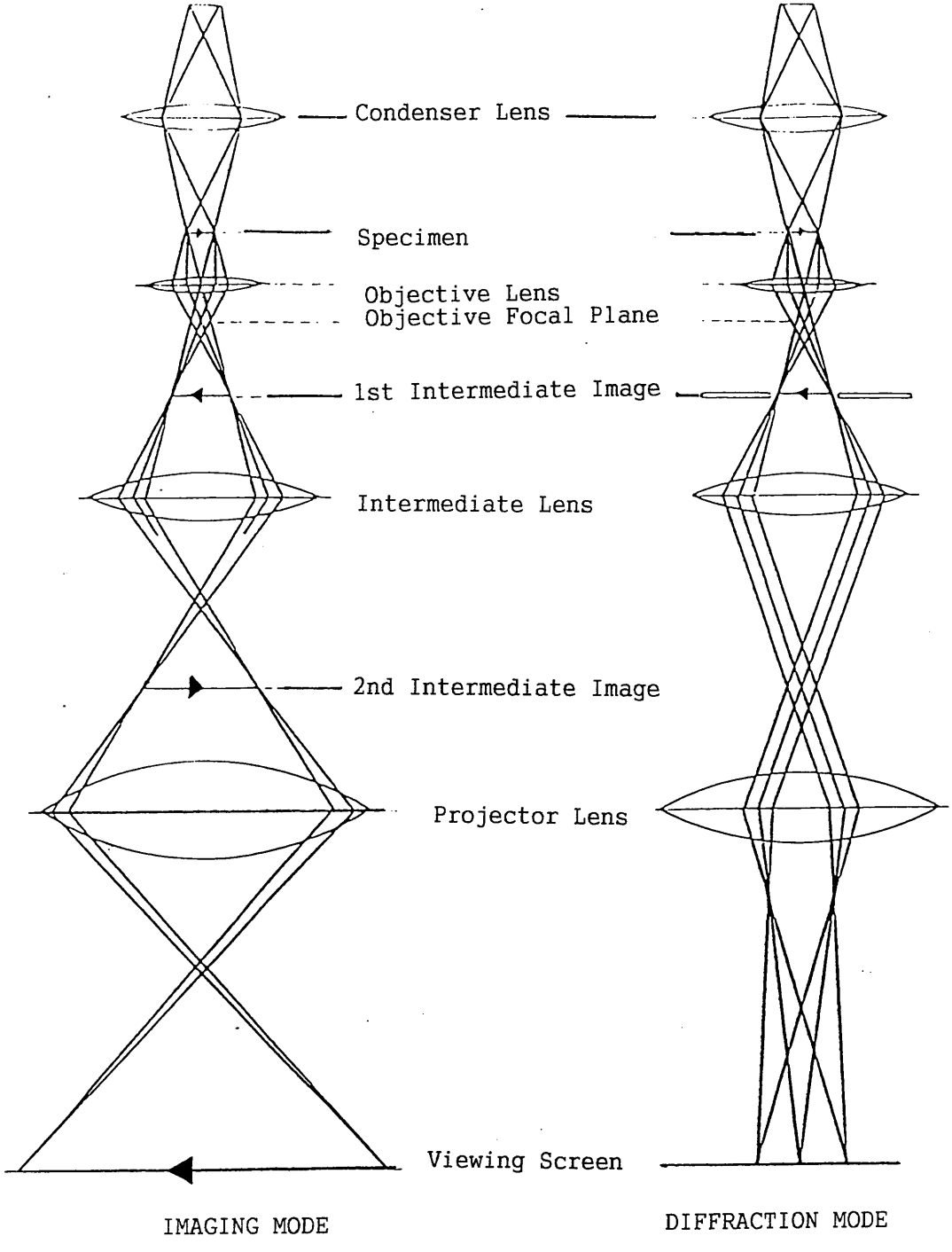

trons. A brighter and more coherent source of electrons can be obtained from a lanthanum hexaboride filament. However, these are not routinely used since they are more expensive and an operating vacuum of 10^{-8} torr is required (Ahmed 1971). The electrons are then accelerated from the gun towards an anode at earth potential. A typical accelerating voltage is 100 kV but microscopes have been built with accelerating voltages of 1000 kV (Uyeda 1990).

Having passed through an aperture in the anode, the electron beam is collimated by the condenser system. This consists of an aperture to allow the electrons in the centre of the beam, which have the greatest coherence, to pass through, and two or more condenser lenses.

Once a coherent beam of electron has been produced it then interacts with the specimen. The undeflected beam together with the electrons scattered by the specimen are then collected and magnified by the objective lens. Further magnification is by the projector lens and an image is projected onto a fluorescent screen. The image can be recorded photographically or by the use of a television camera (Fig. 12).

2.3 Coherence

The coherence of an electron beam refers to their ability to interfere with each other. This is important in the

production of good high resolution images. If the electron source is taken to be the exit plane of the final condenser lens. Then the spatial coherence width X_C is the width at the object plane which is irradiated by coherent illumination. The scattered waves from two atoms separated by less than X_C therefore interfere. If the distance is greater than X_C then no interference can occur as the electrons are scattered incoherently (Spence 1981).

The coherence width is related to θ_C, the semi-angle subtended by the beam at the specimen by the expression:-

$$X_C = \lambda/(2\pi\theta_C) \qquad \text{(ii)}$$

To obtain phase contrast θ_C must be chosen so that X_C is larger than the coarsest detail of interest in the specimen. When this condition is met, images of the object can be formed with optimum contrast at the Scherzer focus.

A tungsten filament emits a relatively incoherent source of electrons, the coherence can be improved by diverging the beam and inserting a small condenser aperture. A compromise must therefore be struck between the need for coherence and the need for brightness. Improvement can be obtained by the use of a LaB_6 filament or a field emitting filament.

The LaB_6 is similar in design and can be used in the

same way as a tungsten filament. It is particularly suitable for high resolution microscopy, where it will give extra brightness and a low energy spread for the emitted electrons.

2.4 Image Formation and Contrast

Image formation can arise from the recombination of scattered and undeviated electron waves, or by the exclusion of scattered waves after passage through the specimen.

There are two main forms of scattering, elastic and inelastic.

2.5 Elastic Scattering

Electrons are scattered elastically when they are deflected by atomic nuclei without any loss of energy. The proportion of electrons elastically scattered increases with increasing atomic number and increasing specimen thickness. In crystalline materials the electrons are scattered by the crystal lattice planes and obeys the Bragg relationship.

$$n \lambda = 2d\sin\theta \qquad \text{(iii)}$$

d is the lattice spacing.

θ is the angle of scattering.

n is an integer.

The scattering amplitude becomes smaller with increasing atomic number and increasing scattering angle.

If the electrons are scattered to such an extent that they are stopped by the microscope column or the objective aperture then image contrast arises. This is also called amplitude contrast or for a periodic specimen, diffraction contrast.

2.6 Inelastic Scattering

Inelastic scattering occurs when the electrons transfer part of their own energy to the atoms of the specimen, undergoing a change in their own energy and therefore a change in their wavelength. These waves contribute an out of focus background to the image, which reduces the contrast in the elastically scattered image. This is known as inelastic phase contrast.

2.7 Phase Contrast

Elastic phase contrast can be obtained if the objective aperture allows the transmission of elastically scattered electrons. These electrons have a longer path length than the unscattered electrons, so they will interfere and give an increase or decrease in amplitude. If the elastic phase contrast occurs as a result of scattering from a periodic structure then a related periodic structure will be imaged. This is the basis of lattice imaging in high resolution electron microscopy. Small periodicities will scatter electrons widely and if

they pass through the objective aperture then they will be focussed by off axis parts of the objective lens. This means that lens aberrations severely limit the resolution of lattices.

The interpretation of contrast is most easily carried out for thin specimens where it can be assumed that only one scattering event occurs. In reality however multiple scattering events do occur, the occurrence of thickness fringes being an example. A rigorous treatment of this is given by Cowley and Moodie (1957).

2.8 The Contrast Transfer Function

Scherzer (1949) considered the theoretical resolution limit of transmission electron microscope using wave mechanics. This took account of the interaction of the incident electron wave with the specimen and then the effect of the microscope in transferring the resultant wave to the image plane. This led to the contrast transfer function (Grinton and Cowley 1971) which is outlined below. It is assumed that the specimen is a weak phase object and that the scattered wave amplitudes are much smaller than those of the unscattered.

The image contrast represented by the intensity transmitted to the image plane can be explained by the consideration of the amplitudes of the elastically scattered electrons and the diffraction pattern they form. Phase

modulations induced by the specimen and by defects in the objective lens are accounted for and the resultant wave amplitudes are combined to form the image. The intensity distribution calculated should then correspond to the image seen in the micrograph.

For a coherent electron wave of unit amplitude the effect of passage through a thin object can be given by:-

$$\Psi_o(r) = \exp[i\sigma\Phi(r)] \qquad \text{(iv)}$$

Ψ_o is the transmitted amplitude of the object wave.

r represents real space coordinates.

i indicates the phase nature of the object.

σ is the interaction constant = $\pi/(\lambda W)$, where λ and W are the relativistically corrected electron wavelength and accelerating voltage respectively.

If the weak phase object approximation holds then the higher order terms in $\sigma\Phi(r)$ can be neglected and (iv) becomes

$$\Psi_o(r) = 1 + i\sigma\Phi(r) \qquad \text{(v)}$$

The Fourier transform of this object gives the transmitted amplitude in the back focal plane (the diffraction pattern) of the objective lens. The lens are not perfect so a phase modulator $\chi(s)$ is included, s represents reciprocal space coordinates. The presence of the objec-

tive aperture is accounted for by the function A(s), with value 1 inside the aperture and 0 everywhere else. The wavefunction in the diffraction plane is then :-

$$\Psi_D(s) = F[\Psi_o(r)]\exp[i\chi(s)]A(s) \qquad \text{(vi)}$$

The resultant amplitude distribution is given by the difference between the undeviated wave $\delta(s)$, and the elastically scattered amplitude distribution represented by (vi). Substituting for $\Psi_o(r)$ from (v) and performing the Fourier transform gives:-

$$\Psi_D(s) = \delta(s) - (\sigma\Phi(r)\sin\chi(s) - i\sigma\Phi(r)\cos\chi(s)) \qquad \text{(vii)}$$

The inverse transform of (vii) corresponds to the image plane and gives the resultant amplitude distribution :-

$$\Psi(r) = 1 - F(\sigma\Phi(r)\sin\chi(s) - i\sigma\Phi(r)\cos\chi(s)) \qquad \text{(viii)}$$

and the intensity distribution in the image plane, i.e. that seen on the micrograph is given by :-

$$I(r) = \Psi\Psi^*$$
$$= 1 - 2\sigma\Phi(r)*F\sin\chi(s) \qquad \text{(ix)}$$

where * indicates the complex conjugate. It must be remembered that the weak phase object approximation is held to be true for the above (Lynch and O'Keefe 1972).
The importance of the $\sin\chi$ is demonstrated by equation (ix) this term is known as the phase contrast transfer function which determines the transfer of information

from an object to the image. For a perfect lens $\sin \chi(s) = 1$, and equation (ix) becomes :-

$$I(r) = 1 - 2\sigma\Phi(r) \qquad (x)$$

in this case the object and the image would be linearly related. The defects in the magnetic lens preclude this possibility. $\chi(s)$ the instrumental phase adjustment factor was developed by Scherzer (1949) to allow for the main lens defects:-

$$\chi(s) = 2\pi/\lambda(\Delta f(\alpha(s)^2/2) - (C_S\, \alpha(s)^4)/4) \qquad (xi)$$

$\alpha(s)$ is the scattering angle in reciprocal space.

C_S is the spherical aberration coefficient of the objective lens.

Δf is the lens defocus value.

The final image is therefore dependent on the oscillatory function $\sin \chi$, and has different values for different spatial frequencies. Figure 13 shows $\sin \chi$ plotted against the reciprocal periodicity ($1/d$ $\text{Å}^{-1} \equiv \lambda/\alpha$), assuming coherent illumination over a range of defocus values.
The optimum defocus value gives a transfer function a value of near unity for the largest range of spatial frequencies without contrast reversal. This was calculated by Scherzer to be

$$\Delta f' \approx 1.2\sqrt{(C_S\, \lambda)} \qquad (xii)$$

The combination of the lens defects lead to the theoretical resolution limit d_{min} of the microscope and is called the Scherzer cut off:-

$$d_{min} = 0.65 C_s^{1/4} \lambda^{3/4} \qquad \text{(xiii)}$$

Great care must be taken in the interpretation of periodic images since the presence of certain periodicities in a micrograph is dependent on the defocus used.

So far it has been assumed that a perfectly coherent electron source is being used. In reality this is not the case so a more complete transfer function must take account of this. This is achieved by the use of an envelope function (Boerchia and Bonhomme). The effect of which on the phase contrast transfer function is shown in figure 13.

The kinematical approximations used in the derivation of the phase contrast transfer functions do not hold for real specimens which are often too thick, which means that multiple scatterings can occur. The more rigorous dynamical treatment devised by Cowley and Moodie (1957) can be applied. In this approach the object is assumed to be made up of many thin slices, each a weak phase object scattering the electrons only once (Buseck et al 1988).

2.9 Electron Diffraction

The transmission electron microscope may be adjusted

FIG. 13

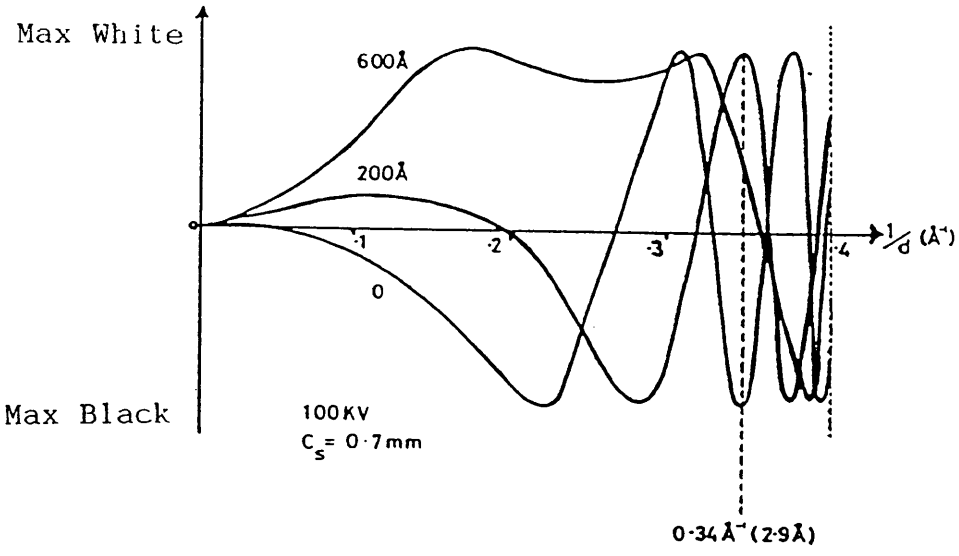

Phase Contrast Transfer Functions for a range of defocus values.

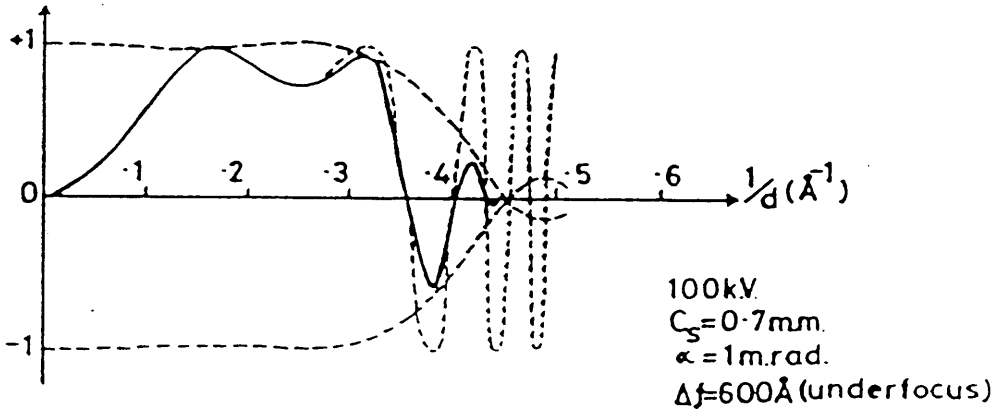

Phase Contrast Tansfer Function modified by damping envelope function. The full line is the product of sin χ and this function.

for use as an electron diffraction camera simply by adjusting the projector lens so that the diffraction pattern which occurs at the back focal plane is focussed on the viewing screen (Fig 12), (Andrews et al 1967).
The area from which the diffraction pattern is to be taken can be selected by the use of an aperture. In order to interfere Bragg's law must be satisfied.

$$n\lambda = 2d\sin\theta \qquad \text{(xiv)}$$

d is the lattice spacing.

θ is the scattering angle.

λ is the wavelength of the electrons.

n is an integer.

from figure 14 it can be seen that the spacing D/2 in the diffraction pattern can be related to the scattering angle θ. This gives:-

$$\tan 2\theta = D/2L \qquad \text{(xv)}$$

since θ is normally very small equations and may be combined to give :-

$$Dd = 2/L \qquad \text{(xvi)}$$

2/L is a constant since it depends on the microscope operating conditions and it is called the camera con-

FIG. 14
Scattering of Electrons

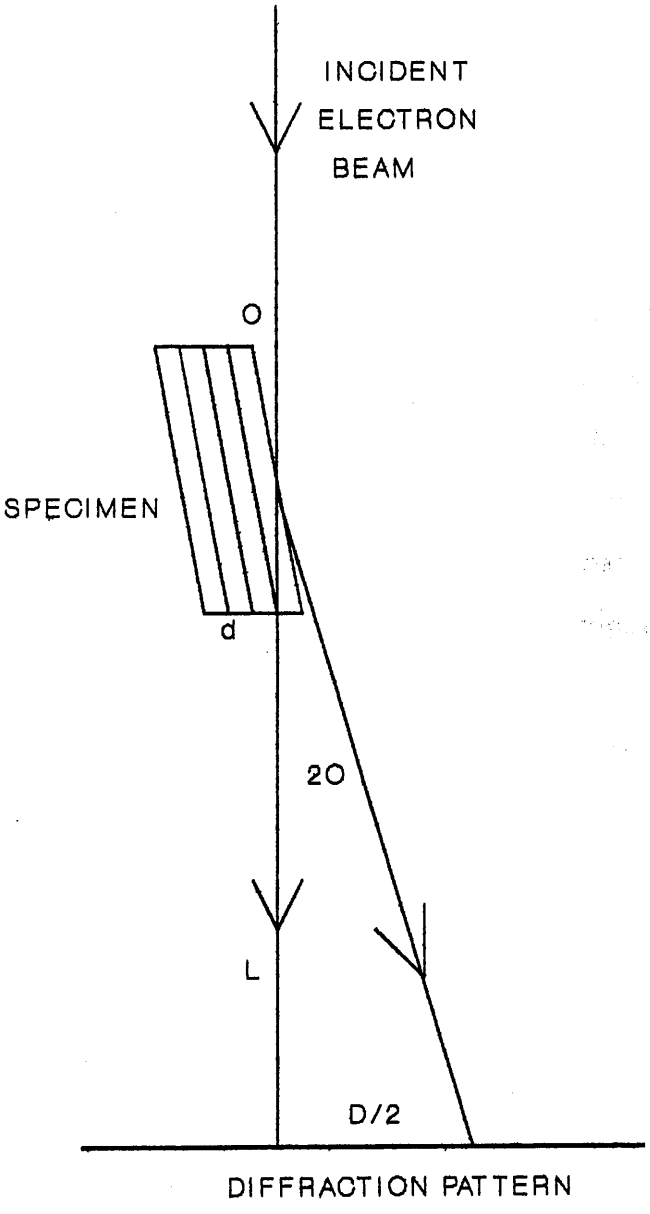

stant. L is the effective camera length and is given by:-

$L = f_o M_1 M_2 M_3$ (xvii)

f_o = focal length of objective lens.

$M_{1,2,3}$ = magnification of intermediate and projector lens.

A standard of known lattice spacing is used to determine the camera length, often graphite or thallous chloride. Diffraction patterns from unknown samples can then be measured accurately and compared to other known spacings, these have been tabulated by the A.S.T.M. Joint Committee on Powder Diffraction Standards (1971). Diffraction spacings can also be compared to calculated spacings from molecular modelling programmes (Voigt-Martin 1990).

Diffraction patterns contain information about the crystallinity of a specimen and also the orientation of the specimen. They can also be used to determine the crystal structure of some specimens (Dorset 1990).

2.10 Radiation Damage

With organic specimens the greatest limitation in obtaining high resolution images is radiation damage caused by the electron beam. As the specimen may be destroyed before sufficient electrons have passed through it to form a good image.

The phenomenon of radiation damage is mainly due to the inelastic scattering of the electron beam (Grundy and

FIG. 15
Radiation Damage

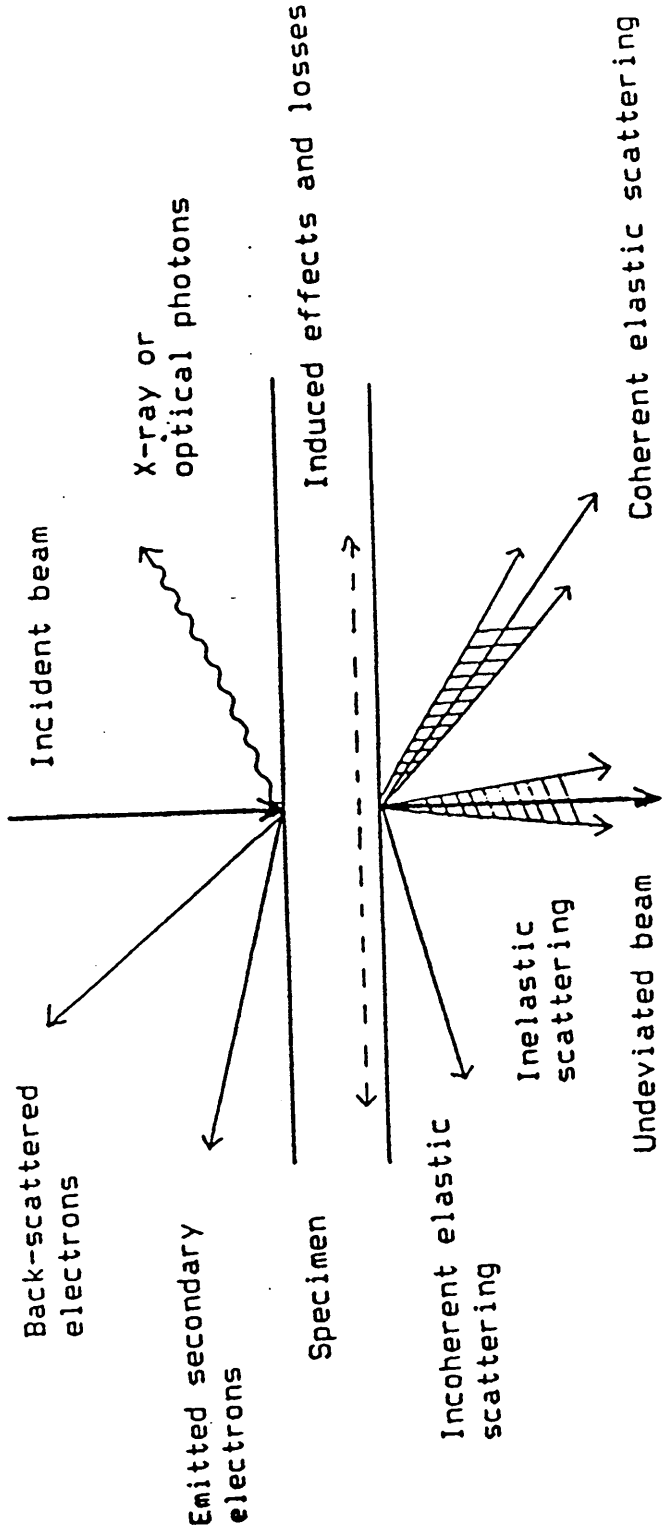

Jones 1976). The energy imparted to a specimen by inelastic collisions may affect a molecule in many ways (Fig. 14). There may be ionisation from valence and inner shells, the formation of excited molecular states, the transfer of energy to an adjacent molecule, the dissociation of excited vibrational states, electron capture and radical reactions. Bond disruption is commonly the result of these processes and a variety of fragmentation products can be observed such as gaseous H_2.

Aromatic materials are considerably more stable than aliphatic materials, this has been attributed to the delocalised molecular orbitals which can distribute the effects of ionisation over the molecular network (Issacson et al 1976). In addition the excited states in aromatic systems can relax by the emission of fluorescent radiation. Aromatic molecules can exhibit a protective influence over aliphatic hydrocarbons by the transfer of energy from one part of a molecule to another (Friedlander and Kennedy 1962).

The excited molecular species initially produced can undergo chemical reactions involving neighbouring molecules. Commonly these are radical reactions, this could be the reaction of a radical with a neutral molecule to produce another radical or it could be the abstraction of a hydrogen atom (Henglein 1984). The reaction will be terminated by the formation of a neutral species or

stable ion. A diffusing electron may be trapped by a lattice defect or by reaction with an electron scavenger such as a halogen atom which reacts to form a stable ion.

It has been observed in some substituted aromatic compounds that molecular fragments released by radiation damage processes remain localised because there is no diffusion route. This is called the "cage effect" (Murata et al 1977).

Radiation damage imposes a limitation on resolution, a theoretical limit has been calculated (Glaeser 1971):-

$$Cd \geq S/\sqrt{(fN_{cr})} \qquad \text{(xvi)}$$

C is the object contrast (typical value 0.1).

d is the minimum object size.

f is the utilisation factor.

N_{cr} is the critical exposure for damage ($e\text{Å}^{-2}$).

S is the signal to noise ratio.

Applying this equation to the polycyclic aromatic naphthacene (Fryer 1978) would suggest a maximum attainable resolution of 0.9 nm however a greater resolution may be obtained by using one of the many techniques to overcome some of the effects of radiation damage. This equation acts as a useful guide to the feasibility of studying a particular specimen.

2.11 Overcoming Radiation Damage

To reduce to a minimum the amount of time an area of a specimen is exposed to the damaging electron beam, minimal exposure techniques have been developed. The sample is only exposed to the beam during the image recording. This is achieved by focussing and setting the exposure times on an area of sample close to the desired area, and then the beam is switched off or deflected while the desired area is brought into position. An image is then recorded.

The use of an imaging system that does not require a high number of electrons to form an image will drastically cut down the damage to the specimen. X-ray film is more sensitive than normal photographic film and has been used successfully to obtain greater resolutions. Unfortunately X-ray film has a coarse grain so it is not routinely used. Television cameras only require low doses of electrons to form a good image and are often used. There is the added advantage that a signal from a television camera is easily digitised, stored on computer and image processed. In low electron dose micrographs the information available in the image is not always easily observed, computer image processing can be used to eliminate noise and to average periodic information thus highlighting any useful information. This is discussed later.

Microscopes with large accelerating voltages will reduce radiation damage by lowering the number of inelastic collisions. The lifetime of some organic substances can be improved by a factor of 3 on increasing accelerating voltage from 100kv to 1MeV (Cosslett 1978).

Support films that are able to conduct heat away from the irradiated area of sample can prolong sample life (Grubb 1974). Fortunately copper grids with a carbon support film are able to do this relatively well. Encapsulating the sample in a carbon film gave a marked improvement in the lives of halogenated aromatic compounds (Fryer and Holland 1983), probably by a method similar to the cage effect.

Cooling the specimen to liquid helium temperatures can increase sample lifetime considerably (Knapek 1982). This is achieved by the "freezing in" of damaged particles preventing fragments from diffusing out of the lattice. The rate of the chemical reactions of any reactive species formed will also be slowed down.

2.12 Electron Microscopy of Organic Crystals

The majority of molecular crystals are organic, and their crystal structures are now routinely determined by X-ray techniques. However it is still desirable to study organic crystals by electron microscopy for a number of reasons. The resolution obtainable from a wave of high

energy electrons is theoretically greater than that from X rays. The limitations in microscope design that prevent attainment of desired resolution are gradually being overcome. The transmission electron microscope allows information from thin films and very small crystals to be gathered, this could not easily be achieved by X-ray crystallography which requires relatively large single crystals. The high resolution lattice images obtained by electron microscopy are of stacks of molecules and are not an average picture of an entire crystal, information about the environment of individual molecules is therefore obtained.

There are however drawbacks in the study of organic crystals, they are very beam sensitive, as a result so only a few aliphatic compounds have been successfully examined (Fryer and Dorset 1987). Preparation of correctly orientated samples is difficult so if a compound cannot be evaporated to form a thin film or will not crystallise as a thin crystal it cannot be easily studied.

Crystals of biological materials such as enzymes and viruses can be crystallised and of course show very large lattices. Images of a biological crystal were obtained from unstained crystals of ribonuclease (Dawson and Watson 1959). Protein electron crystallography is now developing as a powerful tool for studying these large polymers in their native topological situation (Baumeis-

ter et al 1991).

The first phase contrast lattice images of an organic material were obtained of platinum and copper phthalocyanines (Menter 1956), the use of phthalocyanines was convenient for many reasons. They were commercially available pigments whose crystal structures had already been determined (Robertson 1935). The problems of specimen determination and beam sensitivity could also be partially overcome. Phthalocyanines can be prepared as extremely small crystals, small enough to allow microscopy or they can be prepared as thin films since they are very stable to heat and can be evaporated under vacuum onto a substrate. They have also turned out to be relatively stable in the electron beam.

Stability and ease of thin film preparation has also facilitated a good deal of work with polycyclic aromatic compounds. Less stable materials such as paraffins and polymers have also been studied. The methods that can be used to overcome radiation damage to organic specimens are discussed elsewhere.

The first image of an organic molecule was obtained by Uyeda (1972) and his co-workers and was that of hexadeca-chloro phthalocyanine (Fig. 16). This molecule is extremely resistant radiation damage. The image is that of a superimposed stack of molecules so the orientation of the stack is crucial for good imaging. Images of non-

FIG. 16

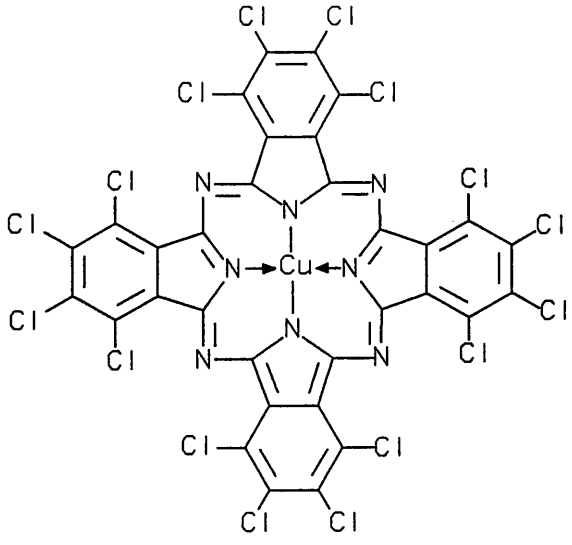

Hexadecachlorophthalocyanine

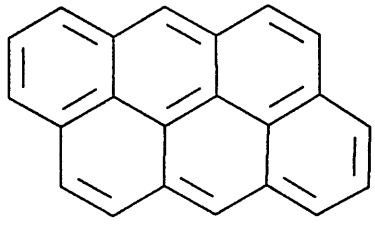

Anthanthrene

chlorinated phthalocyanines have also been obtained for both metal free (Fryer 1979) and metallo phthalocyanines (Murata et al 1976).

Polycyclic aromatic compounds show a similar order of stability to phthalocyanines. The first molecule of this type to be imaged was anthanthrene (Fig. 16) by Fryer (1978) at Glasgow University. The only perinaphthalene to be studied in depth is quaterrylene which was imaged using a 500 kV microscope by Fryer and Smith (1981). Until this point high resolution studies had concentrated on molecules with a superimposable major crystallographic axis. Quaterrylene was imaged in projection down the {110} axis (Fig. 17). This gave an image of the molecular columns despite the molecular planes being slightly inclined to the direction of the electron beam. Images have not been obtained of perylene it being more beam sensitive than quaterrylene.

Crystallographic information of organic materials can be obtained by electron diffraction. Though a diffraction pattern does not look at individual molecules the area of crystalline sample required is still much smaller than that needed for X-ray work. Compared with high resolution imaging there is less radiation damage with electron diffraction since a lower beam intensity is required to form a diffraction pattern than an image. This makes this technique the most suitable for aliphatic compounds

FIG. 17
Crystal Structure of Quaterrylene

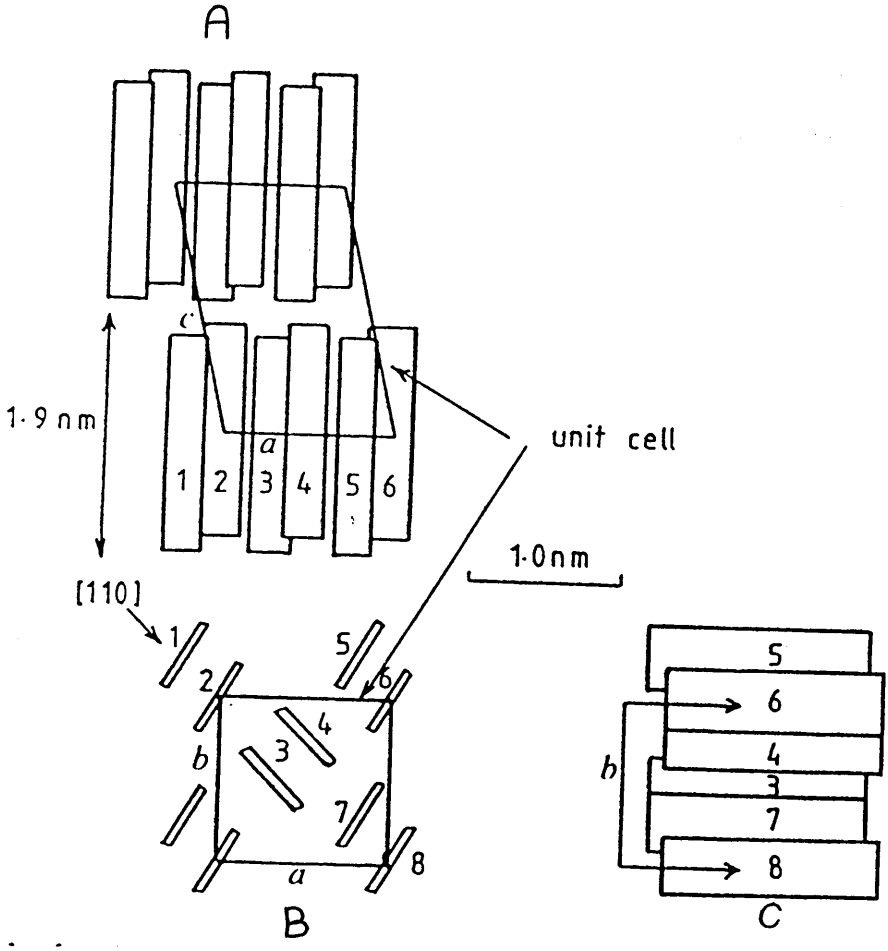

A b axis projection

B c axis projection

C a axis projection

and other beam sensitive materials (Dorset 1985). The dimerisation of anthracene was investigated by Thomas et al (1972) with the lattice parameters being seen to change upon dimerisation, it was also possible to show that the mechanism was dislocation induced. Electron diffraction can be used for phase identification where several phases exist in a very small crystal (Young and Levine 1974).

2.13 Electron Microscopy of Liquid Crystals

Both thermotropic and lyotropic liquid crystal systems have been studied by electron microscopy. The techniques used in each system are however very different. Amphiphilic systems have used replication, freeze fracture, and staining methods (Goodman and Clunie 1974). Using an osmium tetroxide stain it is possible to observe hexagonal phases in potassium oleate micelles and a lamellar phase with sodium linolenate.

The structure of polymeric liquid crystals have recently received much attention due to their potential for technological applications. They are also amenable to high resolution electron microscopy because samples can be well orientated by "poling" in a magnetic field followed by rapid cooling. This has allowed the direct observation of the microstructure and defects. High resolution images have been obtained for a main chain

polymalonate ester and a discotic polymer by Voigt-Martin (1990). The triphenylene based discogen was observed in a hexagonal phase as a disc because of molecular rotation. The triphenylene monomer was also imaged in the crystalline state.

Electron diffraction of liquid crystals only show 1st order reflections due to the motion of the molecules.

In situ electron diffraction studies have been carried out (Hui et al 1990) where the formation of hexagonal smectic phases was observed directly. In the mesophase arcs rather than spots where observed because of the greater disorder than in a crystalline solid.

In smectics and discotics there is some short range order but little long range order. This is most noticeable in electron diffraction where small angle spacings will usually only show first order maxima.

CHAPTER 3: MICROSCOPY TECHNIQUES

3.1 Microscopes Used

Transission electron microscopy was carried out with a JEOL 100C and a JEOL 1200EX transmission electron microscopes.

The JEOL 100C normally operates with an accelerating voltage of 100 kV. It has a top entry specimen stage and cannot be used with a hot stage in the same way as the JEOL 1200EX. The JEOL 100C can be fitted with a high resolution pole piece, but in this study a medium resolution pole piece was used. This gives a maximum lattice resolution of 0.2 nm. It does not have a built in minimum dose system but low electron dosages were achieved using the dark field switch. This could be used to deflect the beam away from the area of interest to allow the specimen to settle, and the beam could be brought back to the selected area once a plate was exposed. The images of anthanthrene (Fryer 1978) were taken on the JEOL 100C using this minimum dose system and the high resolution pole piece.

The JEOL 1200EX operates at 120 kV and has lattice resolution of 0.14 nm. It has a side entry specimen stage that can be tilted by up to 30 degrees. An image intensifier was used to aid focusing and astigmatism correction. The JEOL 1200 EX has a built in minimum dose system. This system allows an area to be selected at very low brightness and the beam deflected to an adja-

cent area were the focus, brightness and the exposure can all be set. The micrograph is then exposed automatically.

3.2 Microscope Hotstage

The JEOL 1200EX can be fitted with a Hexland hotstage which is capable of heating specimens inside the microscope to temperatures in excess of 300°C. Normal copper 3.05 mm grids are used and the stage is heated electrically.

3.3 Image Processing

In high resolution micrographs of periodic objects the signal to noise ratio can be very low, especially when minimum dose systems have been used. Three methods are commonly used to improve the signal to noise ratio, photographic averaging, optical image processing and computerised image processing.

Photographic averaging is carried out by exposing the photographic paper many times while each time moving the periodic image by one repeat unit distance, thus averaging the information in each molecular image over the whole picture. This was successfully used by Fryer and Smith (1981) in their images of quaterrylene.

A laser optical bench may be used for the analysis and noise filtration of images. The lattice image of the

micrograph acts as a diffraction grating and a spot pattern that corresponds to the electron diffraction pattern of the same sample is formed. This optical diffraction pattern may be used to check the resolution and operating parameters of the microscope (Mulvey 1991). It can also detect crystalline areas of the sample that are not normally visible because of noise. A standard grating may be used and the lattice sizes may be measured very accurately. The optical bench may also be used to remove the noise from periodic images. This is achieved by applying a mask to the diffraction pattern formed in the back focal plane of the optical bench, masking out any signals that are not periodic. The image is then reconstructed by means of lenses, is projected onto a screen, and should have a much better signal to noise ratio.

3.4 Computerised Image Processing

The computer is capable of doing many things to an image. It can be enlarged, areas can be cut out and pasted together, contrast reversed, false colour added and of course the signal to noise ratio can be improved. The picture to be stored on computer can be taken directly from a microscope fitted with a television camera or simply taken from the micrograph. The computer stores the image digitally so mathematical manipulation can be carried out.

Image enhancement of periodic objects is normally carried out by Fourier filtering (Misell 1975). The Fourier transform of an image is the equivalent of an optical diffractogram and the Fourier transform of a periodic structure contains the structural information of amplitude and phase in the peaks of the transform. The peaks represent a projection of the reciprocal lattice. Noise is distributed over the whole transform and this may be excluded by the means of a mask. The mask consists of windows placed round these peaks and only signals inside the windows may contribute to the final image. It is important not to make the windows too small as lattice distortions and imperfections in the sampled area broaden the peaks. The final image is obtained by simply performing an inverse Fourier transform calculation.

At Glasgow the SEMPER 6 system is used. This is a high level language that allows great flexibility and can be adapted for most image processing needs.

The diffraction pattern contains no phase information. This information is however available in the image and in the Fourier Transform of the image.

CHAPTER 4: THIN ORGANIC FILM GROWTH

4.1 Specimen Preparation For TEM

The transmission electron microscope can only be used for thin specimens, typically 10-100 nm thick. There are a large number of techniques that can be used to prepare suitably thin samples. The method used depends on the nature of the sample and the information required from it. For organic materials the most common methods are precipitation from solution of suitably sized crystals, physical vapour deposition (PVD), Langmuir Blodgett deposition and for polymers thin sectioning (Fryer 1979b).
Thin films of organic materials are also required for molecular electronic uses so transmission electron microscopy is the ideal instrument to study these films. The techniques used to prepare films for electronic devices are much the same as for microscopy.

4.2 Evaporated Thin Films

Thin films organic compounds can be prepared by evaporation under vacuum onto a substrate this is also known as physical vapour deposition or PVD. Unfortunately not all organic compounds are stable to the heat required for the sublimation under vacuum. This technique has been extensively applied to the phthalocyanines (Uyeda 1977), polycyclic aromatic quinones (Ashida et al 1972) and aromatic hydrocarbons (Fryer 1978). These large flat

molecules have produced well orientated crystalline films under the correct conditions. Typical substrates used are alkali halides, mica and graphite. The types of films that could be formed can be grouped under the following headings polycrystalline, epitaxial in one dimension, epitaxial in two dimensions (a single crystal film) and a continuous single crystal film similar to the bulk crystal.

4.3 Epitaxial Thin Films

An epitaxial layer is one in which a film is arranged on a substrate so that the crystals all have the same orientation because the substrate has had some effect on the growth of the film. Epitaxy may occur in many systems for example metals upon alkali halides, silicon upon sapphire or quartz and alkali halides upon mica (Mathews 1975). In organic systems a good example is phthalocyanine upon muscovite (Ashida 1966).

The structure of the evaporated film is dependent on the surface structure of the substrate and the forces between the adsorbed molecules and the substrate. An empirical relationship has been derived for inorganic crystals which says an epitaxial thin film will be formed if the lattice parameters of the evaporant and the substrate match within 15% (Pashley 1965). This model is harder to apply to organic compounds since these molecules tend to be much larger than the lattice parame-

ters of an inorganic substrate. However if the lattice spacing of the overgrowth is a multiple of the lattice spacing of the substrate epitaxy may still occur (Uyeda and Murata 1982). The first monolayer may become distorted to achieve this correspondence, or dislocations may occur between it and the substrate to achieve a good fit. The epitaxial nature of some phthalocyanine films is explained by Ashida (1966) as resulting from the strong interaction between some of the nitrogens and the K^+ of the substrate. For other molecules such as polycyclic aromatics such strong interactions may not exist and weaker Van der Waal forces must be considered.

When the vapour of the overgrowth material meets the substrate, the formation of the thin film takes place in several stages (Ueda and Mullin 1974). The first is the formation of a distribution of small three dimensional nuclei, these nuclei then grow in size without any increase in their numbers. The further growth in size of the nuclei results in the formation of islands and a decrease in their numbers. Finally a connected network of deposit is formed and this becomes a continuous deposit of material free from holes. This sequence was initially described for metals but the pattern is similar for non metals. The formation of nuclei is important since when an adsorbed molecule has migrated to and

bound to a cluster it is less likely to undergo desorption. Nuclei tend to form at defects sites on the substrate since at these positions there is an excess Gibbs free energy (Green 1973). The phenomenon of migration allows adsorbed molecules to organise themselves in an epitaxial fashion. Migration is possible because molecules are bound to the surface only by weak forces, the activation energy for migration is in general only 10-20% of the energy of the surface adsorbate bond. This means that migration and the formation of evaporated films in general is very temperature dependent.

Substrate temperature effects on the quality of evaporated thin films have been carried out for a range of aromatic compounds and metals by Vincett et al (1977). The films were assessed electrically and by scanning electron microscopy. The optimum substrate temperature for epitaxy was found to be approximately one third of the boiling point of the evaporant. This temperature was explained in terms of bulk thermodynamics and the ease of re-evaporation. These arguments are however not easily applied to organic materials because of the large variations in sticking coefficients (McConnell and Fryer 1991). It is also the case that boiling point data for most organic compounds is unavailable and hard to measure.

The type of substrate used will determine what type of film is formed since the nature of an epitaxial film

depends on the strength of the adsorbate surface bonds. The quality of the surface should also be carefully considered. An adsorbed molecule may find it easier to migrate to the foot of a step or it may become trapped at a vacancy site. Mobility may also be easier along one crystal face of the substrate or the growing film than another (Drauglis et al 1969). Langmuir Blodgett films have been successfully used as substrate for the PVD of a thin film of an amphiphilic diacetylene heptacosa-10,12-diynoic acid (Inoue et al 1989).

The formation of evaporated thin films of perylene has been investigated (Debe 1982) and (Fan et al 1972). The latter study found that on a gold substrate perylene will lie with its ab plane parallel to the surface. With large planar aromatic molecules the mode of stacking on the substrate may vary (figure 18). The mode depends on the type of substrate. For example coronene will stack vertically on KCl but not on mica.

It is possible to improve the quality of metal thin films by annealing but this approach has not proved particularly successful for planar organic molecules. This is because of the strongly preferred direction of growth along the column axis (Fryer 1979b), so if the plane of the molecules is not perpendicular to the substrate the all that will be achieved will be a thickening of the film.

FIG. 18

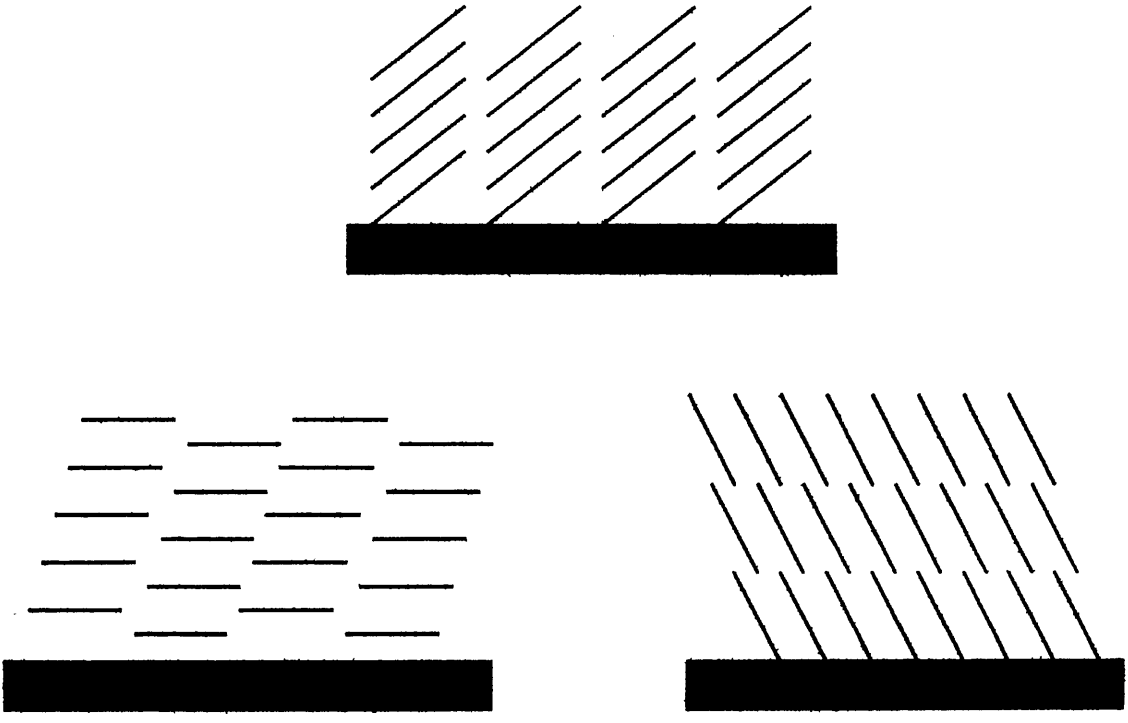

GROWTH OF MOLECULAR CRYSTALS ON A SUBSTRATE

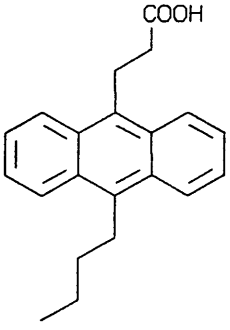

9-Butyl-anthryl-
propionic acid

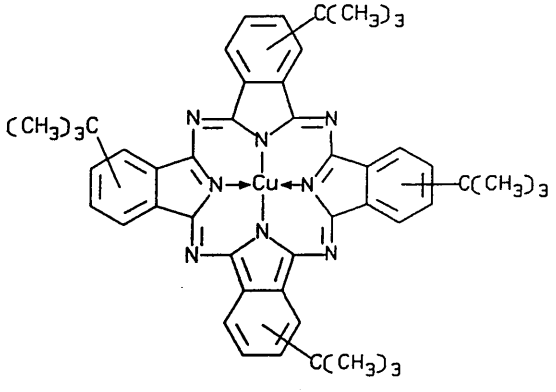

Tetra-t-butyl-
phthalocyanine

4.4 Langmuir Blodgett Films

Langmuir Blodgett (LB) films were first made by Irving Langmuir (1917) and Katharine Blodgett (1935). They deposited monolayers of fatty acids onto the surface of water and then deposited films onto solid substrates. More recent work has extended the uses and the range of compounds that can be used (Kuhn and Mobius 1971). Some of the potential uses are optical coatings, electro-optical devices, gas sensors and for microbeam lithography (Roberts 1984).

A Langmuir Blodgett film is formed by depositing a solution of a small quantity of a suitable material, such as stearic acid, onto a liquid surface, normally purified water. The solvent is then allowed to evaporate and a mono-molecular layer is produced. This layer can then be compressed until a quasi solid one molecule thick is formed. Compressing the layer helps order the molecules. For example with stearic acid the polar heads are immersed in the water and the hydrophobic tails are left pointing upwards. Monolayers can be removed from the liquid surface and coated onto a substrate surface by dipping or raising the substrate through the monolayer. Films many molecules thick can be built up in this way. Alternating layers of different materials can also be formed. Few naturally occurring compounds are suitable for LB film formation so new compounds are being de-

signed. The classic LB film forming molecule contains a polar hydrophilic head and a hydrophobic tail. Stearic acid is a good example, it possess a water soluble carboxylic acid head, and a long alkyl chain tail. A suitable molecule must also be soluble in a volatile solvent such as chloroform or xylene. It must also be insoluble in water.

Recently LB film forming molecules have been designed with aromatic groups incorporated an example is 9 butyl-anthryl propionic acid (Fig. 18), (Roberts 1984). Porphyrin derivatives have also been used (Bull and Bulkowski 1983). Phthalocyanine derivatives have recently received a lot of attention because of their many useful properties and their stability. The problem of their insolubility in suitable solvent has been overcome by peripheral substitution. Roberts et al (1983) were the first to prepare a LB film of a phthalocyanine with a tetra-t-butyl- phthalocyanine. Films of an asymmetrically substituted phthalocyanine that mimics a fatty acid has been prepared by Cook et al (1989).

The first lattice image of an LB film monolayer was obtained by Fryer et al (1985) with tetra-t-butyl- phthalocyanato copper (Fig. 18). As might be expected the monolayer was extremely sensitive to the electron beam and low dose methods with exposures as low as 30 ms, had to be used. Along with the images diffraction stud-

ies were able to give information about the ordering of the monolayer. Different orientations and an "island" structure were observed. Other LB films studied by transmission electron microscopy include tricosenoic acid (Peterson 1984), a thorium hexafluoroacetyl acetone complex (Baumeister and Hahn 1973) and Uyeda et al (1987) have used dark field microscopy to study monolayers of stearic acid.

CHAPTER 5: EVAPORATED THIN FILM METHOD

5.1 Equipment and Materials

The perylene was used as purchased from the Aldrich Chemical Company and has a stated purity of greater than 99%.

The quaterrylene used was synthesised in Glasgow University by Andrew Craig (1988).

The KCl was purchased from Agar Scientific, as 1cm cubes and was cleaved into plates 1cm square. The mica was also purchased from Agar Scientific. The carbon was evaporated from two carbon rods.

An Edwards 306 coating unit which is capable of a 10^{-7} torr vacuum was used to prepare all thin films and to evaporate the carbon.

5.2 Preparation Of Perylene Thin Films

Thin films of perylene and were prepared by evaporation under high vacuum. All films were prepared at 10^{-6} torr. A liquid nitrogen cooled cold trap was present. The substrate onto which the film is deposited was mounted on a holder. The substrate holder could be heated to 300°C electrically or cooled to -40°C by a cold finger system with liquid nitrogen. The temperature was measured with a calibrated copper constantan thermocouple with a digital readout.

The substrates used were KCl and mica. Unfortunately

the thin films prepared on mica could not be separated from the substrate so all results are from KCl. To obtain a clean substrate surface the KCl was cleaved with a razor blade to expose an unstepped (100) face. The KCl was then heated under vacuum to 300°C to desorb any gases and allowed to cool to desired temperature. The cooling rate was slow, so over the period of the evaporation the substrate temperature (T_S) was held to be constant.

The material to be evaporated was weighed and placed in a molybdenum boat. The boat was then resistively heated, and over a period of one minute the perylene was allowed to evaporate. The substrate was then allowed to return to room temperature before the coated KCl was removed.

To prepare the thin film for transmission electron microscopy a thin layer of amorphous carbon was evaporated under vacuum onto the KCl. This carbon acts as a support for the film. The thin film and the carbon were then separated from the KCl by floating off with distilled water. The perylene film was then transferred onto 3.05mm copper grids and allowed to dry.

The thickness of the films prepared could be calculated (Holland 1956) assuming a sticking coefficient of unity. However the sticking coefficient will decrease as the temperature of the substrate is increased. The distance

between the boat and the substrate was 12cm except for the 20°C film were it was 10cm.

Conditions for Perylene Thin Film Preparation

Substrate Temp T_S	Weight of Perylene	Calculated Film Thickness
-40°C	2.2mg	4.3nm
-20°C	3mg	5.9nm
0°C	2.5mg	4.9nm
20°C	1.3mg	5.9nm
40°C	2.7mg	5.3nm
60°C	5mg	9.8nm
80°C	5mg	9.8nm
100°C	5mg	no deposition

5.3 Preparation of Quaterrylene Thin Films

Evaporated thin films of quaterrylene were prepared by a similar method as was used with perylene. The only differences being that quaterrylene has a higher boiling point so the best films were deposited with higher substrate temperatures, and the substrate distance was held at 10cm.

Conditions for Quaterrylene Thin Film Preparation

Substrate Temp T_S	Weight of Quaterrylene	Calculated Film Thickness
20°C	5mg	20.2nm
60°C	6mg	24.3nm
200°C	5mg	20.2nm
250°C	3mg	12.1nm

Calculated spacings for alpha perylene

a= 1.135 b= 1.087 c= 1.031 beta= 100.8°

(100) 1.11 nm

(001) 1.01 nm

(010) 1.09 nm

(110) 0.78 nm

(011) 0.74 nm

(101) 0.69 nm

(111) 0.58 nm

CHAPTER 6: RESULTS AND DISCUSSION

6.1 Perylene Thin Films Results

-40°C. This was the lowest temperature at which perylene thin films were prepared. Plate 1a shows that it is composed of many small crystals which are often fused. The crystals are approximately $2.7x10^5nm^2$ in size and have a square shape reflecting the symmetry of the KCl substrate. There is a variation in contrast among the many crystallites, indicating vertical misalignment with some of the crystals having no major Bragg axis parallel to the electron beam. It could also indicate variations in film thickness.

The diffraction pattern (plate 1b) is arced but indicates that the crystals of perylene all have their ab (001) face parallel to the substrate surface. The arcing is caused by individual crystals being rotated relative to each other. But still with a common face on the substrate.

	$d_{observed}$	$d_{calc.}$	assignment
plate 1b	1.16	1.11	(100)
	1.12	1.09 nm	(010)

-20°C. The crystal size (plate 2a) is similar to that of the -40°C film. However in this film nucleation has occurred not only on the KCl surface but

PLATE 1 PERYLENE

T_S = -40°C

1A 17800 X magnification

1B 1.3 nmcm constant

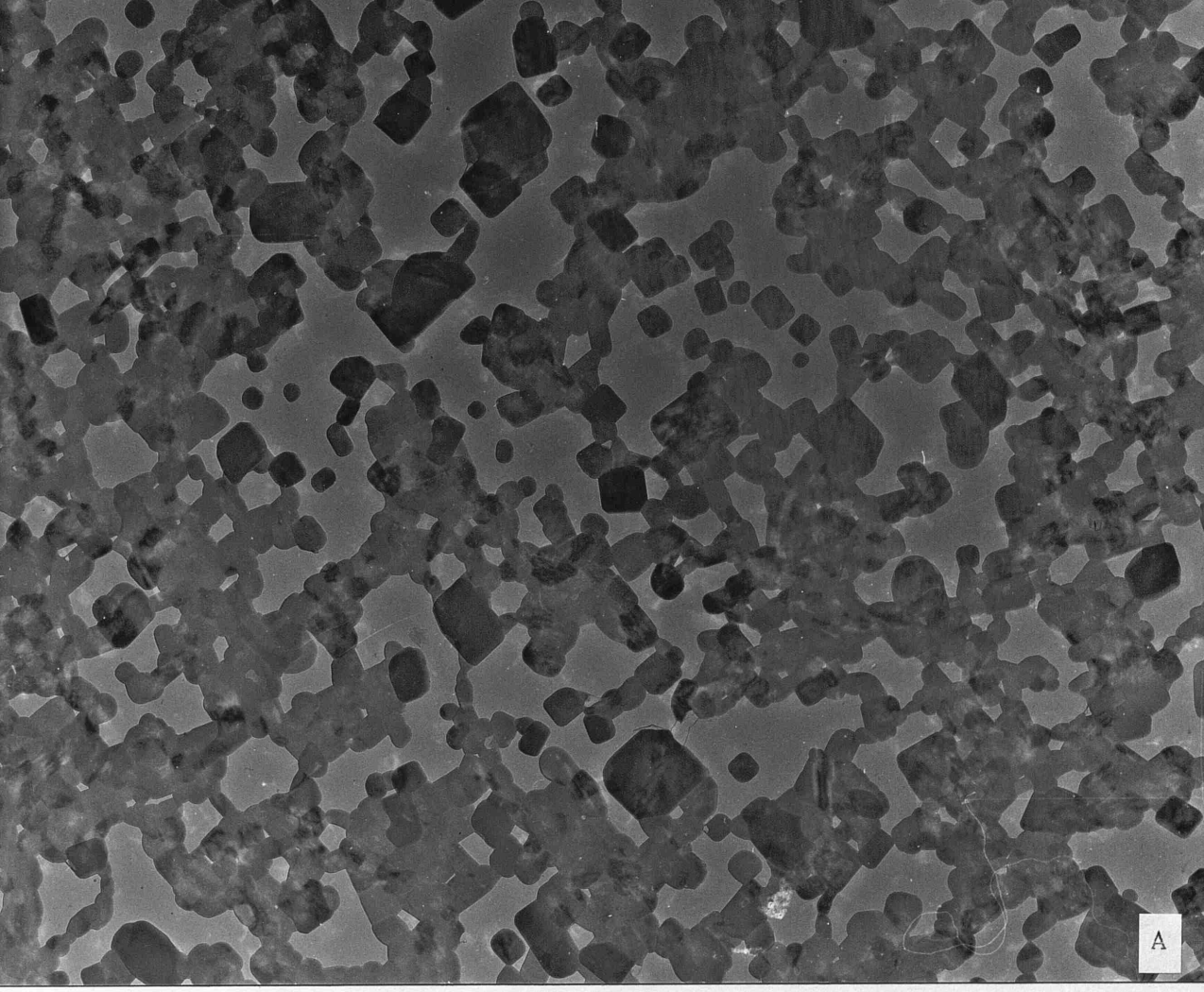
A

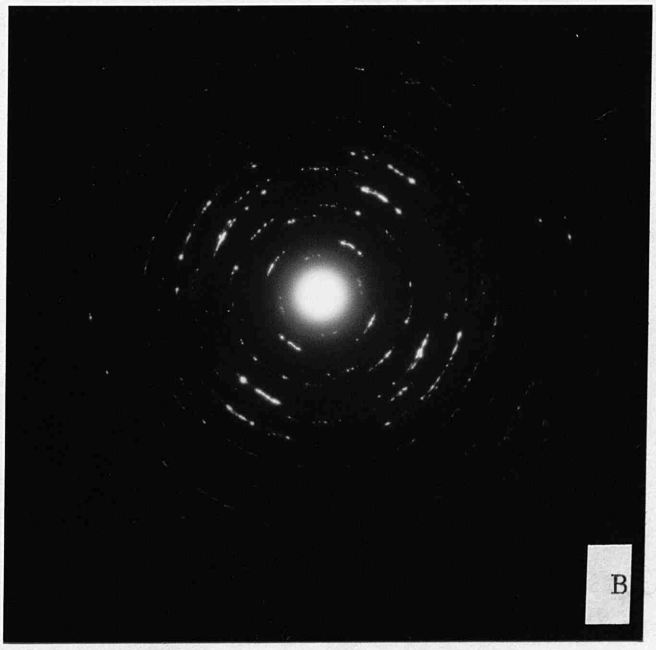
B

PLATE 2 PERYLENE

T_S = -20°C

2A 17800 X

2B 1.3 nmcm

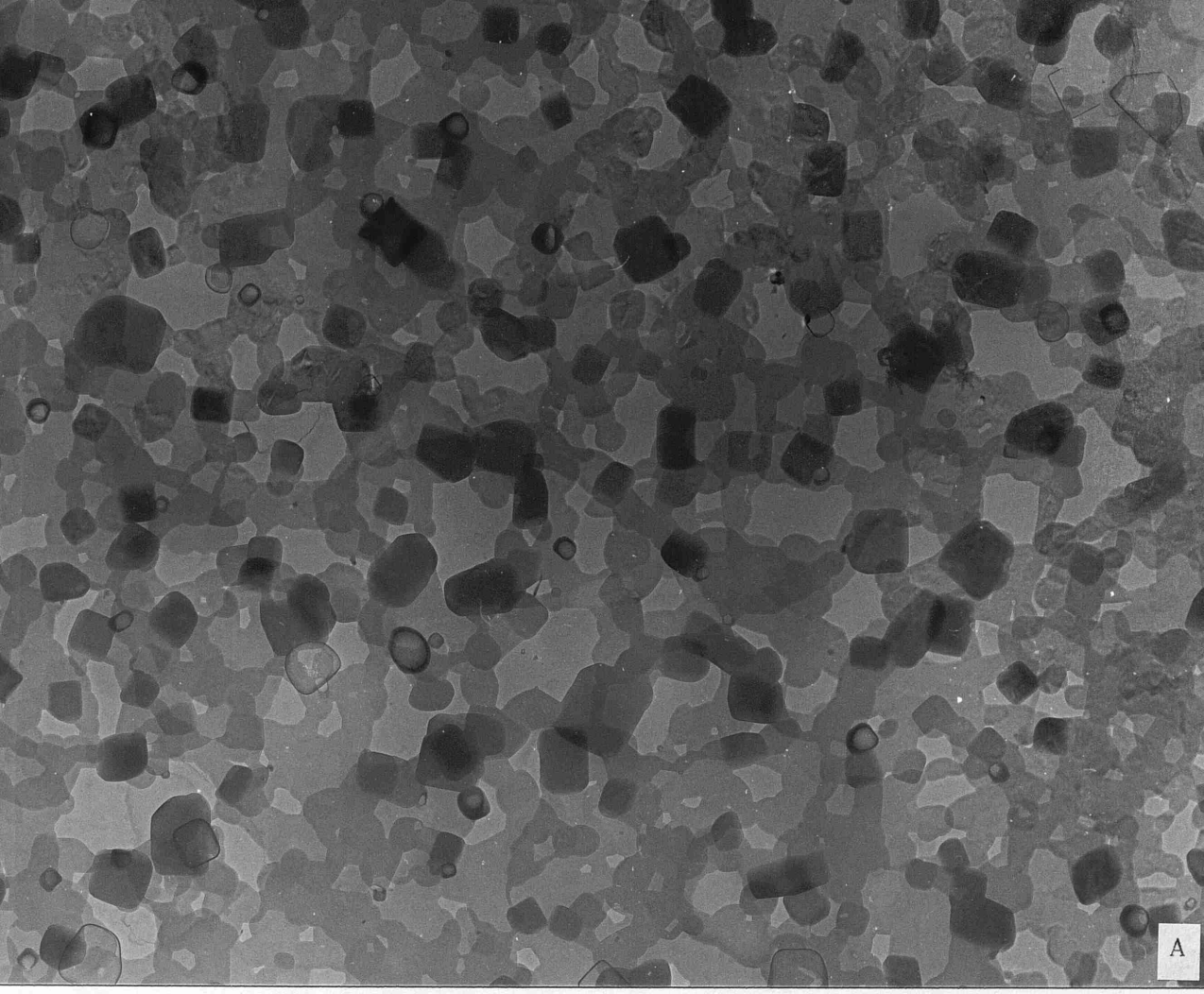
A

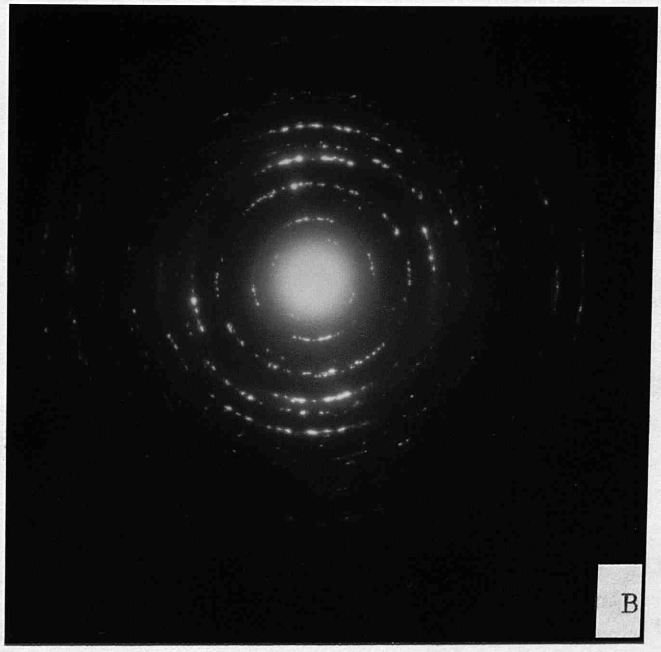
B

also on the deposited perylene, giving two layers. The second layer gives a darker contrast and may be thicker or perhaps aligned differently with respect to the electron beam compared with the lower layer. The diffraction pattern (plate 2b) shows that again the ab (001) face of the perylene is parallel to the substrate. The diffraction pattern is still arced.

	$d_{observed}$	$d_{calc.}$	assignment
plate 2b	1.12	1.11	(100)
	1.05	1.09 nm	(010)

0°C. More perylene was used in this film and the result is a more continuous film (plate 3a). The crystal size and shape is similar to that of the previous films. Many small crystals can be seen on the outside of the larger crystals on the substrate. The diffraction (plate 3b) pattern again shows the ab (001) face parallel to the substrate. It also now shows not only arcing but rings. This is due to the much larger number of crystals giving many more orientations.

	$d_{observed}$	$d_{calc.}$	assignment
plate 3b	1.08	1.09 nm	(010)

20°C. There is a large change in the appearance of the deposited film when the temperature of the

PLATE 3 PERYLENE

T_S = 0°C

3A 17800 X

3B 1.3 nmcm

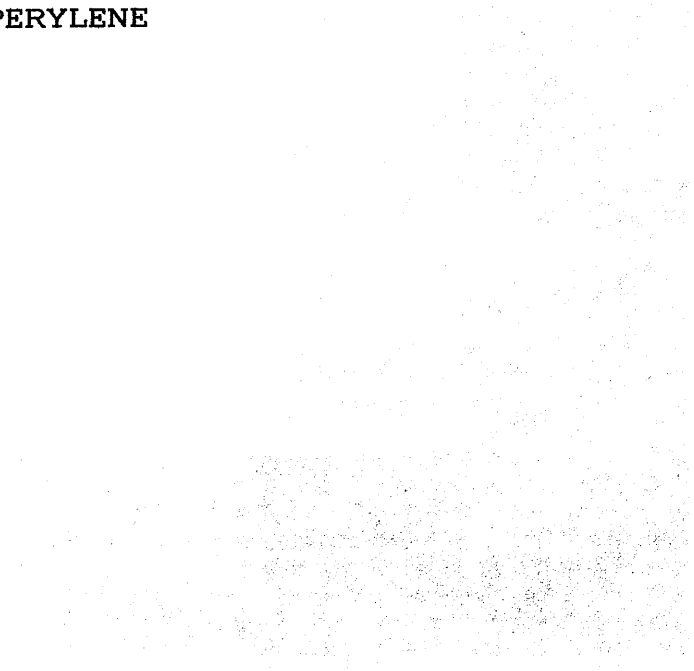

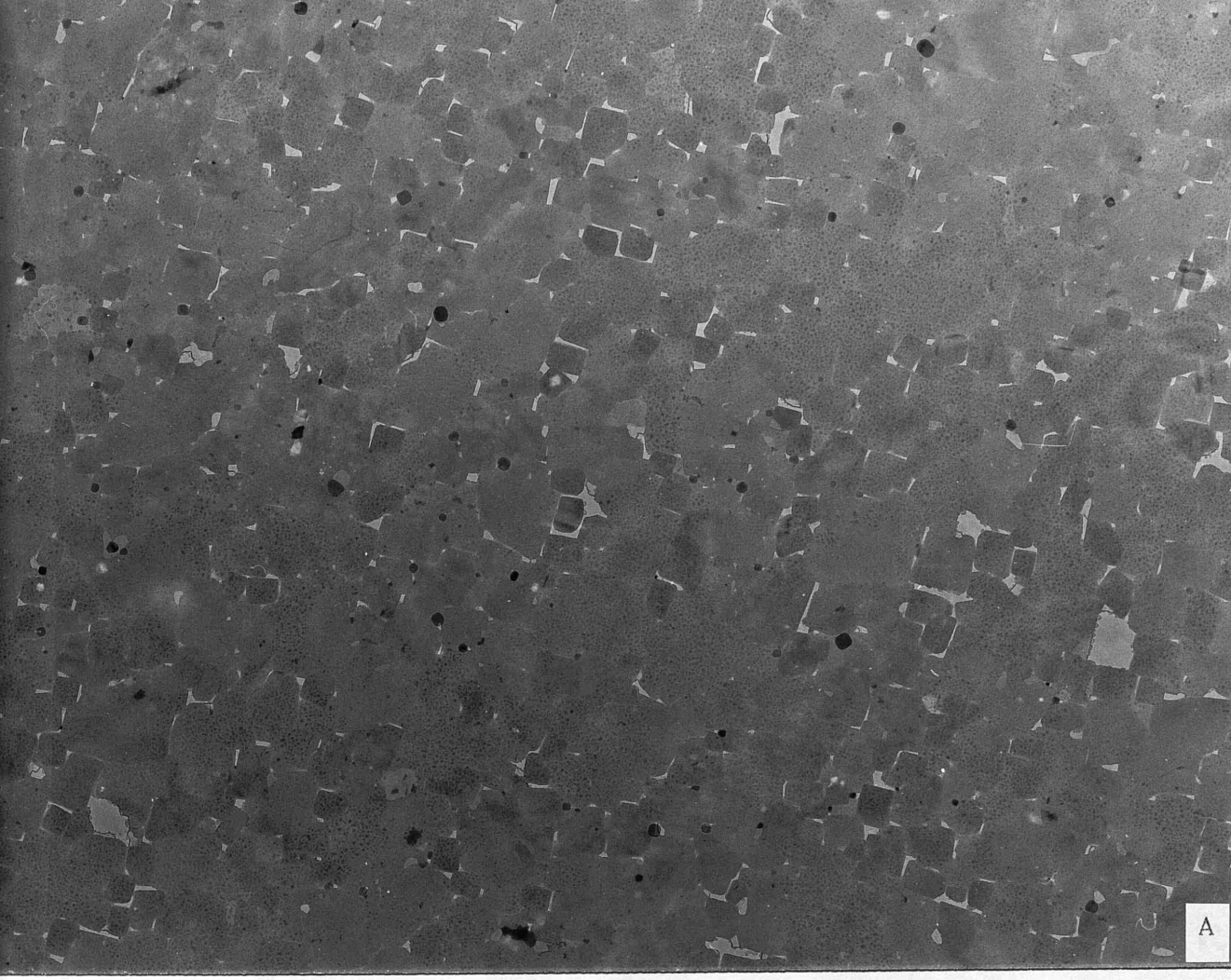
A

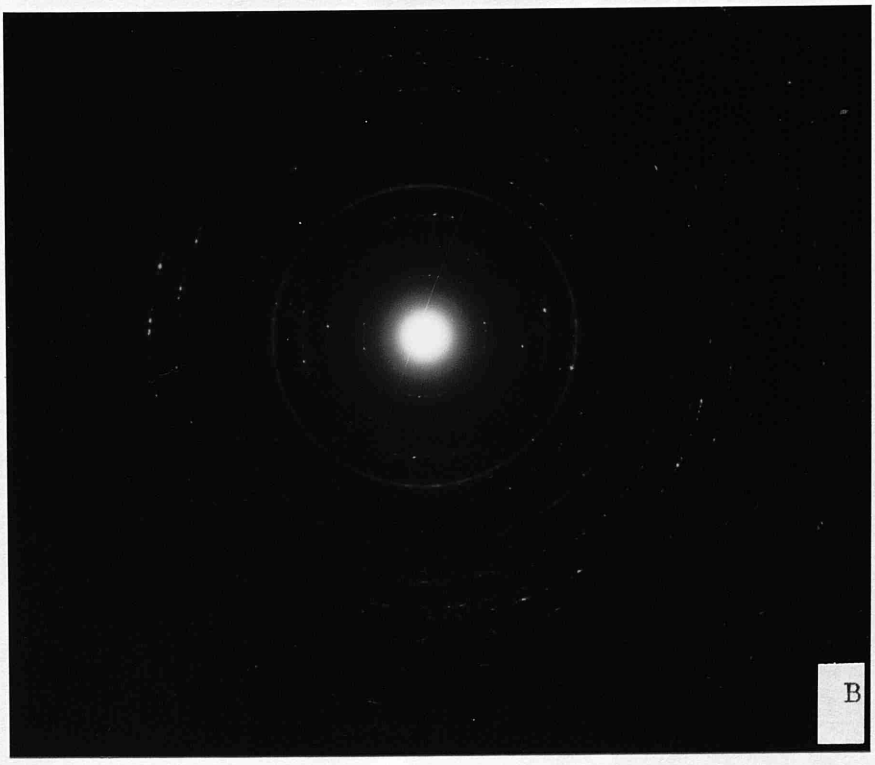
B

PLATE 4 PERYLENE

T_S = 20°C

4A 17800 X

4B 1.6 nmcm

4C 1.6 nmcm

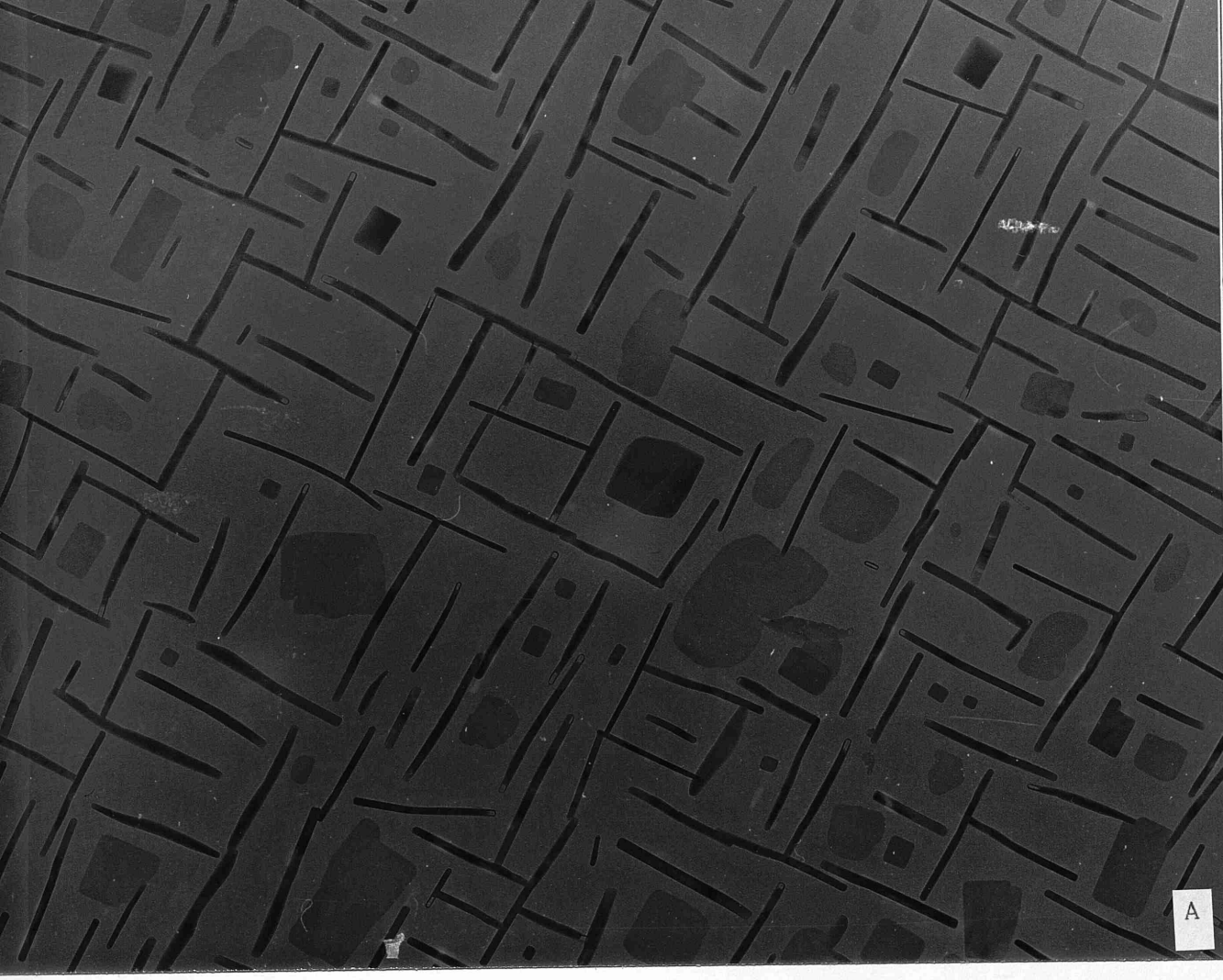
A

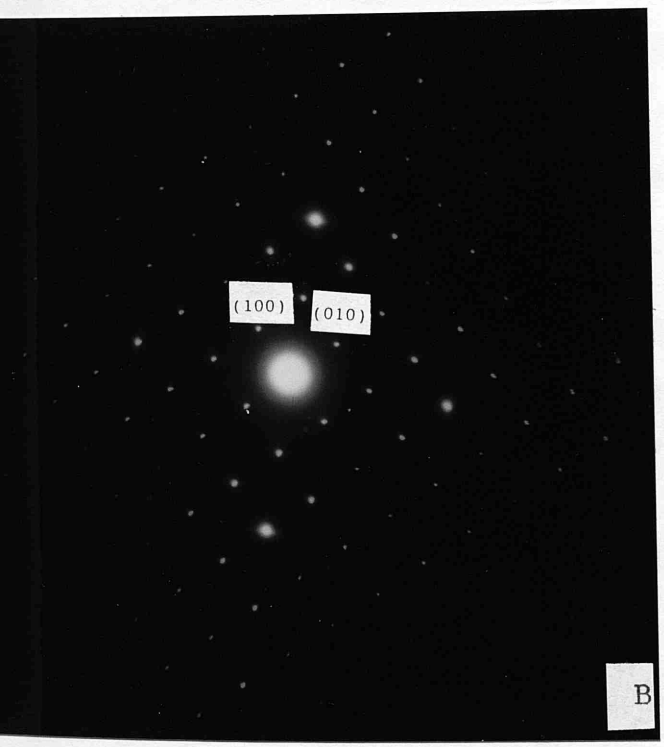
(100)
(010)
B


C

substrate is increased by 20°C. Two crystal types are present (plate 4a) and they may be described as "raft" and "needle" like. The raft like single crystals are of various sizes with their ab (001) faces parallel to the substrate. The diffraction pattern (plate 4b) is that of a single crystal. The needle type crystals also give a single crystal diffraction pattern (plate 4b) but this time it is the (hk0) face that is parallel to the substrate, the (001) face is now perpendicular to the KCl. This diffraction pattern appears only as a line of spots because of the shape of the needles. The needles are arranged in a square fashion reflecting the symmetry of the KCl surface. However the arrangemant of the crystals does deviate slightly from the square pattern suggesting that surface interactions are not strong. Relatively few of the crystals overlap with each other and each crystal occupies a large area of substrate surface.

	$d_{observed}$	$d_{calc.}$	assignment
plate 4b	1.11	1.11	(100)
	1.09	1.09nm	(010)
plate 4c	1.02	1.01	(001)

40°C. Plate 5a. This preparation temperature gave a

PLATE 5 PERYLENE

T_S = 40°C

5A 17800 X

5B 1.2 nmcm

5C 1.2 nmcm

5D 1.2 nmcm

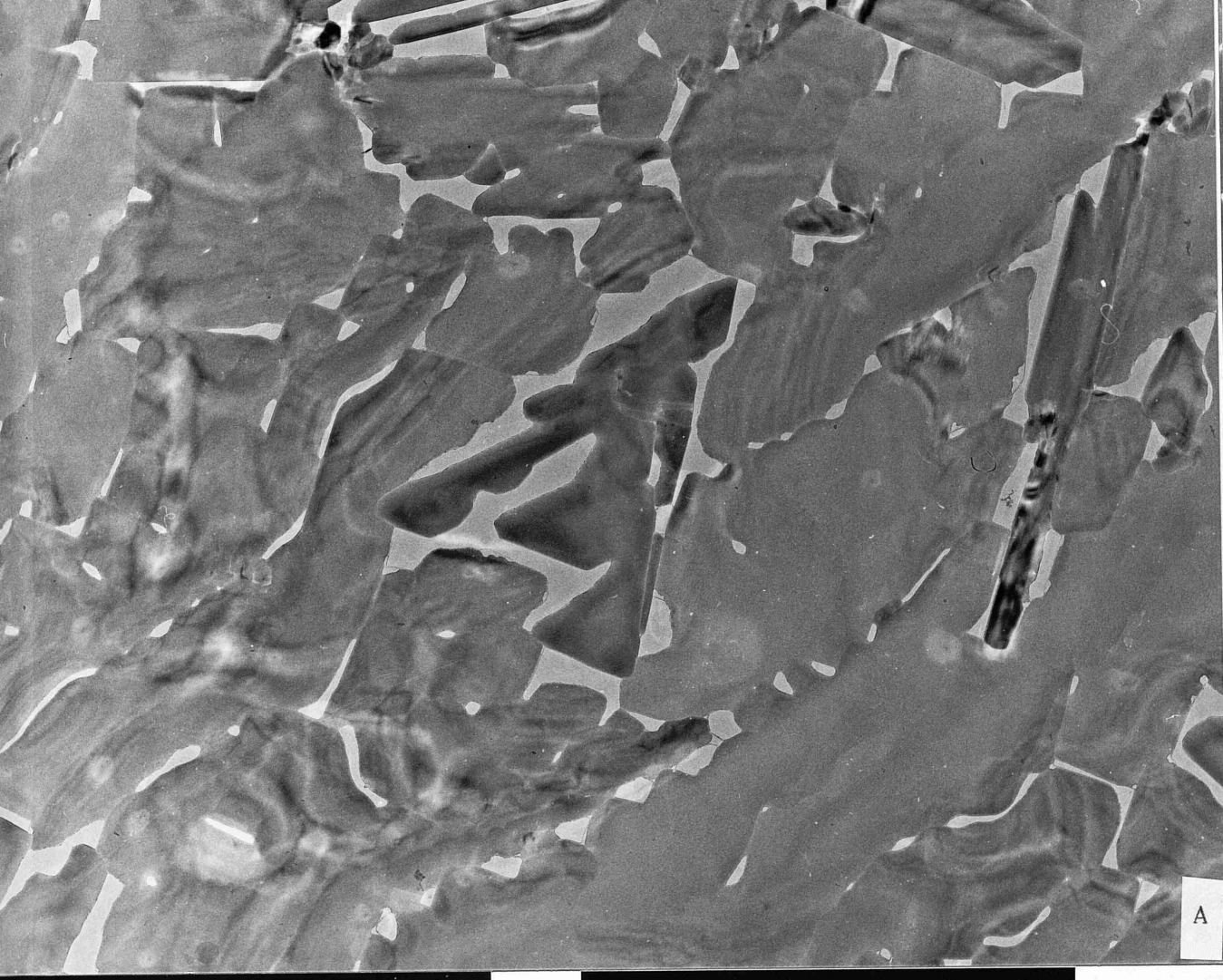
A

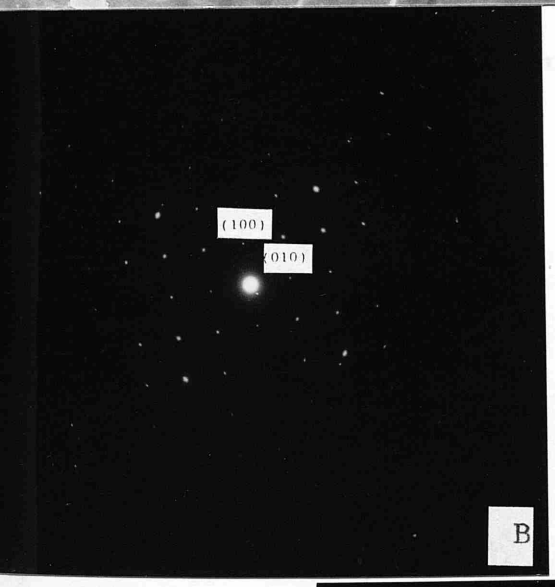
(100)
(010)
B

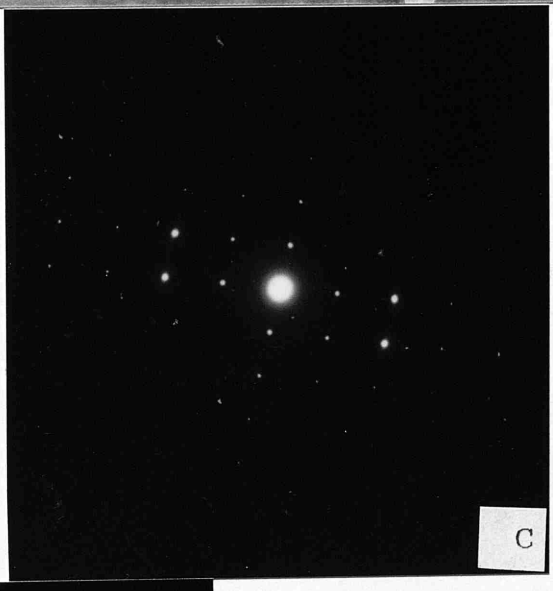
C


D

much more extensive film. The square arrangement can still be seen although the greater substrate coverage makes it less clear, needle like crystals can be seen embedded in the film. There is strain contrast visible since the growth of the large crystals has been constrained by their neighbours. There are three diffraction patterns visible the ab (001) (plate 5b) and the (hk0) (plate 5c) that have been seen before and a new pattern (plate 5d) that can be attributed (as with plate 5b) to a view down onto the ab (001) face. However there are now systematic absenses probably caused by a different zone axis being imaged.

	$d_{observed}$	$d_{calc.}$	assignment
plate 5b	1.11	1.11	(100)
	1.08	1.09	(010)
plate 5c	1.02	1.01	
	.77		
plate 5d	1.08	1.09	
	.37	.37 nm	

60°C. Plate 6a. This is a well arranged film with large square type crystals predominating. The amount of material evaporated was double that of the previous 40°C film but the coverage is similar. Around

PLATE 6 PERYLENE

T_S = 60°C

6A 17800 X

6B 1.2 nmcm

6C 1.2 nmcm

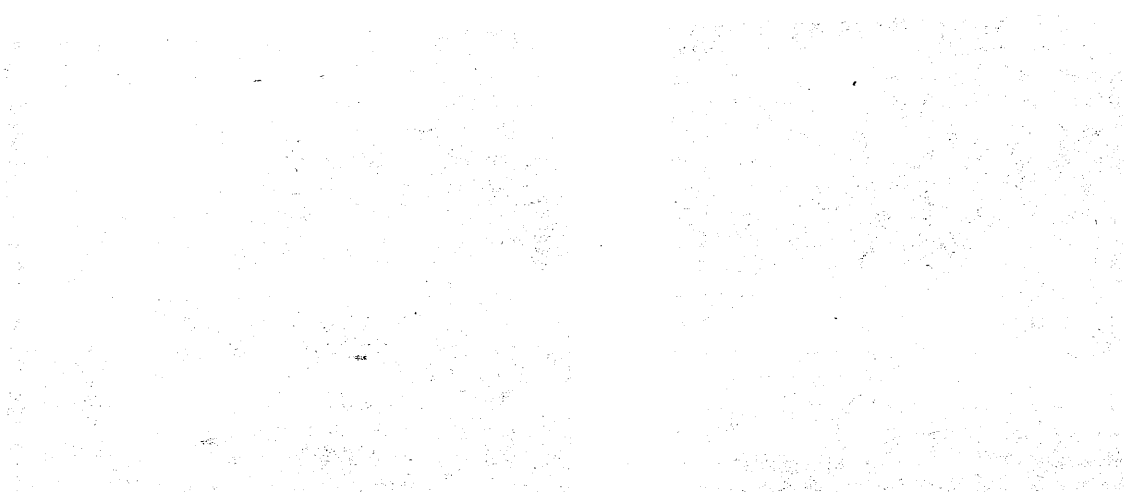

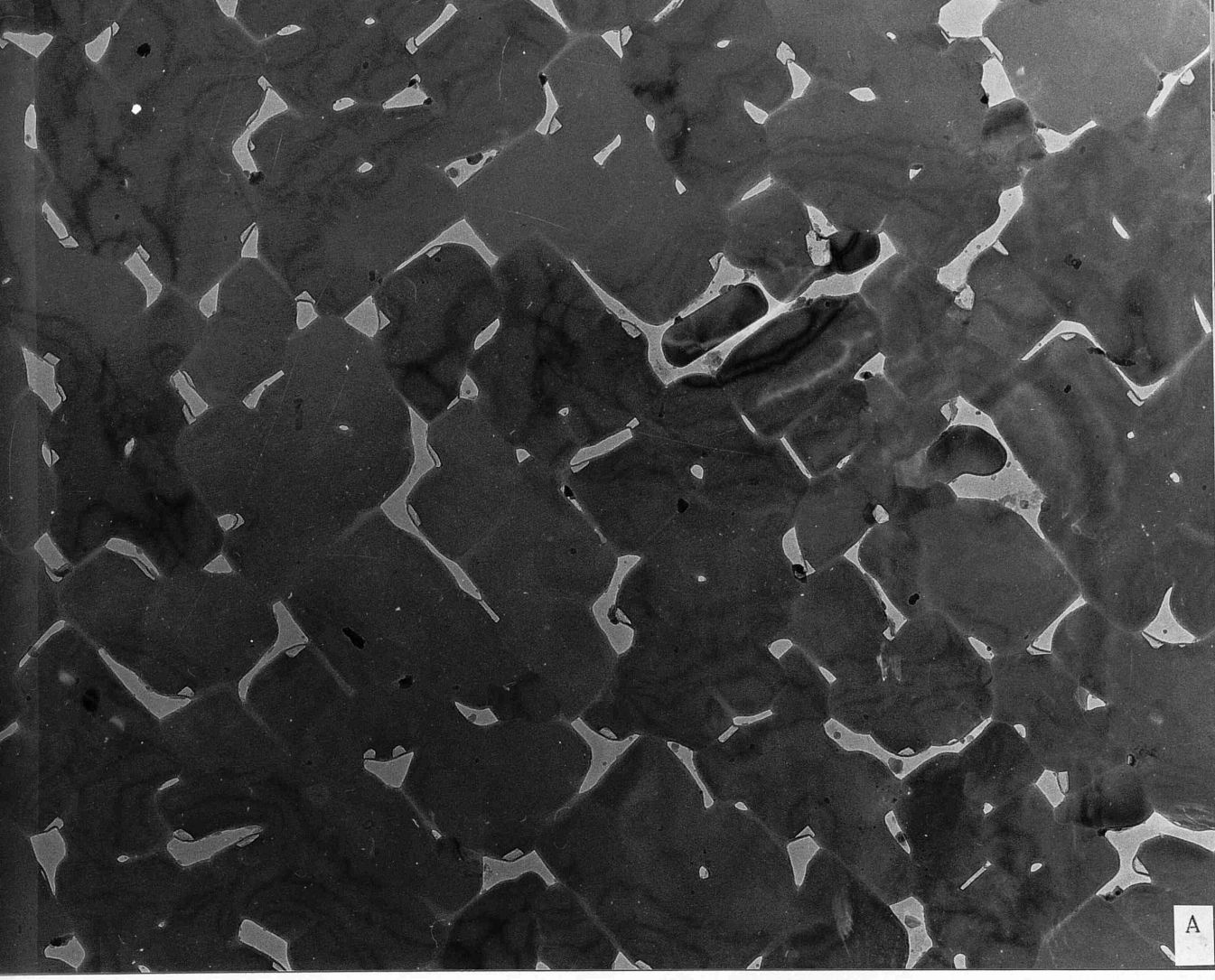
A

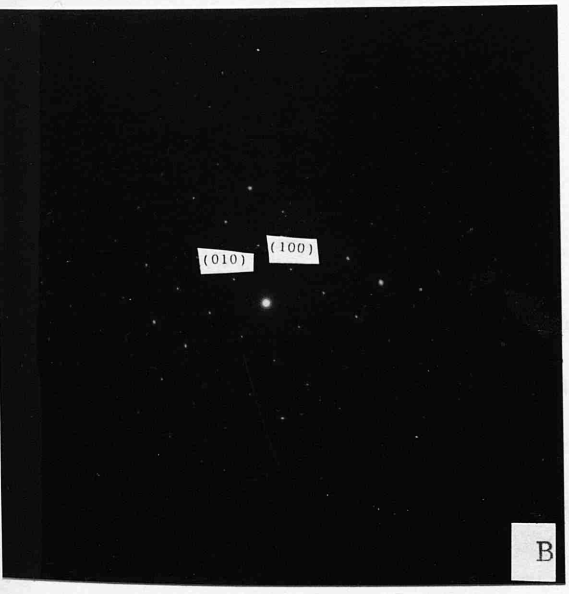
(010)
(100)
B

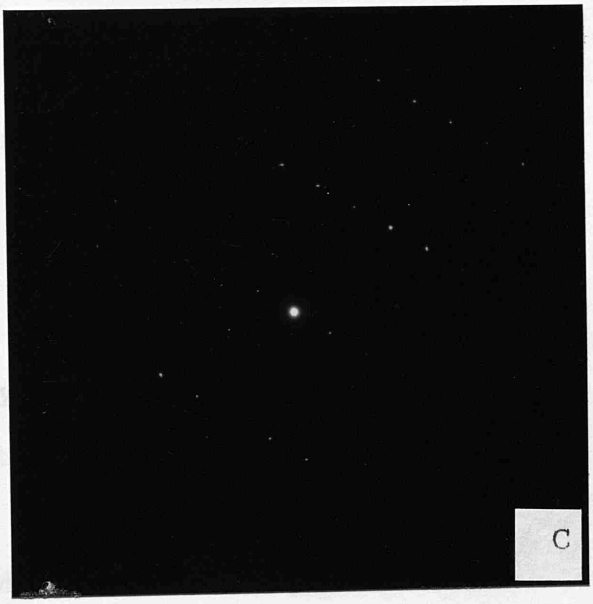
C

the edges of some of the crystals there are dark lines which are not Fresnel fringes. This is probably impurity that has been pushed to the periphery of the growing crystals. Since these lines of impurity can be seen to lie beyond the edges of the crystals it is likely that there has been some re-evaporation from these regions leaving the impurity behind. There is now only diffraction patterns of the ab (001) face visible (plate 6b & 6c). For this reason this film can be regarded as being close to a single crystal film.

	$d_{observed}$	$d_{calc.}$	assignment
plate 6b	1.11	1.11	(100)
	1.09	1.08	(010)
plate 6c	1.09	1.08	
	.37	.37 nm	

80°C. Plate 7a. This is similar to the previous 60°C film in that we have a well aligned, square single crystal film. However the surface coverage is lower than would have been the case if the sticking coefficient was unity. The crystals are large and there are large spaces between them. The lines of deposited impurity caused by re-evaporation are very evident but the area bounded by such impurity lines

PLATE 7

T_S = 80°C PERYLENE

7A 17800 X

7B 1.2 nmcm

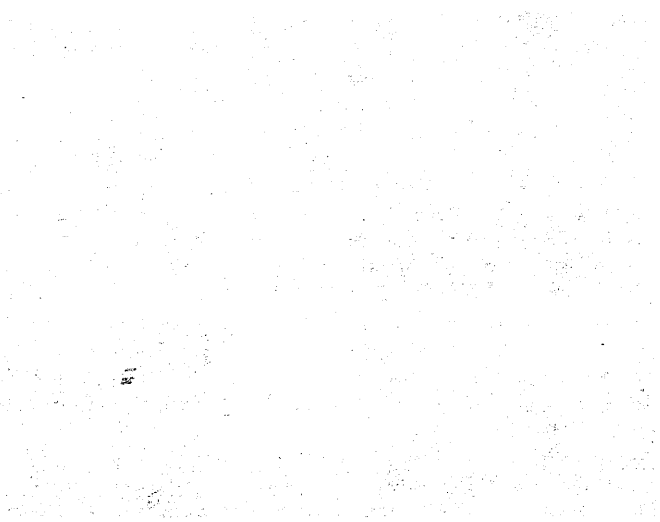

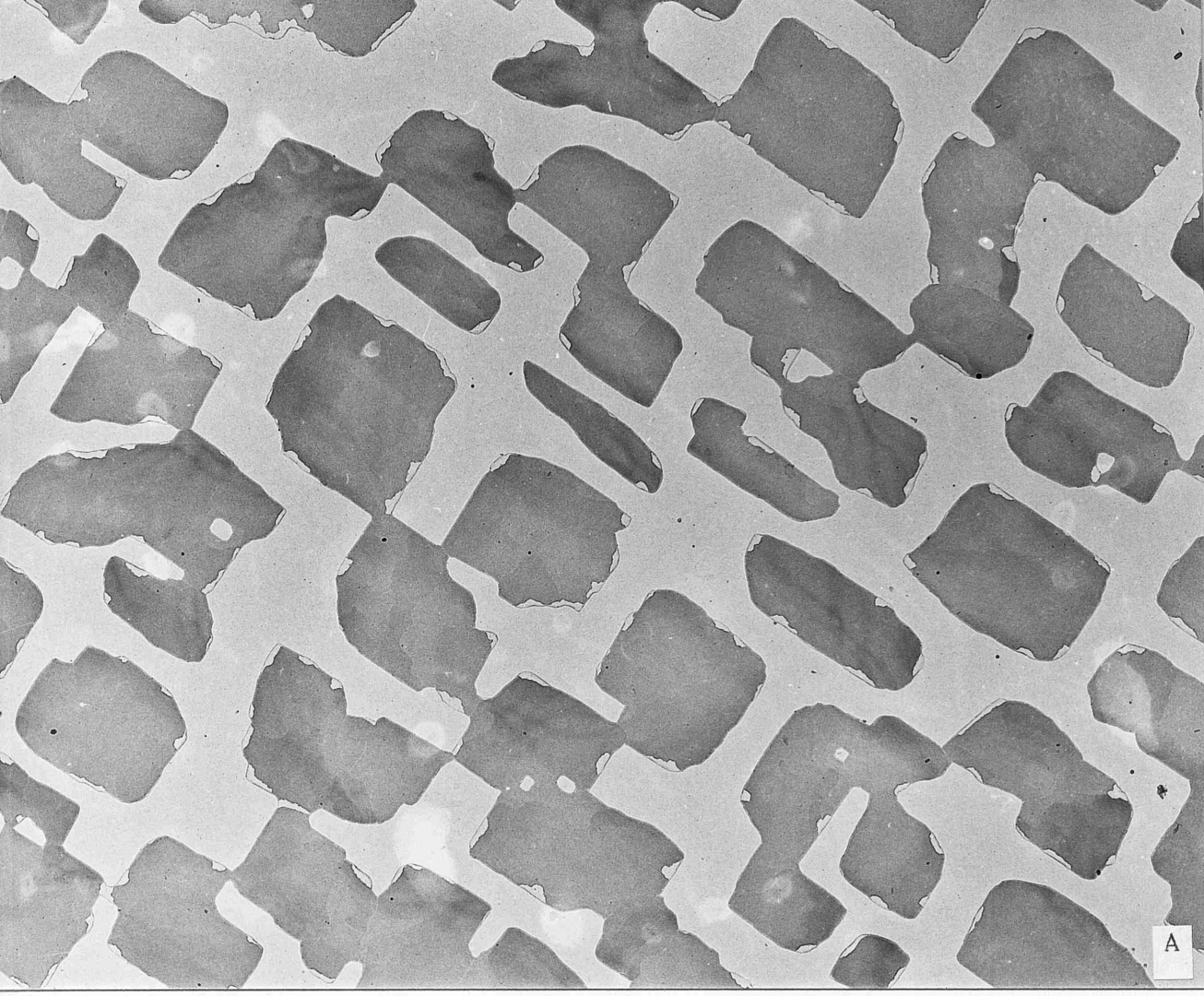
A

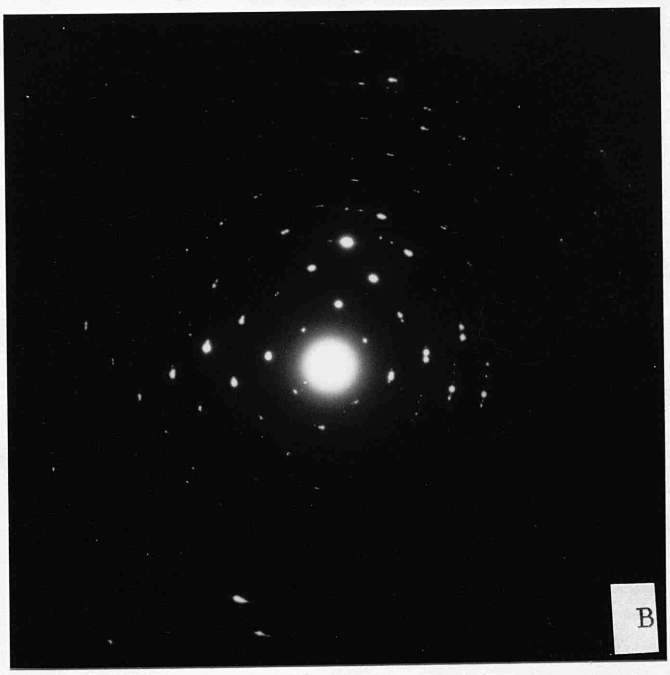
B

is small suggesting that the major loss of perylene from the surface occurs before nucleation. There is now only one ab (100) diffraction pattern visible (plate 7b).

	$d_{observed}$	$d_{calc.}$	assignment
plate 7b	1.09	1.11	(100)
	1.06	1.08 nm	(010)

100°C. An experiment was carried out at this temperature but no perylene was deposited on the substrate.

6.2 Quaterrylene Thin Films Results

20°C This low temperature film (plate 8) was made up of tiny irregularly shaped crystallites with a diameter of approximately $4x10^{-7}$ m. No diffraction pattern could be obtained.

60°C (plate 9). This film is composed of small round crystallites of $6x10^{-7}$ m in diameter. There is some aggregation of the crystallites. No diifraction pattern could be obtained.

PLATE 8 QUATERRYLENE

T_S = 20°C

8A 17800 X

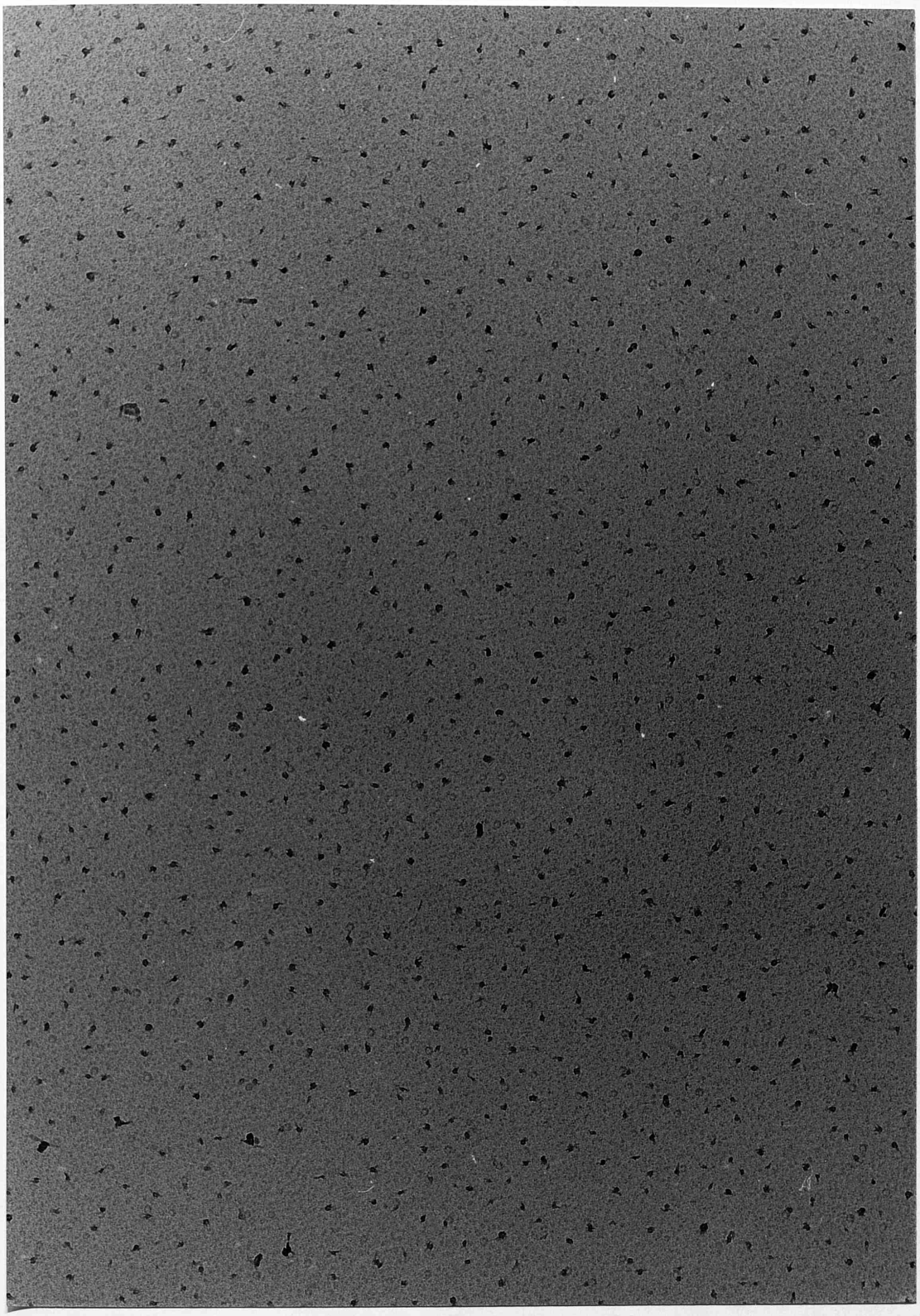

PLATE 9

T_S = 60°C

9A 17800 X

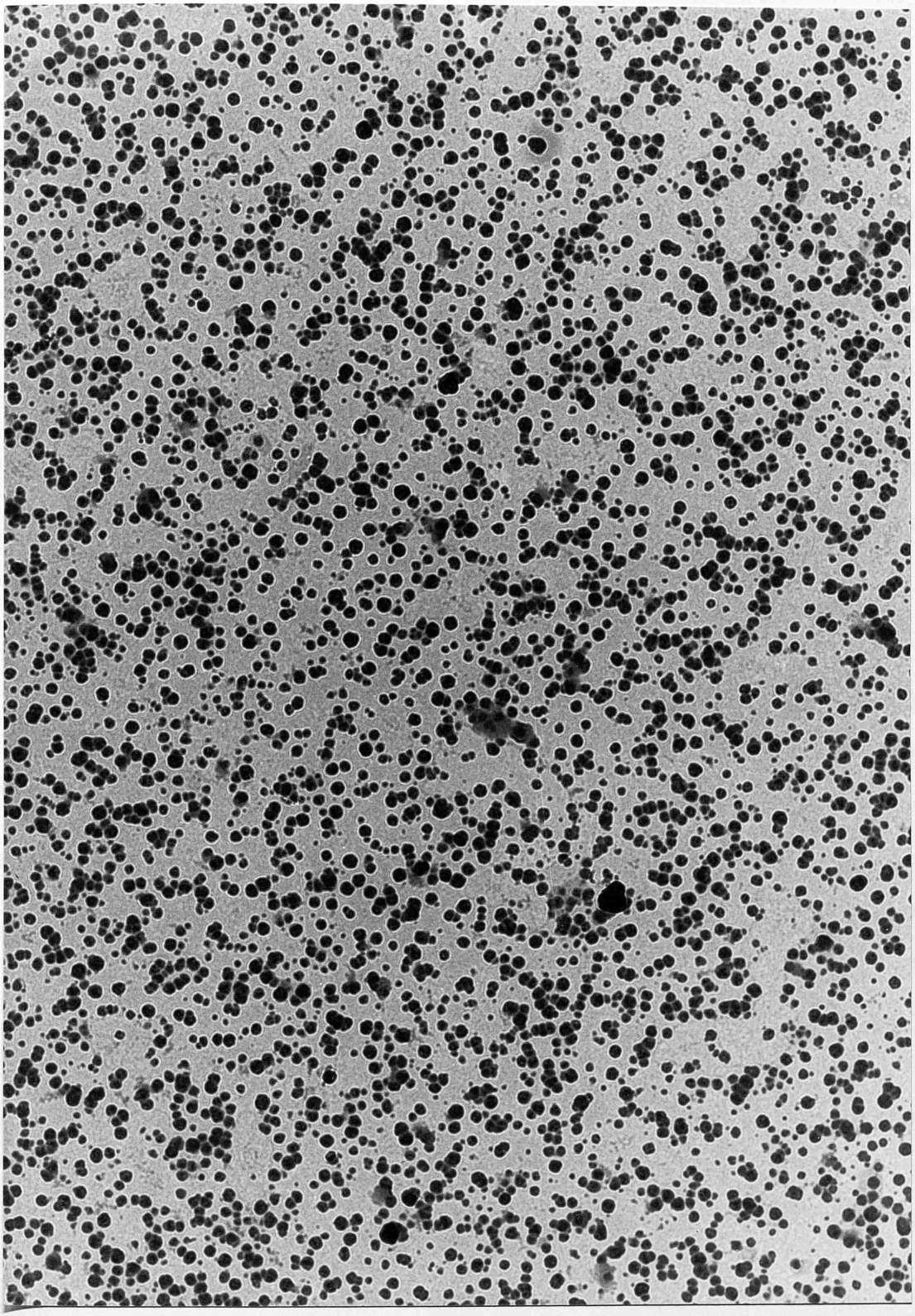

200°C (plate 10a). The temperature was increased dramatically to 200°C since the films at lower temperatures were not showing signs of improvement. There is good coverage of the substrate but the substrate does not seem to be imposing any order on the film. The lower film is covered with islands of larger thicker crystals. The diffraction pattern (plate 10b) is arced, showing that the film is only partially crystalline and still quite disordered.

255°C (plate 11a). The film consists of areas of lower contrast in which the ordering of the KCl substrate is evident and "islands" of greater contrast. The film is of a very high crystallinity. Medium resolution (plate 11b) shows large areas where the lattices are continuous, they measure 0.64 nm probably the (200) spacing. Crystalline diffraction patterns are also seen (plates 11c, 11d & 11e).
Plate 11c and 11e appear to consist of two patterns superimposed upon one another, and may indicate an over growth of one layer of quaterrylene upon another.

PLATE 10 QUATERRYLENE

T_S = 200°C

10A 17800 X

10B 2.3 nmcm

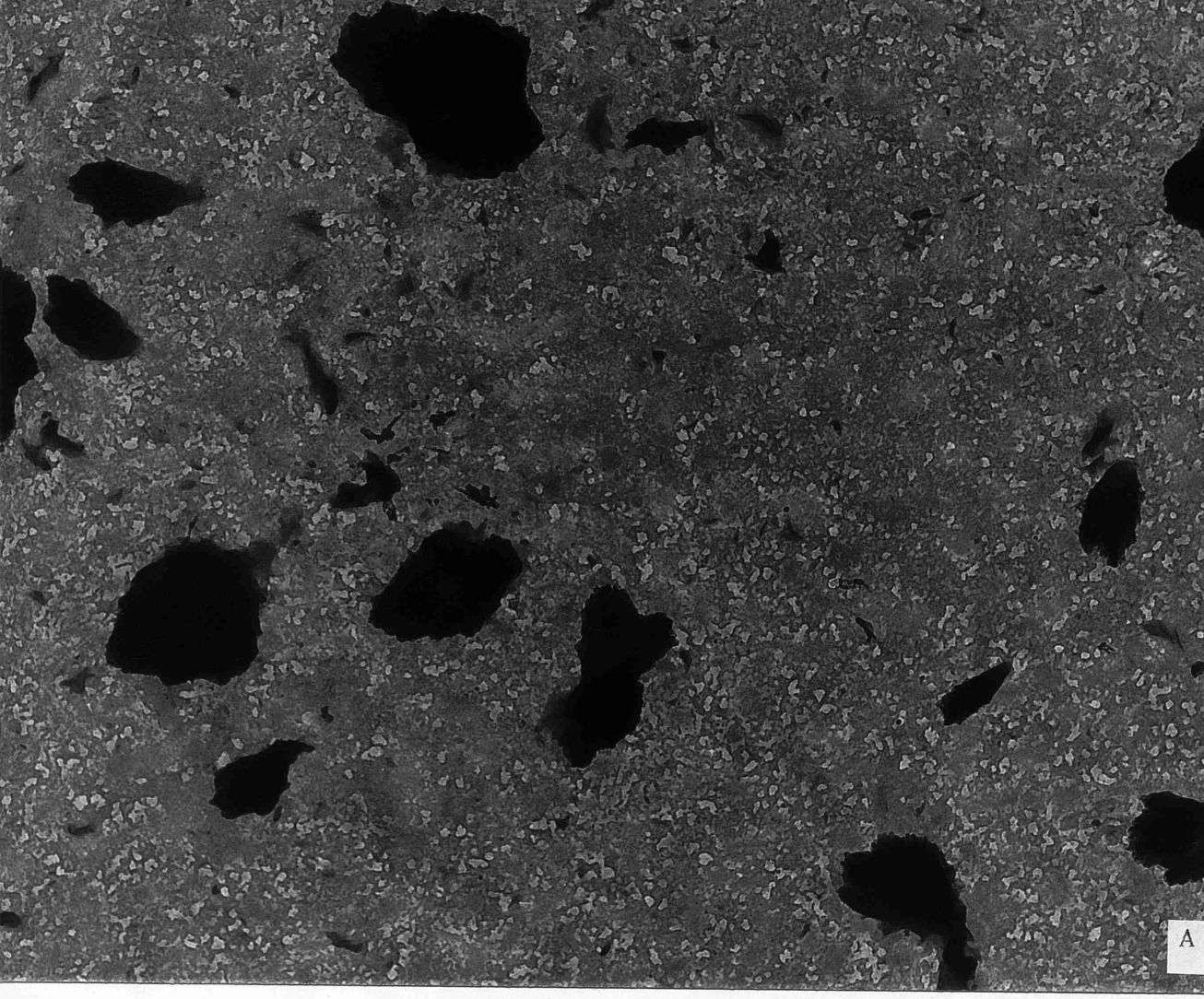
A

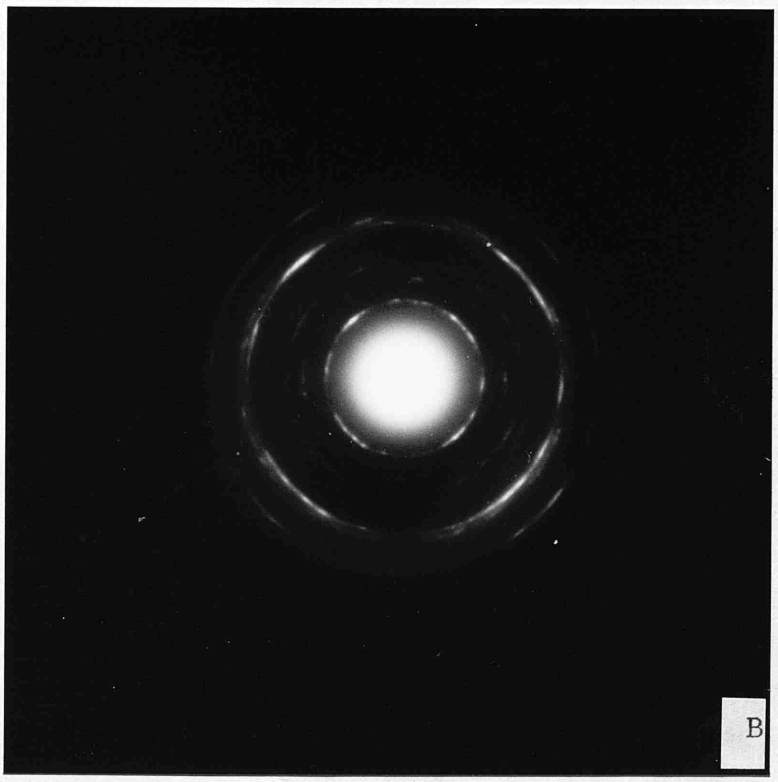
B

PLATE 11 QUATERRYLENE

T_S = 255°C

11A 17800 X

11B 781250 X

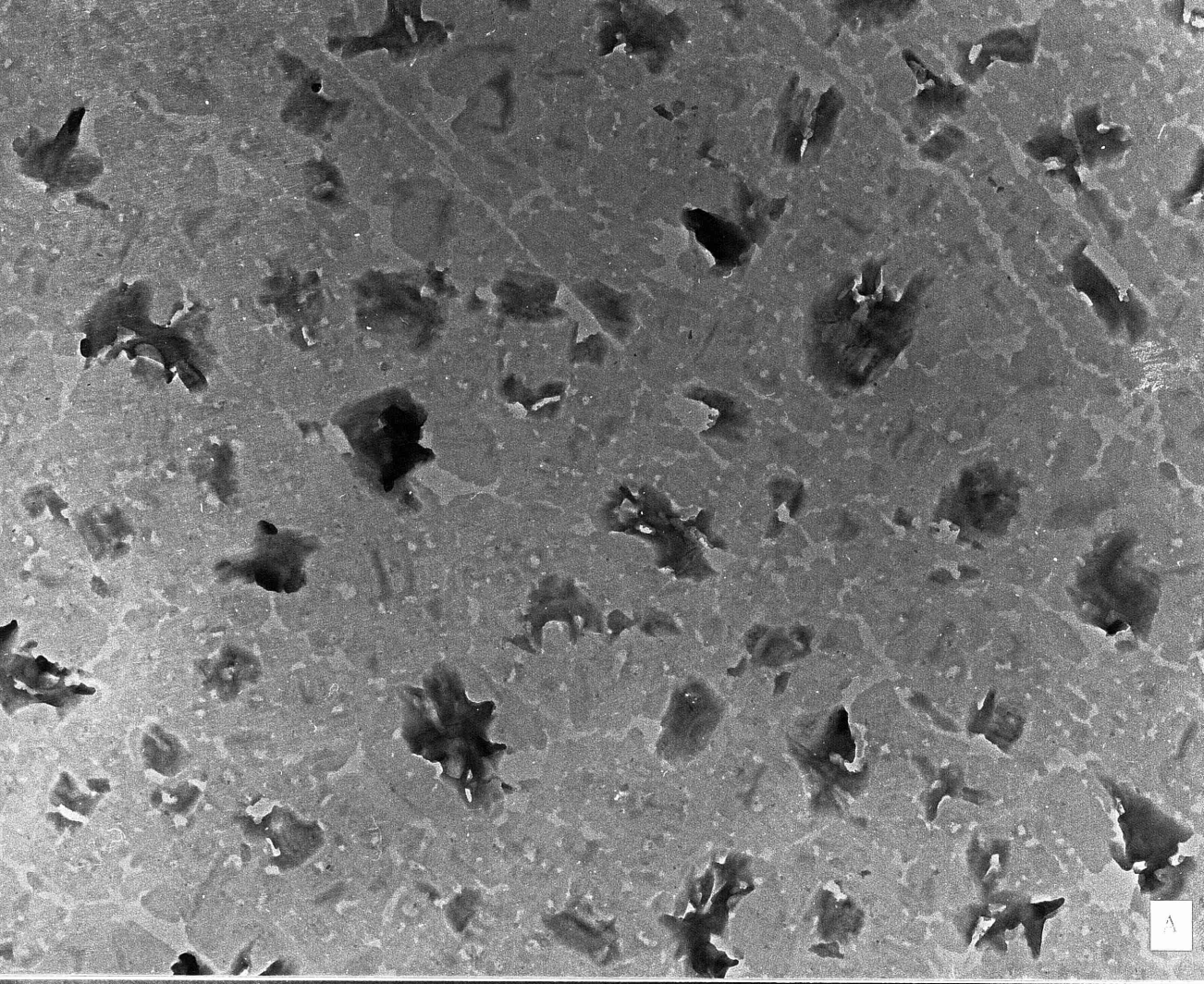
A


B

PLATE 11 QUATERRYLENE

T_S = 255°C

11C 1.5 nmcm

11D 1.5 nmcm

11E 1.5 nmcm

11F 740555 X


C


D


E

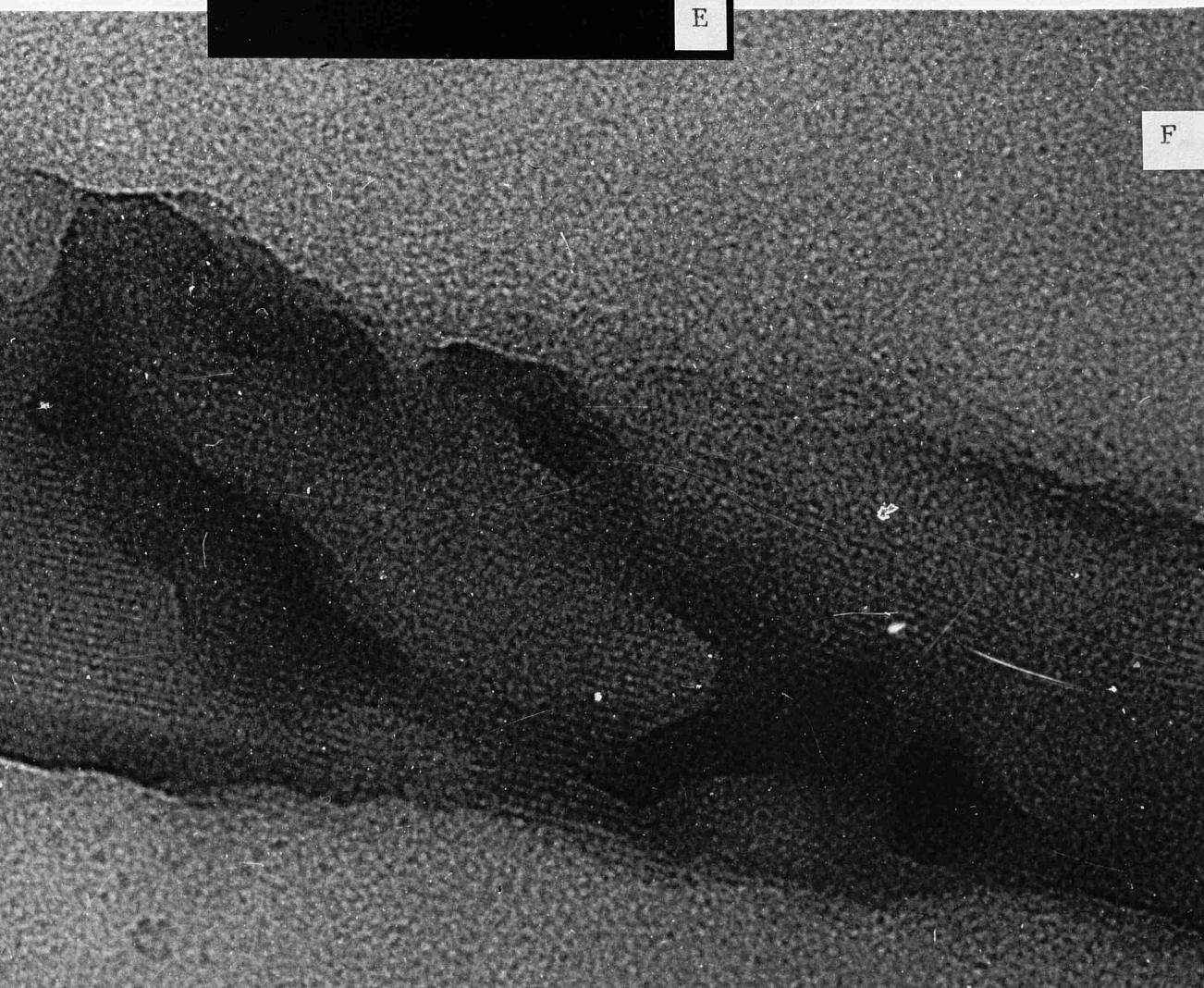
F

PLATE 12 QUATERRYLENE

T_S = 255°C

12A Unfiltered Image

12B Power Spectrum

12C Filtered Averaged Image

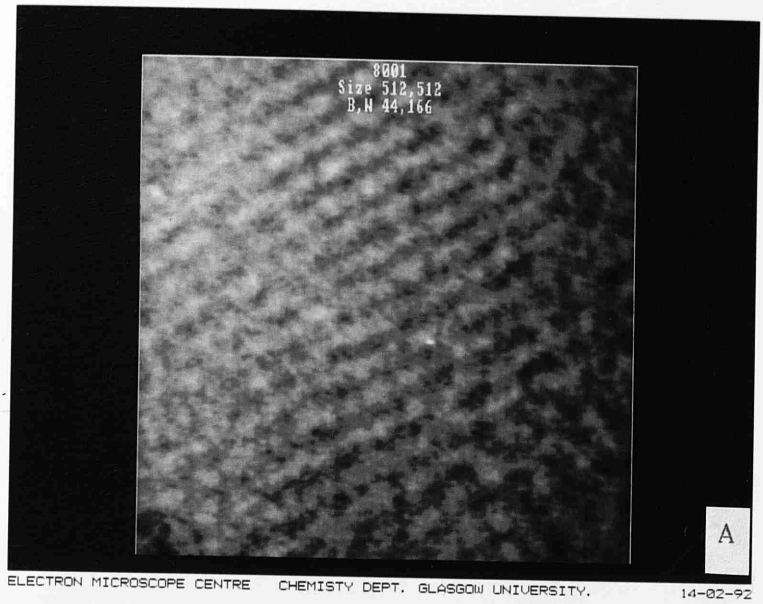

ELECTRON MICROSCOPE CENTRE CHEMISTY DEPT. GLASGOW UNIVERSITY. 14-02-92

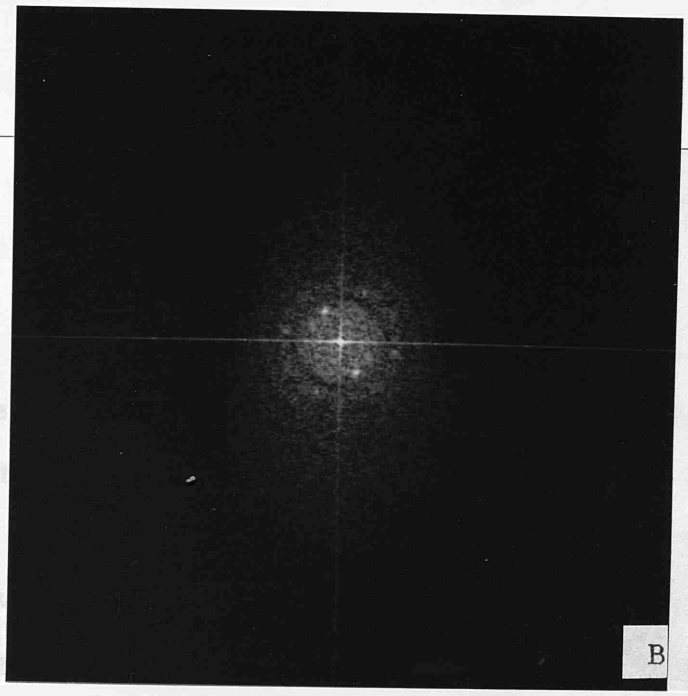

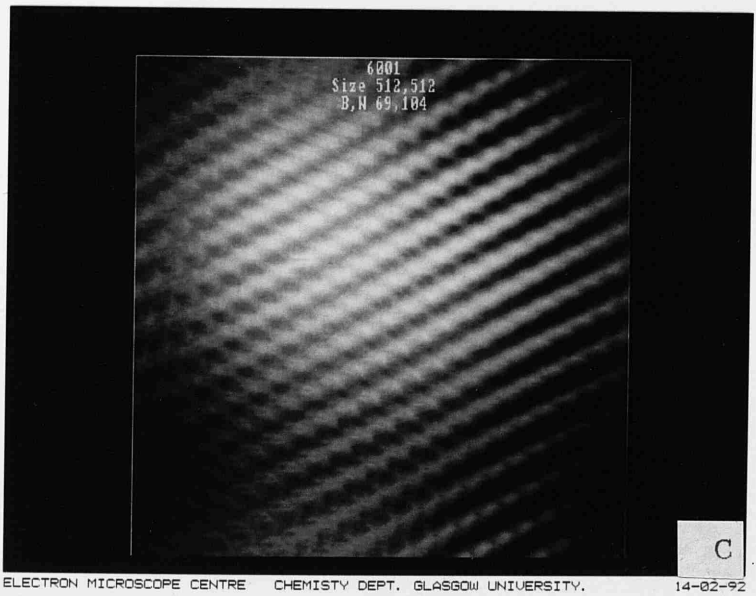

ELECTRON MICROSCOPE CENTRE CHEMISTY DEPT. GLASGOW UNIVERSITY. 14-02-92

	$d_{observed}$	d_{calc}	assignment
plate 11c	1.93	1.89	(001)
	1.45		
plate 11d	1.18	1.09	(100)
	1.02	1.06	(010)
plate 11e	1.93	1.9	
	1.48		
	0.39	0.37 nm	

The islands present a different crystal face to the electron beam (plate 11e) and crossed lattices 1.8 nm x 1.1 nm are seen. The corresponding diffraction pattern is shown (plate 11c). The high resolution micrograph was image processed using the SEMPER VI system (Plate 12a). The power spectrum shows the same maxima as the small angle spacings in plate 11e. It does not show any other spacings, probably because of the small area of lattice images that can be chosen to be filtered. The final filtered image is shown in plate 12c.

6.3 Perylene Thin Films Discussion

Many things may affect the properties of a thin film deposited by PVD. Most important are the nature of the substrate and the temperature of this substrate (T_S). The aim of this study with perylene and KCl was to investigate how the deposited perylene thin films would be affected by a gradual increase in substrate temperature, and to find the conditions for the deposition of a single crystal film.

The effect of increasing the substrate temperature is clearly shown in plates 1-7. In every case only α-perylene was observed. There is no evidence that the β-perylene modification at any temperature.

The most easily noticeable thing about the films deposited at lower temperatures is the small size of the crystals and their great number. This is caused by the large number of nucleation points. The low temperatures allow much of the evaporated perylene to be adsorbed and for nucleation and growth of crystals to take place even at relatively unfavourable sites on the substrate. However crystals are not only growing on the substrate they are also growing on the surface of deposited perylene. This is observed at temperatures of 0°C and below. This second layer of perylene adopts different

orientation from the material on the KCl as can be seen from the darker contrast of these crystals. At -40 and -20°C deposition onto perylene would appear to be favourable since the crystals in this second layer are large and there are many gaps on the KCl surface. At 0°C growth on the perylene is less favoured since there are few gaps in the film and the crystals that are growing on the perylene are very small. Once the substrate temperature is raised further growth only occurs on the KCl. This reflects the strong interaction of the perylene with the KCl. Diffraction confirms that there is a favourable interaction between the ab (001) face of the α-perylene unit cell and the KCl surface, the ab orientation parallel to surface is observed at all temperatures. This is the only orientation stable enough to be deposited at 80°C when other orientations which are present when T_S is lower are no longer deposited. The ab face of perylene and the KCl surface both have a square symmetry which although of different dimensions will aid adhesion.

The diffraction patterns of films deposited at 0°C or less show arcing of the spots. This is caused by slight misalignment of the crystals, which still have their ab face parallel to the substrate but the crystals are rotated relative to each other. At 0°C as well as arcing

there are rings. These rings are probably caused by the very small crystallites growing on the perylene surfaces which have many different orientations.

An increase in temperature to 20°C causes a large change in the appearance of the film. Two morphologies are seen and they are arranged in a square array. There are some small deviations from this symmetry suggesting that alternative fits are possible. The needles which give a single order diffraction pattern (plate 4c) do not overlap with other crystals, this suggests that their growth is along the long axis. At higher temperatures the full diffraction pattern from this type of crystal is observed (plate 5c). It is likely that at 20°C the growing needles did not posses enough energy to overcome a boundary to their growth in that direction. That boundary could be due to impurities, substrate misfit, or it may be that migration of an adsorbed molecule is easiest along that axis of the crystal.

40°C appears to be near the optimum temperature for crystalline film growth. At this temperature there is good coverage of the substrate and the crystals formed are large. The crystals have grown together leaving small holes between themselves, and where they meet there is the appearance of a grain boundary rather than

two fused crystals. The appearance of strain contrast is due to the size of these crystals. The strain contrast probably accounts for the appearance of a new diffraction pattern (plate 5d) though this pattern is still consistent with the ab face of the perylene being parallel to the substrate.

Films deposited at 60 and 80°C are of very regular size and shape. There are now no diffraction patterns for any orientations other than ab face parallel. This is therefore the most stable orientation. There is evidence of re-evaporation with lines of impurities bounding the crystals. This might suggest that impurities will restrict the size of crystal that can be grown by evaporation onto a substrate. The need for very pure evaporant and a very clean substrate surface is clear.

The optimum temperature (T_o) for a single crystal film of perylene is probably between 40 and 60°C. Vincett et al (1977) reported that T_o for smooth films of anthracene, pyrene and phthalocyanine was approximately one third of the boiling point. The smoothness was assessed by scanning electron microscopy and took no account of crystallinity of the film. For perylene (b.p. 350-400°C) this would give a temperature of around -50°C for a smooth film. There is a dominant interaction at -40°C, the ab face being parallel to the substrate suggesting that the

one third boiling point guide could be applied to this system. But to make a crystalline film $T_S \approx$ 50°C or half the boiling point is required. Often films are grown at room temperature and then annealed to improve the crystallinity of the film. A general observation is that a temperature of greater than half the melting point is required. 50°C is equal to 60% of the melting point of perylene, suggesting that a process similar to annealing is occurring.

6.4 Quaterrylene Film Growth Discussion

Increasing the substrate temperature clearly improved the crystallininty of the evaporated quaterrylene thin films. At the lower substrate temperatures the films were composed of tiny crystallites and gave no clear diffraction pattern. This suggests that the films were amorphous. With the large increase in T_S to 200°C the film became partially crystalline, and then with a relatively small increase in T_S to 255°C a crystalline film with large domain size was produced. A similar effect was seen in the perylene films where an increase of 20°C changed the film from polycrystalline to one composed of many epitaxially orientated crystals.

There are three different orientations in the crystalline film that are observed by electron diffraction. The observed diffraction patterns correspond to the known crystal structure of quaterrylene (Kerr et al 1975) in

some spacings. Plate 11d matches fairly well with the known ab face of quaterrylene. With this face parallel to the substrate the long quaterrylene molecules are standing upright on the KCl surface. This is the orientation that is observed over the largest area of the film and is consistent with the previous PVD studies on large planar aromatic molecules (Inokuchi et al 1961), which also show that the molecular axis will lie perpendicular to the substrate. Occasionally observed was the pattern shown in plate 11e. These spacings cannot be attributed to the known structure of quaterrylene since the long axis is only 1.48 nm long. It is likely that the substrate is having an effect on this structure. Closer examination of plate 11e shows two spots corresponding to 1.93 nm. This spacing occurs again in the diffraction pattern shown in plate 11c. This again is not easily ascribed to the known crystal structure. This pattern was only observed superimposed on top of the pattern in plate 11e. It is likely that this structure is an epitaxial layer that will only form on top of the domain in plate 11e.

Lattice images were observed in both domains. The specimen tilt stage was not used so only some orientations were correctly aligned. 0.64 nm lattices are seen, this is a view down on the ab face. However the (200) lattice planes are viewed, because of the orientation. There

were 1.9 nm and 1.16 nm lattices visible in the "island" areas these are the (001) and the (101) spacings respectively. The underlying quaterrylene layer does not appear to contribute to the image, it will however contribute to the background noise.

CHAPTER 7: SYNTHESIS OF SUBSTITUTED PHTHALOCYANINES

7.1 Experimental Aims

The aim of this work was to prepare a range of different phthalocyanine liquid crystals for study in the electron microscope. The phthalocyanines that were produced were all peripherally substitued with the dodecyloxy moiety. It was hoped to produce two polymeric compounds containing the phthalocyanine unit. One a spinal columnar phthalocyanine siloxane polymer and the other having the phthalocyanine as part of the polymer main chain. Octadodecloxyphthalocyanine and its copper complex have both been prepared previously Simon et al (1987), but no electron microscopy of phthalocyanine liquid crystals has been carried out.

The metal free octadodecloxyphthalocyanine was first prepared by a method that involved first the alkylation of catechol and then the bromination of the aromatic ring. In this preparation the catechol was dibrominated and then alkylated, therafter the method was the same as Simon et al (1987). The yield of phthalocyanine from the diimino-isoindoline is very low. No attempt was made to optimise this yield as only small quantities were required for electron microscopy.

The copper octadodecloxyphthalocyanine can be made by several different routes. The one that was chosen here is the tetramisation of the dibromo-didodecyloxy benzene in the presense of a large excess of cuprous cyanide. Unfortunately this led to problems in the purification of the product, since this copper

phthalocyanine could not be purified by chromatography on silica gel. Finally gel permeation chromatography was used. An alternative route would have been to prepare the metal free phthalocyanine and then to insert the copper by the use of a strong base. This would have given a quantitative yield and few purification problems. This route was not used because of the small quantities of metal free phthalocyanine available.

The route to the silicon dihydroxy phthalocyanine is given by Sauer and Wegner (1989) and this was followed quite closely. Again the yields of the phthalocyanine products are low. The polymerisation of the dihydroxy-octadodecloxymethylphthalocyanine has been reported by Simon et al (1988). The corresponding octadodecloxyphthalocyanine has not been reported as a siloxane polymer. In fact the siloxane prepared by Simon was an oligomer with only 20% of the product containing more than three phthalocyanine units. Seperation of the oligamers according to molecular size is possible by gel permeation chromatography. In this study the oligomerisation is monitered by U.V./vis. spectroscopy, but no determination of chain length could be made.

The attempt to incorporate the octadodecloxyphthalocyanine into the main chain of a polymer was unsuccessful. It was hoped incorporate one diimino-isoindoline group with functionalised side arms into a phthalocyanine with three of the ordinary side arm indolines. The hydroxyl groups at the end of the chains would then have been used to form a polyester. The functiona-

lised side arms were prepared by a series of well known reactions (Whiting et al 1983). The reasons for the failure of this synthesis were the difficulty in substitution of the aromatically bonded bromine by nitriles, and the separation of the final phthalocyanine products from the reaction mixture. The failure of the aromatic substitution was unexpected since a similar reaction had been successful for the didodecylphthalonitrile. A reason may be the cuprous cyanide which should probably have been stored in an inert atmosphere. Another possible explanation is that there was hydrogen bonding between the first nitrile to be added to the ring and the hydroxyls on the chains, thus giving some degree of hindrance to further substitution on the ring. It was anticipated that purification of the reaction mixture from the assymmetrically substituted phthalocyanine would be difficult. However a combination of difficulties arising from small amounts of starting material, low yields of phthalocyanines and a multitude of products visible by thin layer chromatography prevented isolation of any of the desired product.

Instrumentation

U.V./visible spectra were obtained using a Perkin-Elmer Lambda 9 spectrophotometer.

NMR spectra were obtained on Bruker AM 200 and WP 200 spectrometers (200 MHz, FT-NMR), and on a Perkin-Elmer RS32 (90 MHz, continuous wave). All samples were referenced internally to solvent references.

Infra-red spectra were obtained on a Phillips FTIR 963 spectrometer. All samples were prepared as 8mm KBr discs.

Mass spectra and micro analysis were carried out as a service by Glasgow University Chemistry Dept.

Chemicals

Chemicals were purchased from Aldrich Chemical Co. Ltd. and were used as received unless otherwise stated.

7.2 Experimental

4,5-dibromocatechol 1

Catechol (91g) which had been recrystallised twice from toluene and dried in vacuo was dissolved in glacial acetic acid (400ml) and cooled in an ice bath, liquid bromine (265g) was added slowly and the mixture was stirred for 3 hours. Most of the acetic acid and the unreacted bromine was then removed by rotary evaporation, water (500ml) was then added and off-white crystals formed. After recrystallisation from toluene the product was obtained (126g, 51%), m.p. 106-110°C, (lit 118-120°C).

M.S. m/z 269/267/265 (M^+-1).

$C_6H_4O_2Br_2$	Calc. %	C 26.8	H 1.49
	Found %	C 26.8	H 1.26

4,5-didodecycloxy-1,2-dibromobenzene 2

Dibromocatechol 1 (36g) and potassium carbonate (35g) were added to dry distilled dimethylformamide with overhead stirring under nitrogen. 1-bromododecane (95g) was added and the mixture was stirred at 95°C for 24 hours. After cooling the reaction was drowned in water (1.5l). The water was extracted with chloroform (3x200ml) which was washed with 1M NaOH (2x500ml). After drying (Na_2SO_4) the chloroform was removed by rotary evaporation to leave a red oil. The product was obtained as a white solid (76g, 99%),m.p. 51-52°C (lit. 50.9°C) by recrystal-

FIG. 19

Synthesis of Octakis(dodecyloxy)phthalocyanine

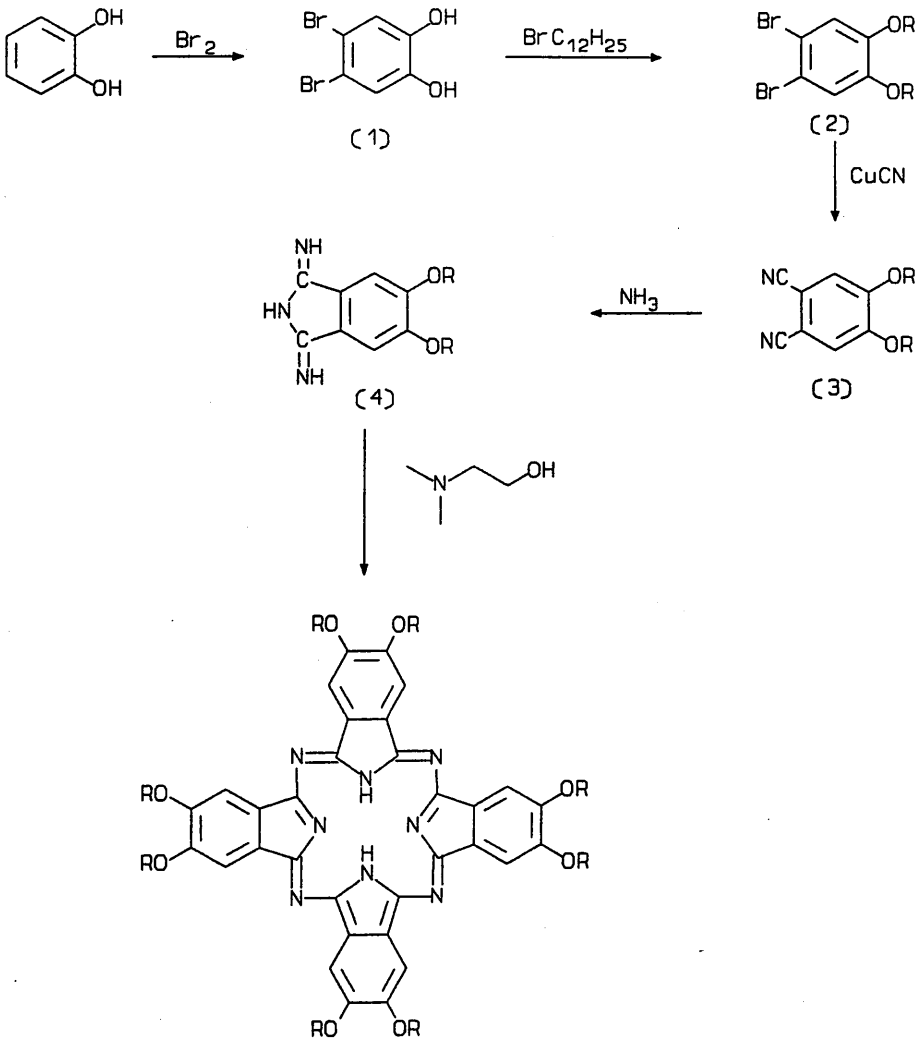

R = $C_{12}H_{25}$

lisation from ethyl acetate.

M.S. m/z 606/604/602 (M^+).

^1H nmr ($CDCl_3$) δ= 0.95 (m, $C\underline{H}_3$), 1.2-1.5 (m, $C\underline{H}_2$), 3.9 (t, $OC\underline{H}_2$), 7.09 ppm (s, arom).

4,5 didodecyloxy-phthalonitrile 3

Didodecycloxy-dibromobenzene 2 (16g) and cuprous cyanide (8g) were added to dry, distilled and degased dimethylformamide (125ml). This mixture was stirred in an atmosphere of dry nitrogen under reflux for 24 hours. The reaction was drowned in concentrated ammonia and the brown solid that was precipitated was collected by filtration. The brown solid was extracted with hot acetone. A white solid was obtained after removal of the acetone by rotary evaporation. Recrystallisation from petrol (b.p. 60-80°C) yielded the desired product 3 as white crystals (11.2g, 85%), m.p. 103-104°C (lit. 103.5°C).

M.S. m/z 496 (M^+).

I.R. (KBr) 2230 (C≡N), 1595,1525 (C=C), 2960, 2920, 2850, 1470 (CH_2, CH_3), 1295, 1095 (C-O) cm^{-1}.

$C_{32}H_{52}O_2N_2$ Calc. %	C 77.2	H 10.2	N 5.6
Found %	C 77.0	H 10.0	N 5.5

4,5-didodecyloxy-diimino-isoindoline 4

To a flask fitted with a double surface reflux condenser and a

bubbler was added the phthalodinitrile 3 (2.5g) dissolved in dry distilled propanol (25ml); sodium (0.4g) was then added. Gaseous ammonia was bubbled through this mixture for 2 hours at room temperature and 4 hours at 60°C. After cooling, water (100ml) was added and the yellow/green precipitate was collected by filtration and dried in vacuo (2.5g, 96%) m.p.> 130°C. No recrystallisation was attempted as this can lead to decomposition. Complete reaction of the phthalonitrile was confirmed by the disappearance of the C≡N stretch at 2230cm^{-1}.

M.S. m/z 514 (M^+).

I.R. (KBr) 3400 (NH), 2960, 2920, 2850, 1470 (CH_2, CH_3), 1650 (C-N), 1445 (C=N), 1290, 1050 (C-O) cm^{-1}.

$C_{32}H_{55}N_3O_2$	Calc. %	C 74.0	H 10.7	N 8.2
	Found %	C 71.9	H 10.6	N 6.9

2,3,9,10,16,17,23,24-octadodecyloxy-phthalocyanine 5

The di-imino-isoindoline 4 (1.5g) was dissolved in 10ml of dry distilled dimethylamino-ethanol and refluxed for 16 hours. To the resultant green mixture was added water (50ml). This solution was extracted with chloroform. Removal of the chloroform left a green solid which was recrystallised twice from chloroform/acetone and washed with hot diethyl ether. The product was obtained as green crystals (50mg, 3%). Further purification was achieved by column chromatography on silica, eluent chloroform.

U.V./Vis. ($CHCl_3$) λ= 701, 664, 428, 346 nm.

D.T.A. (Heating rate 10°C/min) onset 90°C, max 95°C.

I.R. 3290 (N-H), 2920, 2850, 1470 (CH_2, CH_3), 1100 (Ar-O-C), 1270 (Ar-O), 745 (Ar-O-C) cm^{-1}.

$C_{128}H_{210}N_8O_8$	Calc. %	C 77.2	H 10.6	N 5.6
	Found %	C 76.6	H 9.0	N 5.6

Dichlorosilicon(IV)-octakis(dodecyloxy)phthalocyanine 6

Quinoline (20ml) was dried over potassium hydroxide, and distilled under vacuum from zinc dust. To the quinoline was added the diiminoisoindoline 4 (1g) and silicon tetrachloride (4ml). The mixture was heated rapidly to 190°C in an atmosphere of nitrogen. The reaction was allowed to reflux at 160°C for a further two hours. After cooling the reaction was drowned in water (50ml) and the green precipitate collected by filtration. The solid was dissolved in chloroform and dried (Na_2SO_4). The chloroform was then removed by rotary evaporation to leave the product as a green solid (20mg, ≈1%). T.L.C. (eluent $CHCl_3$) 2 spots, R_f = 0.1,0.2 indicating that some hydrolysis had occurred.

U.V. λ= 681, 652, 613, 429, 358, 340 nm.

Dihydroxysilicon(IV) octakis(dodecyloxy)phthalocyanine 7

Amberlyst A26 ion exchange resin in the chloride form

FIG. 20

Synthesis of Dihydroxysilicon-octakis(dodecyloxy)phthalocyanine

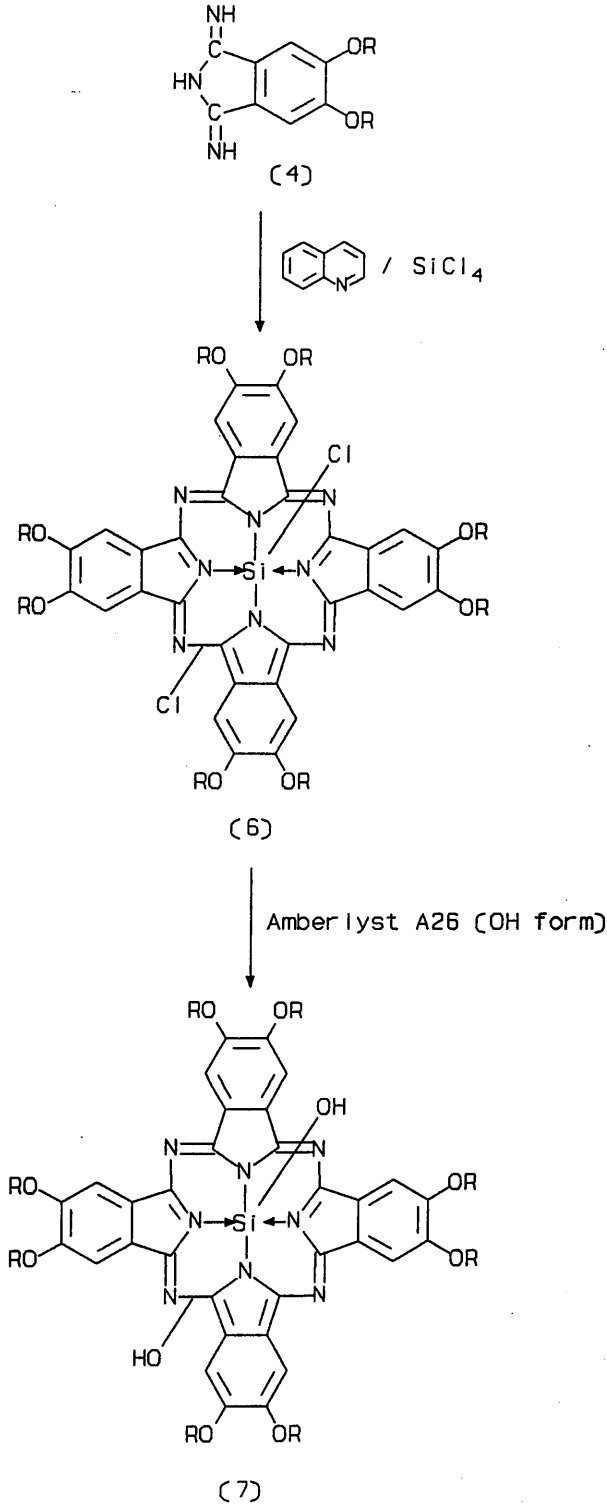

was converted to the -OH form by stirring at 70°C in 10% NaOH for 2 hours then after washing with water until free of chloride ions the resin was washed with tetrahydrofuran and the diethyl ether and dried in vacuo. The dichlorophthalocyanine 6 (20 mg) was dissolved in dry distilled dichloromethane (50ml) and the amberlyst resin (5g) was added. The mixture was gently refluxed for 4 hours. After removing the resin by filtration and the dichloromethane by rotary evaporation (using the lowest possible heat) the product was obtained as a green solid. Further purification was achieved by column chromatography.

U.V. λ= 685, 617, 431, 354, 299, 234 nm.

^{1}H nmr ($CDCl_3$) δ = -2.35 (bs, SiO<u>H</u>), 0.89 (m, OC<u>H</u>$_3$), 1.3 (m, C<u>H</u>$_2$), 4.5 (bm, OC<u>H</u>$_2$), 8.95 (s, arom).

I.R. 3520 (OH), 3010 (CH_2, CH_3), 2400 (NH), 1470 (CH_2, CH_3), 1255 (Ar-O), 1050 (C-N) cm^{-1}.

<u>Polysiloxane-octakisdodecyloxyphthalocyanine 8</u>

The dihydroxysilicon-phthalocyanine 7 (1mg) was heated in air, in an oven at 180°C for 24 hours. The progress of the polymerisation was monitered by U.V./visible spectroscopy (Fig. 19).

U.V. λ= 552, 334, 292 nm.

I.R. 3020 (CH_2, CH_3), 2400 (NH), 1600, 1425 (Si-O), 960 (Si-N) cm^{-1}.

FIG. 21

Synthesis of Polysiloxaneoctakis-(dodecyloxy)phthalocyanine

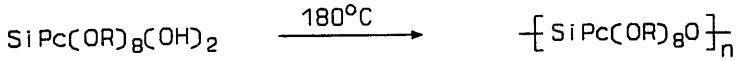

(7) (8)

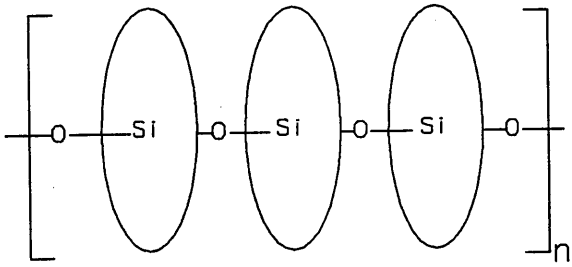

= octakis(dodecyloxy)phthalocyanine

$(C_{128}H_{208}N_8O_{10}Si)_n$	Calc. %	C 74.8 H 10.2 N 5.5
	Found%	C 62.4 H 8.5 N 5.6

Octadodecyloxyphthalocyanato-copper(II) 9

Didodecyloxy-dibromobenzene 2 (1.5g) and cuprous cyanide (1.5g) were added to dry distilled dimethylformamide and the mixture was refluxed under nitrogen for 24 hours. After cooling the reaction mixture was drowned in concentrated ammonia (50ml) and the precipitate collected by filtration. The collected solid was washed with diethyl ether and acetone. The product was finally isolated by recrystallising from chloroform/acetone and centrifuging to collect the solid as a fine powder. Further purification was carried out by gel filtration (eluent $CHCl_3$). The solid was dried in vacuo to give product (0.1 mg).

U.V. λ= 675, 625, 410, 335, 280 nm.

I.R. ($CHCl_3$) 3480 (O-H), 3020, 2980 (CH_2, CH_3), 2400, 1600, 1520, 1425, 930 (Cu-O) cm^{-1}.

$CuC_{128}H_{208}N_8O_8$	Calc. %	C 75.0	H 10.0	N 5.6
	Found %	C 73.5	H 9.8	N 5.7

Lactone of 12-hydroxydodecanoic acid 10

Methylene dichloride (350 ml) and acetic anhydride (250 ml) were stirred together in a 2 litre flask fitted with a double surface reflux condenser, an overhead stirrer and cooled in an ice bath. Hydrogen peroxide 30% (200 ml) was added slowly; after stirring for one hour maleic anhydride (200g) was added,

FIG. 22

Synthesis of Octakis(dodecyloxy)-phthalocyanato-copper(II)

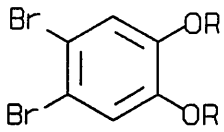

(2)

6xCuCN

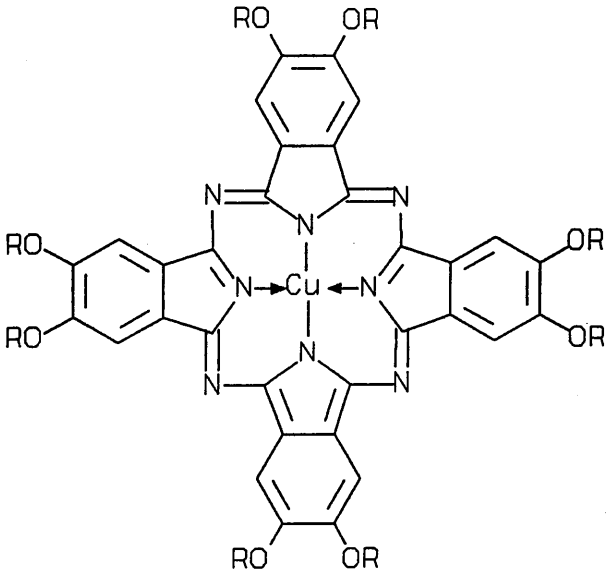

(9)

R = $C_{12}H_{25}$

the mixture was then stirred for a further one hour and the ice bath was then removed. After a further two hours cyclododecanone (50g) was added and the reaction was allowed to reflux for fifteen hours. The mixture was then cooled and the separated maleic acid was filtered off. The filtrate was washed in turn with water (3 x 200ml), 10% potassium hydroxide (2 x 150ml), 10% sodium sulphite (2 x 150ml) and water (2 x 200ml). After being dried (Na_2SO_4) the filtrate was evaporated to give the lactone 10 as a yellow oil (40g, 74%).

I.R. 2930, 2860 (C-H), 1735 (RCOOR) cm^{-1}.

M.S. m/z 198 (M^+).

^1H nmr δ = 1.4 (m, CH_2), 1.7 (t, CH_2), 2.3-2.4 (m, OCH_2), 4.1 (t, $COOCH_2$)

12-hydroxydodecanoic acid 11

The lactone 10 (27g) was added to a solution of sodium hydroxide (20g) in methanol (100ml) and the mixture was heated under reflux for one hour. The solvent was then removed on a rotary evaporator. Water (300 ml) was added and the solution was extracted with diethyl ether (2 x 100ml). The aqueous layer was then acidified with concentrated HCl, the precipitated acid was collected, dried in vacuo and recrystallised from acetone/petrol (b.p. 60-80°C) to afford the acid (22g, 82%), m.p. 80-83°C (lit. 84-85°C).

I.R. 2910, 2850 (C-H), 2550 (O-H), 1690, 1705 (C=O) cm^{-1}.

M.S. m/z 198 (M^+-18), 186 (M^+-30).

FIG. 23

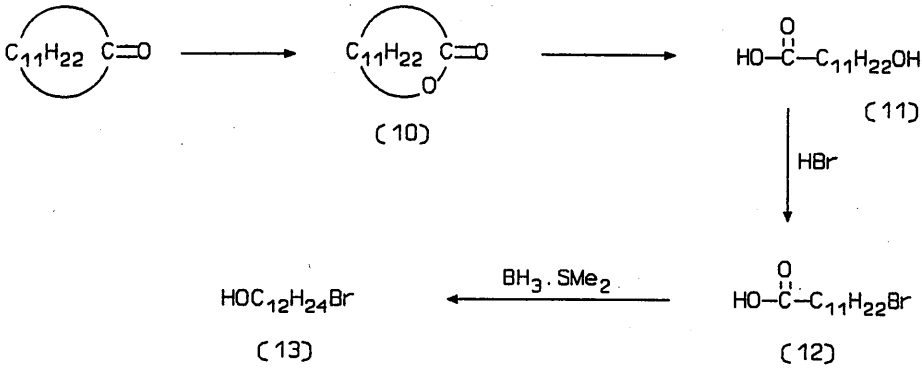

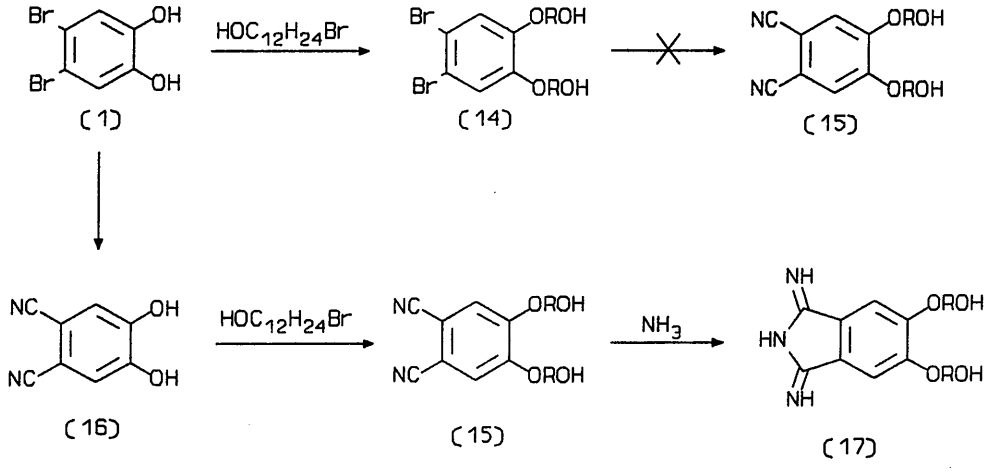

R = $C_{12}H_{24}$

$C_{12}H_{24}O_3$	Calc. %	C 66.06	H 11.9
	Found %	C 66.85	H 11.13

12-Bromododecanoic acid 12

Acetic anhydride (75ml) was added slowly to 47% hydrobromic acid (22ml)followed by the hydroxy acid 11 (19.6g) and the mixture was heated at 100°C for 3 hours. The solvent were then removed by rotary evaporation, The dark residue was recrystallised from petrol (b.p. 40-60°C) to give the bromo acid as an off white solid (14.8g, 59%).

M.S. m/z = 280/278 (M^+).

$C_{12}H_{23}O_2Br$	Calc. %	C 56.6	H 8.18
	Found %	C 56.8	H 8.19

12-bromododecan-1-ol 13

12-bromododecanoic acid 12 (20.5g, 0.073 mol) was dissolved in 200ml of dry distilled tetrahydrofuran; borane-dimethyl sulphide (50ml, 2M) was added slowly with ice cooling and the mixture was stirred under a constant stream of nitrogen for 3 hours. The mixture was then gently refluxed for 2 hours and finally left to stir at room temperature for a further 16 hours. Water (250ml) was slowly added with ice cooling. The tetrahydrofuran was removed by rotary evaporation and the mixture was then extracted with diethyl ether (5x100ml). The

diethyl ether was then washed with in turn 10% sodium carbonate (2x200ml) and water (2x200ml). After drying (Na_2SO_4) the solvent was removed by rotary evaporation to leave a yellow oil. The bromo alcohol was obtained as a low melting point white solid (9g) by recrystallisation from light petrol and as a less pure yellow oil. Vacuum distillation at 1mmHg and 110°C gave pure white solid.

m.p. 31°C (lit. 32°C)

M.S. m/z = 248 (M^+)

4,5-di-(12-hydroxydodecyloxy)-1,2-dibromobenzene 14

-typical procedure.

Dibromocatechol (2.69g, 0.01m) was dissolved in dry distilled dimethylformamide 20ml, potassium carbonate (2.8g, 0.02m) was added and the mixture was stirred at room temperature under nitrogen. The bromo alcohol 13 (8g, 0.03m) was added and the reaction was heated to 90°C for 24 hours on an oil bath. After cooling water (100ml) was added and the mixture was extracted with chloroform (3x100ml). After washing with 1M NaOH (2x100ml) and drying (Na_2SO_4) the chloroform was removed by rotary evaporation to leave a red oil. A pale pink solid was then obtained by recrystallisation from ethyl acetate (m.p. 45-48°C).

M.S. m/z = 638/636 (M^+)

$C_{30}H_{52}O_4Br_2$	Calc. %	C 56.6	H 8.18
	Found %	C 56.8	H 8.19

^1H nmr δ= 7.1 (s, arom), 3.9 (t, OCH_2), 3.6 (t, CH_2OH), 1.7 (m,

$C\underline{H}_2$), 1.2-1.4 (bm, $C\underline{H}_2$).

4,5,di-(12-hydroxydodecyloxy)-phthalonitrile 15

4,5-di-(12-hydroxydodecyloxy)-1,2-dibromobenzene 14 (1g) and cuprous cyanide (0.45g) were added to dry distilled dimethyl formamide (5ml) and refluxed under N_2 for 16 hours. Concentrated ammonia was then added and the precipitate which was formed was collected by filtration. The solid was extracted with hot acetone, dried (Na_2SO_4) and the acetone was then removed by rotary evaporation and the resulting solid recrystallised from ethyl acetate to give impure product. Further purification was attempted by column chromatography (O-alumina, eluent ethyl acetate/light petrol) but no product could be obtained. Mass spectroscopy showed the major product to be the mono-bromo mono-nitrile derivative.

M.S. m/z = 589 (M^+).

4,5-dicyanocatechol 16

Dibromocatechol 1 and cuprous cyanide were added to distilled degassed dimethylformamide and refluxed under N_2 for 16 hours. After cooling the mixture was drowned into a 10% solution of $FeCl_3$ in 2M HCl (150ml), and stirred at 70°C for 1 hour. After cooling the solution was extracted with ethyl acetate. The ethyl acetate was dried (Na_2SO_4) and evaporated to leaved a purple solid (0.95g) Recrystallisation from ethyl acetate/

petrol and then toluene/ methanol gave the product as an off white solid (0.6g, 20%).

M.S. m/z = 160 (M^+)

^1H nmr (CD_3OD) δ= 7.75 (s, arom).

4,5,di-(12-hydroxydodecyloxy)-phthalonitrile 15

Dicyanocatechol (100mg), potassium carbonate (260mg) and bromo-dodecanol 13 (500mg) were added to dimethylformamide (1.5ml) and heated under N_2 at 100°C for 16 hours. The reaction was drowned in water and then extracted with chloroform (3x50ml). After washing with 10% NaOH (2x30ml) and water (2x30ml) the solution was dried (Na_2SO_4) and the chloroform removed by rotary evaporation. The solid produced was impure by thin layer chromatography (eluent 50:50 ethyl acetate:petrol) so it was recrystallised a from ethyl acetate/ 60-80 petrol. Further purification was then carried out by column chromatography on O-alumina (eluent ethyl acetate/60-80 petrol) to give product as an off white solid (40mg, 38%) m.p. 106-108°C.

^1H nmr δ= 1-1.7 (bm, $C\underline{H}_2$, $C\underline{H}_3$), 3.6 (t, $C\underline{H}_2$-OH), 3.95 (bm, O-$C\underline{H}_2$), 7.05ppm (s, arom).

M.S. 529/528 (M^+), 510 (M^+-18)

4,5,di-(12-hydroxydodecyloxy)-diimino-isoindoline 17

The phthalonitrile 15 (20mg) and sodium metal (10mg) were

FIG. 24

Synthesis of an asymmetrically substituted phthalocyanine

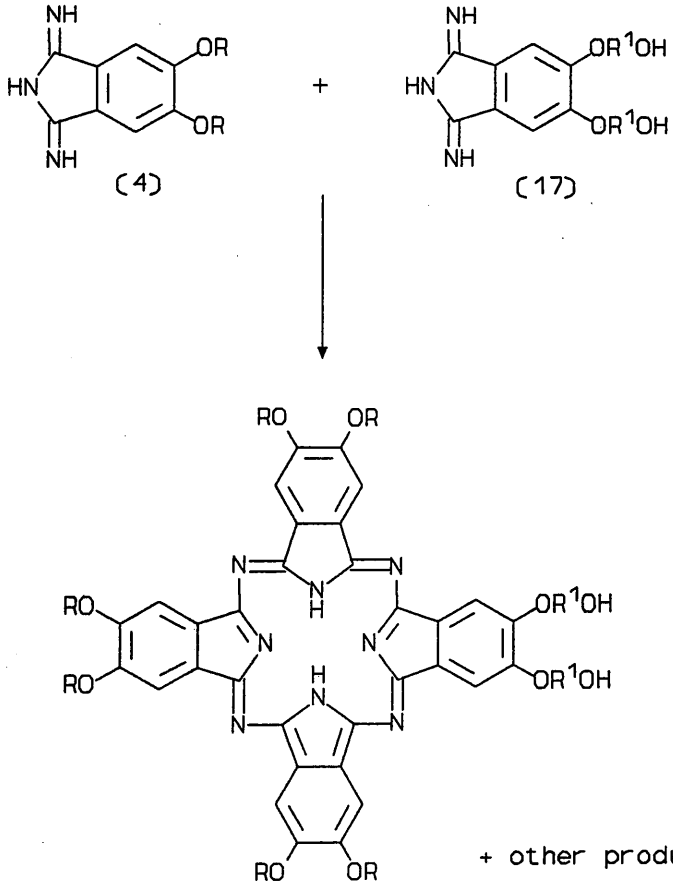

R = $C_{12}H_{25}$

R^1 = $C_{12}H_{24}$

dissolved in dry propanol (10ml). Gaseous ammonia was bubbled through the refluxing solution for 8 hours. After evaporation of the propanol and washing with water the product was obtained as a yellow solid. The product was then immediatly used in the next reaction.

2,3-(12-hydroxydodecyloxy)-9,10,16,17,23,24-octadodecyloxy-phthalocyanine 18

The dihydroxy-diiminoisoindoline 17 (20mg) and the diiminoisoindoline 4 (180mg) were refluxed in dry distilled dimethylamino-ethanol (10ml) for 24 hours. After cooling, the reaction was drowned in water (30ml) and extracted with chloroform (3x30ml). T.L.C. (eluent chloroform) showed many spots. The chloroform was then evaporated and the resulting solid was washed with hot ethyl acetate. Further purification was then attempted by column chromatography (eluent $CHCl_3$) but none of the desired products could be isolated.

CHAPTER 8: PHTHALOCYANINE THIN FILM GROWTH

8.1 Preparation of Thin Films of Phthalocyanines

The methods by which thin films of octadodecloxyphthalocyanines may be prepared are limited. Physical vapour deposition was attempted with no success. The heat required for sublimation causing the decomposition of the molecule. Langmuir Blodgett films have been made of specially substituted phthalocyanines (Cook et al 1987), but not for octadodecloxyphthalocyanines. A dimeric octadodecloxyphthalocyanine has been shown to form Langmuir Blodgett films.

The technique that proved most successful in this study is the solution casting method, this was casting a dilute solution onto the surface of water and allowing the solvent to evaporate leaving a thin film on the surface of the water. In Langmuir Blodgett films the surface film is compressed thus increasing the order of this layer. However with method the film is not compressed and the phthalocyanine molecules are allowed to order themselves on the water surface. Using this method films were prepared of the metal free, copper, silicon dihydroxy and siloxane octadodecloxyphthalocyanines.

8.2 Film Preparation on a Water Surface

General Method

A solution ($\approx 4 \times 10^{-5}$% w/v) of the appropriate octadode-

PLATE 13

OCTADODECYLOXY-PHTHALOCYANINE

WATER CAST FILM

13 585000 X

material for electron microscopy was by the casting on water as described above. When examined at low magnification the film appeared smooth and no features could be seen. At higher magnifications small areas of lattices were visible (plate 13a). The lattice lines were often curved and many broken areas and dislocations could be seen. Two lattice sizes were measured 1.9 nm and 2.6 nm (plate 13b). In some places the lattices appear to be crossed but this is probably due to overlapping areas. Two types of diffraction pattern can be seen (plates 13c & 13d). Plate 13c shows spacings of 3.2 nm and 0.57 nm, corresponding to the distance between the stacks of phthalocyanines and the molten paraffinic spacings. Plate 13d shows spacings of 2.7 and 4.6 nm.

8.5 Crystallisation From Benzoic Acid

Benzoic acid (0.2g) and a small amount of the phthalocyanine 5 (1mg) were placed between two freshly cleaved sheets of mica along with two carbon coated microscope grids. The mica was heated on a hotplate until the benzoic acid melted and the phthalocyanine 5 dissolved. The benzoic acid was allowed to slowly cool and solidify. The sheets of mica were then separated and placed in a high vacuum (10^{-7} torr) for 24 hours. The benzoic acid evaporated leaving the microscope grids and the precipitated phthalocyanine.

No features were visible at low or high magnification. In

PLATE 13

OCTADODECYLOXY-PHTHALOCYANINE

WATER CAST FILM

13B 1316000 X

13C 1.5 nmcm

13D 1.5 nmcm


B

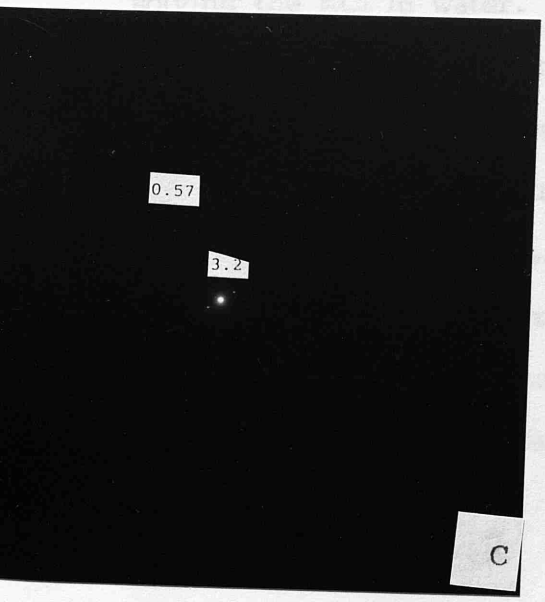
0.57
3.2
C

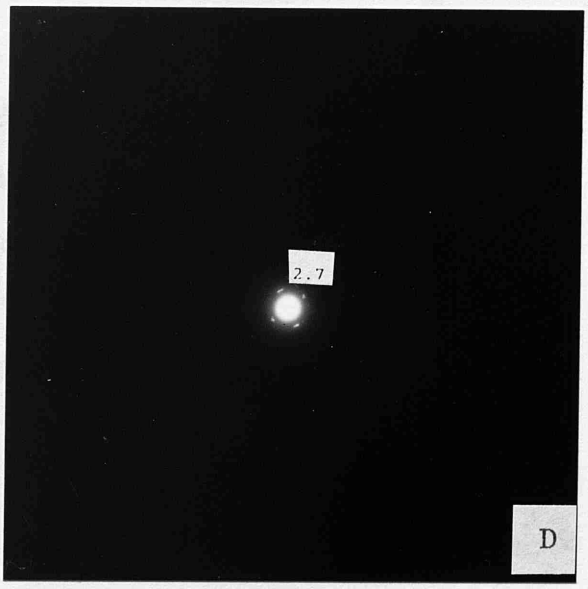
2.7
D

the diffraction mode two patterns were visible. Plate 14a shows two arcs corresponding to a spacing of 3.0 nm, a broad halo at 1.1 nm and another halo at .53 nm. This is probably the same projection that is seen in the water cast films. The second pattern was observed very rarely (plate 14b), it is a hexagonal pattern with second order spots with a spacing of 2.79 nm, a halo was also seen at 0.52 nm. This is a view down on top of hexagonally packed discotic phthalocyanines.

8.6 Crystallisation from Chloroform

The third method of sample preparation was a simple crystallisation. Four drops of the phthalocyanine 5 solution (4.6×10^{-5}% w/v) in chloroform were placed on the surface of a cleaved KCl crystal and the solvent was allowed to evaporate. The KCl was then coated with carbon and the film was transferred to a grid by dissolving the KCl in water.

Low magnification electron microscopy revealed that the phthalocyanine had crystallised into small cigar shaped crystals (plate 15a). At higher magnification no lattices were visible probably as a result of the crystals being too thick. Diffraction revealed two patterns. Plate 15b shows spacings of 2.7 nm and 0.46 nm corresponding to a side on view of the stack. Plate 15c shows arced spots at 2.7 nm.

PLATE 14

OCTADODECYLOXY-PHTHALOCYANINE

CRYSTALLISED FROM BENZOIC ACID

14A 1.5 nmcm

14B 1.5 nmcm

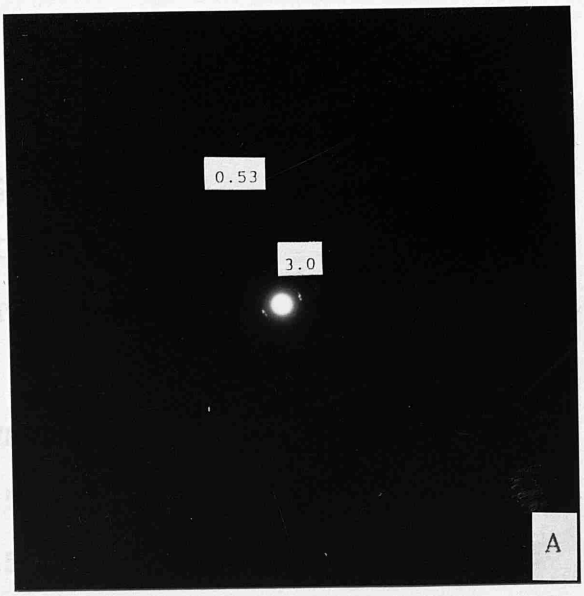

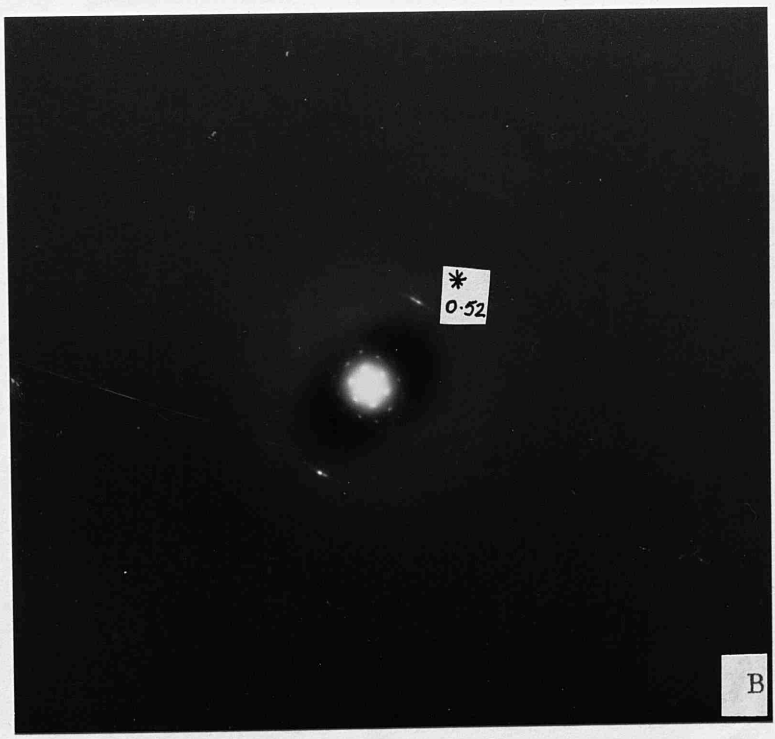

*This is the (001) spacing from some residual benzoic acid.

PLATE 15A

OCTADODECYLOXY-PHTHALOCYANINE

CRYSTALLISED FROM CHLOROFORM

15A 17800 X

15B 1.5 nmcm

15C 1.5 nmcm

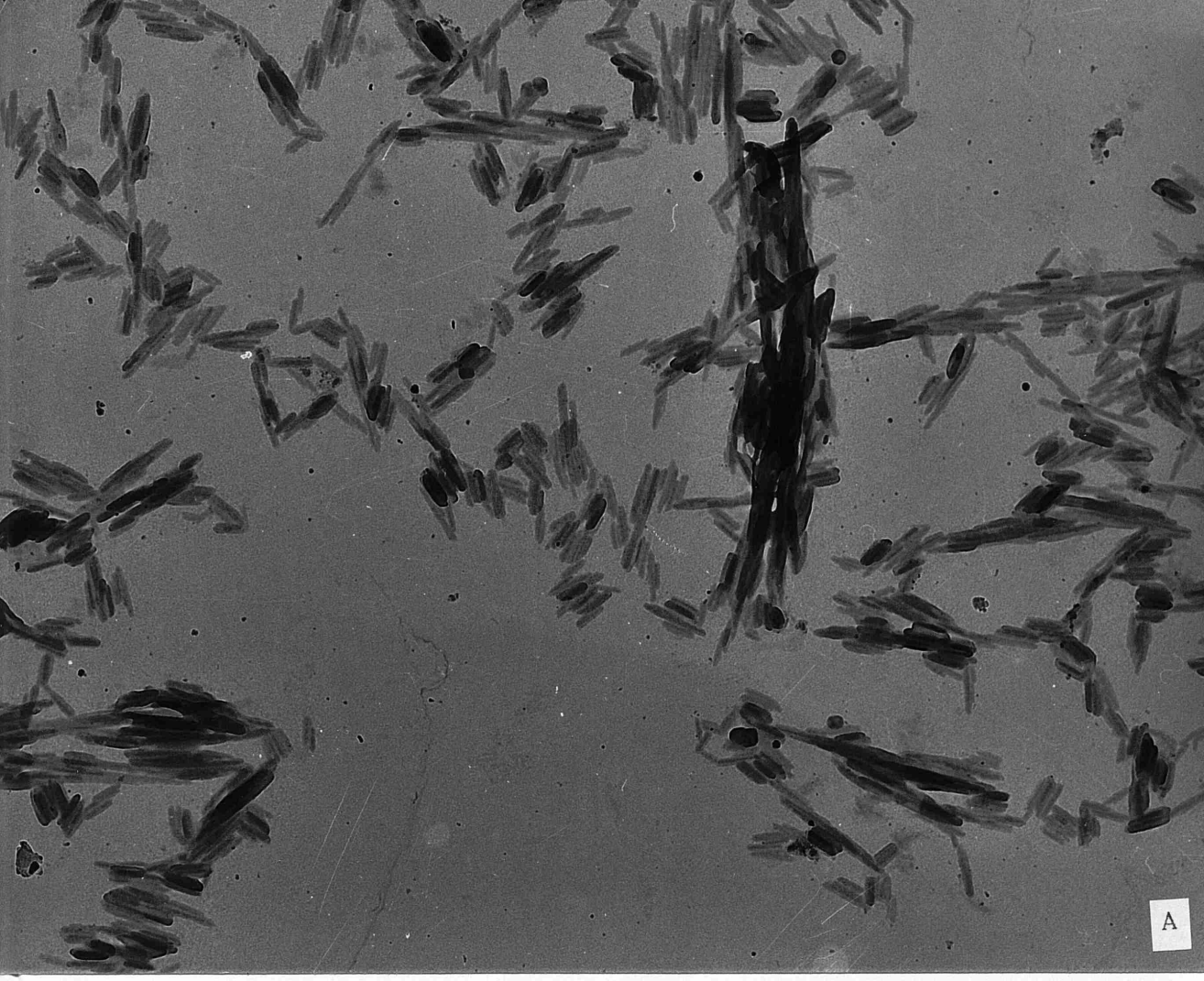
A

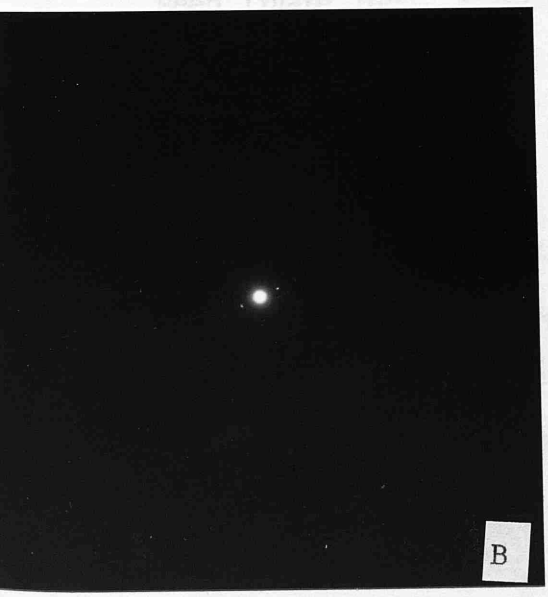
B

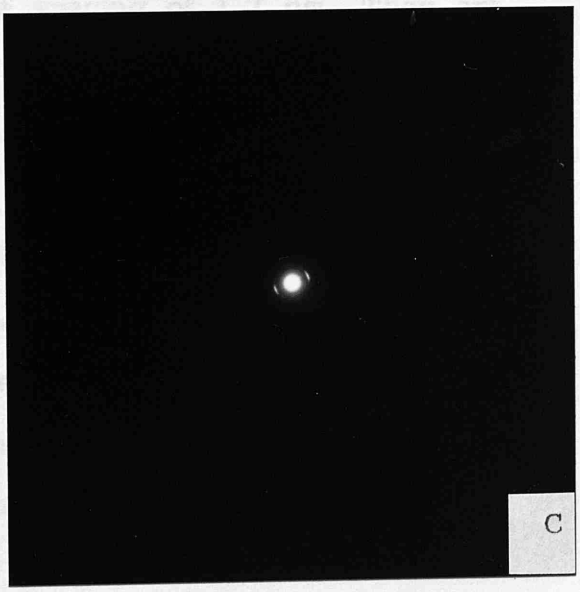
C

8.7 Other Attempted Sample Preparation Methods

Attempts were made to prepare samples of the phthalocyanine 5 by two other methods, both of which proved unsuccessful. Firstly the solution was dropped onto KCl as above but with the KCl heated to 150°C which is above the mesophase transition temperature, this it was hoped might increase the crystallinity of the sample. Rapid cooling of a heated sample was also tried with liquid nitrogen but this proved to have no effect on the sample.

8.8 Octadodecloxyphthalocyaninato-copper 5

Films of the copper complex were prepared by casting a solution on the water surface as described above. At low magnifications small crystallites of irregular shape could be seen (plate 16a).

At higher magnifications very disordered lattices can be seen (plate 16b). They show a spacing of 1.7 nm. They are most clearly visible in the areas in between the crystals, since the film will be thin enough for lattice imaging in these areas.

Diffraction does not show the 1.7 nm spacing probably due to the extreme disorder. The only pattern visible is made up of six spots arranged in a rough hexagon (plate 16c). There are spacings, 0.44 nm. The spots are very beam sensitive and as a result appear slightly arced.

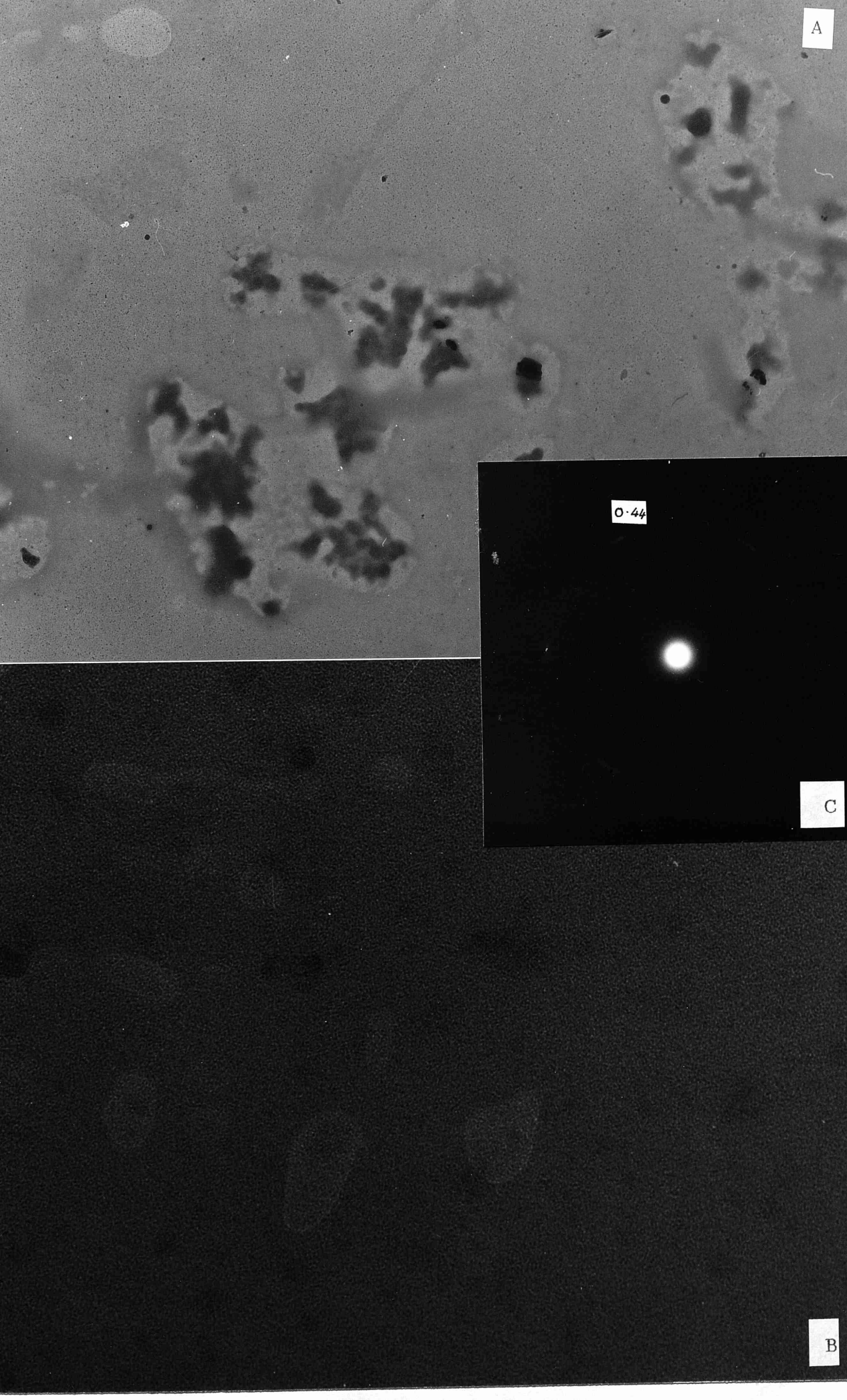
A
0·44
C
B

8.9 Dihydroxysilicon-octadodecloxyphthalocyanine 8

Films of this material were prepared by casting on water as described above.

No features could be discerned at high or low magnifications.

In the diffraction mode the pattern in plate 17a was observed. Only the inner spots are of a crystalline nature, they measure at 2.83 nm, the outer rings are very diffuse and they measure 1.71 nm, 0.40 nm, 0.33 nm.

An attempt was made to cast a film of this material on the surface of water which was then heated on a hot-plate to 90°C. The mesophase formation temperature of this particular material is expected to be below 90°C (by analogy with the octadodecloxy-methyl-phthalocyanine (Piechocki 1982)). However no change was observed in this film compared to the normal method of sample preparation.

8.10 Octadodecloxyphthalocyanine-polysiloxane 9

Films of this material were prepared for electron microscopy using the previously described casting on water method.

Again at low magnifications no features were visible. At higher magnifications lattices could be seen (plate 18a). These areas of crystallinity were different from those in the metal free phthalocyanine, in that they tended to be longer and narrower. The lattices are 2.5 nm and 2.0

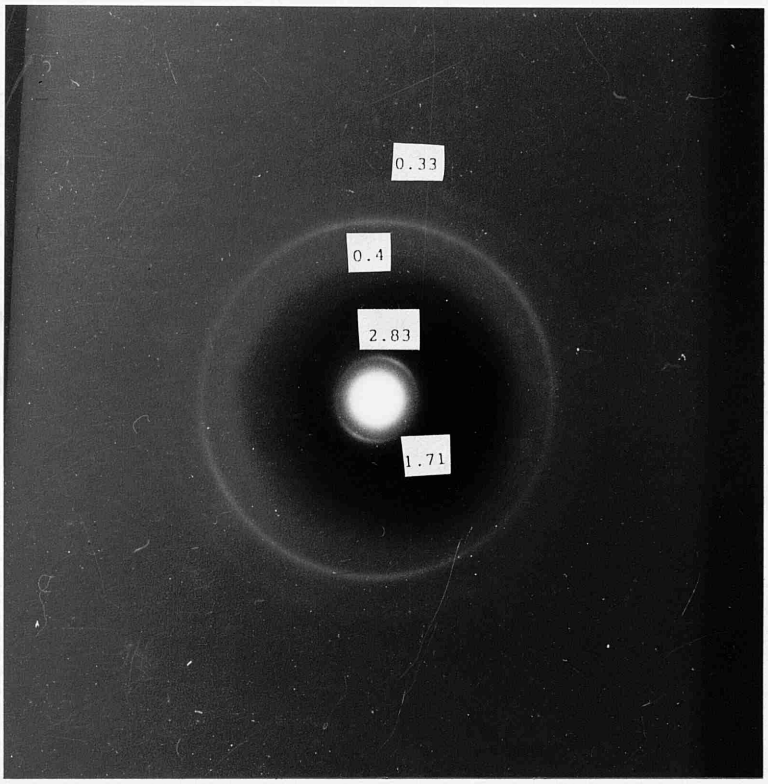

PLATE 17

DIHYDROXY-SILICON-OCTADODECYLOXY-PHTHALOCYANINE

WATER CAST FILM

17A 3.2 nmcm

PLATE 18

POLYSILOXANE-OCTADODECYLOXY-PHTHALOCYANINE

WATER CAST FILM

18A 320000 X

18B 2.4 nmcm

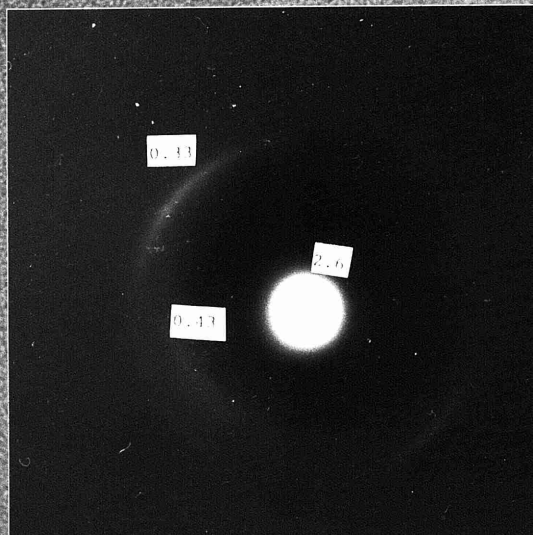
0.33
2.6
0.43

nm in size. They are short, irregular and dislocations can be seen. It was noticeable that this sample was con siderably more stable in the electron beam than earlier samples. The lattices are undulating, this is probably a reflection on the packing mismatch between the phthalo-cyanine molecules and their paraffin side chains (de Gennes 1984). The lattices all run in the same direction.

Electron diffraction showed a largest spacing of 2.6 nm with slight arcing. At right angles to these were larger arcs of 0.33 nm in size. There are also rings present at 1.23 nm and at 0.43 nm. No second order spots were observed.

It has proved possible to "freeze in" the liquid crystal structure of mesophases in other polymeric samples. This was attempted with this polysiloxane by heating a micro-scope grid with the sample, between two glass slides to 150°C. The slides were then plunged into liquid nitrogen and the sample allowed to warm to room temperature. No noticeable effect was observed in the sample.

8.11 Hotstage Electron Microscopy

All the octadodecloxyphthalocyanine derivatives studied are known to form liquid crystalline phases at elevated temperatures. Using the hot-stage, the changes in the spacings as measured by diffraction were assessed at temperatures of up to 150°C. No lattice images could be

PLATE 19

OCTADODECYLOXY-PHTHALOCYANINE

WATER CAST FILM

ON MICROSCOPE HOTSTAGE

19A 2.6 nmcm

19B 2.6 nmcm

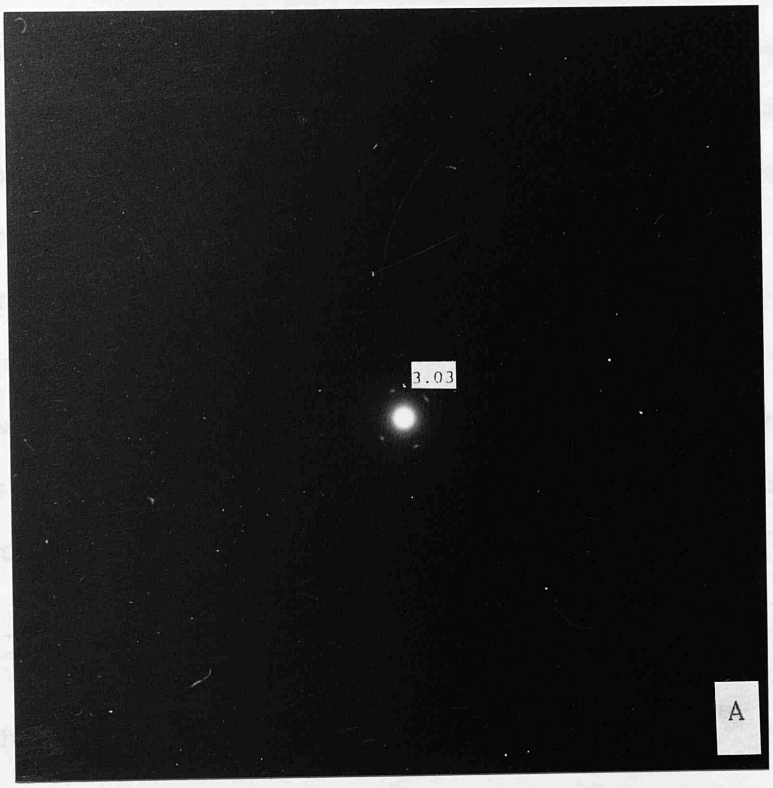
3.03
A

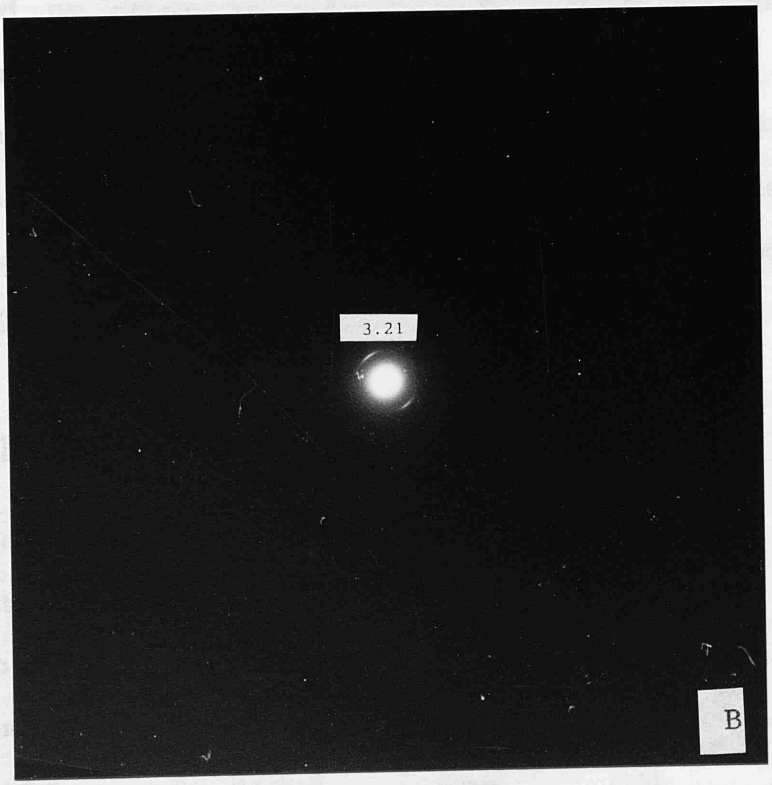
3.21
B

found because of the difficult alignment of the hotstage. The samples that were studied are the same as those studied at room temperature. No special grids or supports were needed as the copper grids and carbon films proved adequate.

The hotstage was always brought to the desired temperature slowly. Before a picture was taken the power was switched of to the electric heater in the sample holder as the current in the heater interfered with the electron beam.

8.12 Octadodecloxyphthalocyanine

When heated to 100°C the size of the largest spacing increased to 3.03 nm (plate 19a). On further heating to 150°C this became 3.21 nm (plate 19b). No other spacings and no other projections were visible at these higher temperatures.

The sample prepared by crystallisation from benzoic acid was examined at 132°C (plate 19c). Two arcs at right angles to each other were visible, their spacings were 3.01 nm and 0.34 nm.

8.13 Other Samples

Samples of the copper, silicon-dihydroxy and polysiloxane octadodecyloxyphthalocyanines were examined at 150°C. However no diffraction patterns were obtained. The temperature at which the loss of the diffraction patterns occurred was not observed.

8.14 Discussion

All the octadodecyloxy-phthalocyanines examined have been observed to order themselves to a greater or lesser degree when cast from solution onto a water surface. The aggregation of phthalocyanine molecules is a much observed phenomenon (Sielcken et al 1987).

Samples of the metal free octadodecyloxy-phthalocyanine were prepared in several ways and casting on water was the best method by which any order was observable by transission electron microscopy. Large randomly orientated crystalline domains were observed to have formed on the water surface. These domains were seen to be long and narrow in shape. This was expected since it is a result of the highly anisotropic packing generally observed in phthalocyanines. In this case there is a stronger attraction between the planar surfaces of the phthalocyanines than between the peripheral side chains.

X-ray powder diffraction at elevated temperatures of metal free octadodecyloxy-phthalocyanine has shown that in the mesophase there is an intercolumnar spacing of 3.5 nm (Masurel et al 1987). However in this study spacings of 1.9, 2.6 and 3.2 nm have all been observed. The smaller intercolumnar distances of 1.9 and 2.6 nm which were observed as lattices could be explained in two ways. The molecules may be packing in a tilted manner (Fig. 25), a similar packing arrangment has been observed

FIG. 25

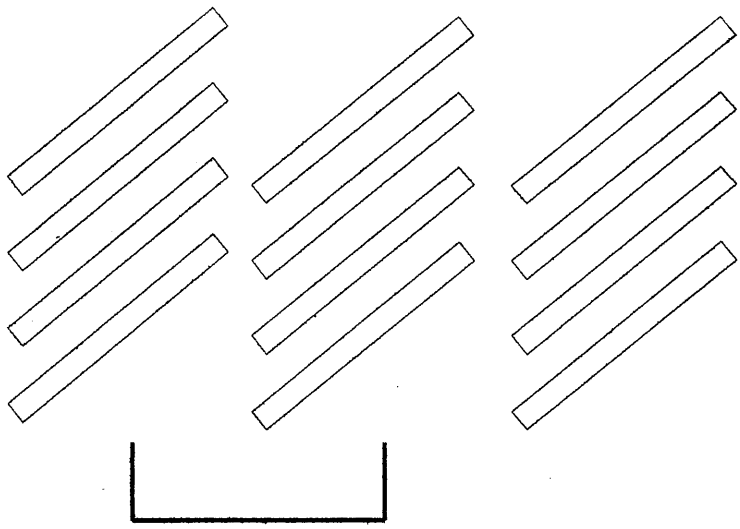

1.9 nm

Tilted Packing on Water Surface

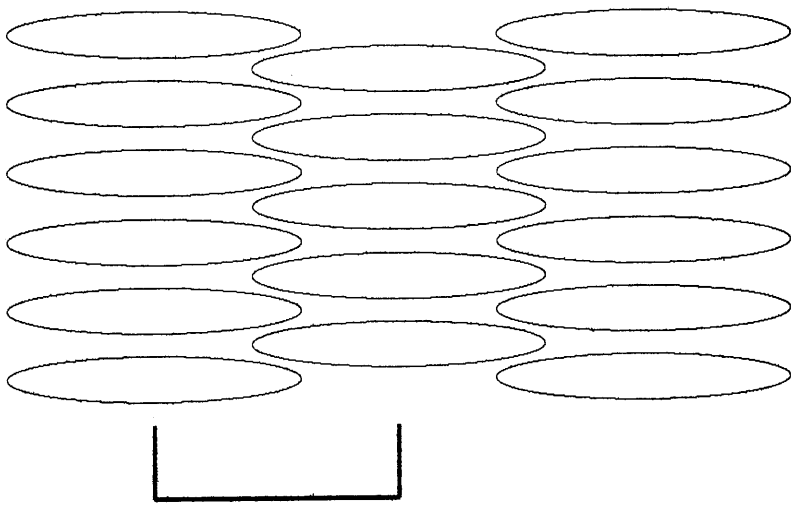

2.6 nm

Interleaving of Substituted Phthalocyanines

Note about the tilted packing:- There is no direct evidence for this packing mode.

in monolayers of tetra-t-butyl-phthalocyanines (Fryer 1985). The other possible explanation is that there is some degree of side chain overlap. This overlap or interleaving would be encouraged by the hydrophobic side chains proximity to the water surface. It is likely that only the 1.9 nm lattice is called by a tilted packing. The 2.6 nm lattice spacing is also observed by diffraction with a 0.46 nm spacing at right angles (Fig. 25).

The areas of crystallinity would appear not to be discrete crystals since at the edge of the crystalline areas the lattices become more disordered and broken. The lattices are islands of well ordered molecules surrounded by amorphous material. On moving across a film in the diffraction mode some reflections due to the phthalocyanine were always visible. However the carbon film would obscure any differences in contrast due to holes in the film.

Transmission electron microscopy in the imaging mode is unable to tell us any more about the crystal packing since the resolution is limited by the extreme beam sensitivity of this material. Electron diffraction shows two types of packing with different inter columnar spacings of 2.7 and 3.2 nm. Both diffraction patterns show reflections due to the paraffin side chains at 4.6 and 5.7 nm respectively. The paraffin reflections are weak and diffuse due to their semi-molten state. They are at right angles to the large spacings showing that in the 2.7 and 3.2 nm cases they are packing discoticly and not

in a tilted manner. Some degree of interleaving must therefore be occurring since the large spacing as measured by X-ray methods is 3.5 nm. The 1.9 nm spacing was not observed by diffraction. It is probable that this is a tilted packing (Fig. 25) with an angle between the molecular plane and the column axis of 56°.

Molten benzoic acid has been used as a solvent for the recrystallisation of paraffins (Wittman et al 1983). However with metal free phthalocyanines peripherally substituted with paraffins it did not give the discreet crystals hoped for. It did reveal two projections of a stack of phthalocyanines. The side on view which had been seen before plus a view down on top of a stack of hexagonally close packed phthalocyanines. This orientation could not be prepared by any other method. The spacing of 2.7 nm suggests that there is some overlap between side chains (Fig. 26). However the diffraction pattern is of several orders so the this overlap is not causing too great a disruption to the lattice. Areas possessing this orientation were observed very infrequently and were difficult to reproduce.

Copper octadodecyloxy-phthalocyanine appeared at first sight to be a poor material to examine by electron microscopy. The only lattices visible were very broken and disordered, the spacing of these being 1.7 nm. These lattices are probably the same as the tilted phase that was visible in the metal free phthalocyanine. Again

FIG. 26

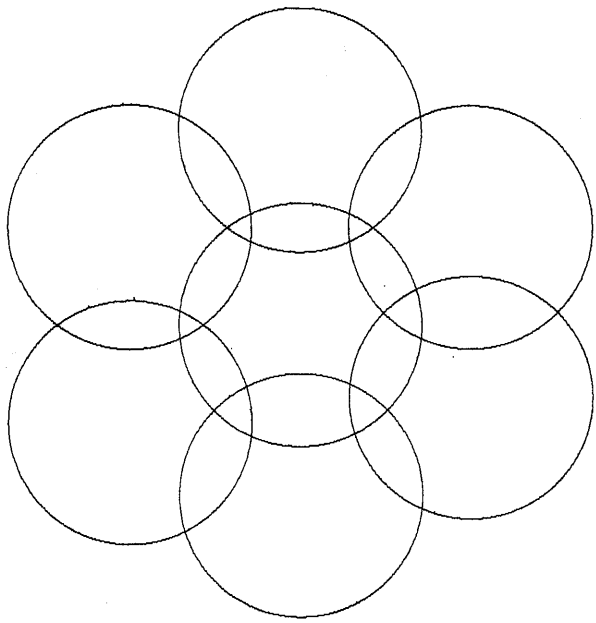

Hexagonally Packed Phthalocyanines

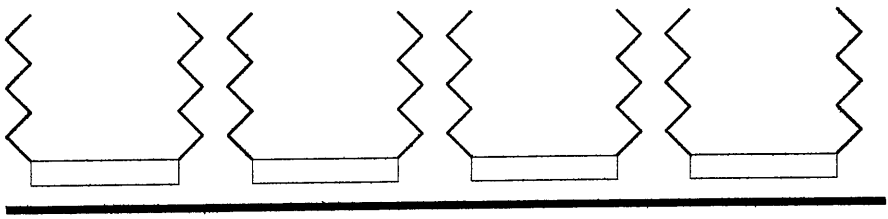

Copper phthalocyanines on a water surface

electron diffraction did not show this large spacing. The only pattern observed by diffraction was an orthorhombic arrangement of six spots, four with a spacing of 0.40 nm and two of 0.44 nm. This is similar to the arrangement observed in long chain paraffins (Kitaigoroskii 1973) and in this case is caused by the packing of the long chain side arms on the phthalocyanines. The spots were usually sharp and the pattern was common throughout the film. An arrangement of the phthalocyanine molecules lying flat on the water surface with the paraffinic chains pointing vertically would fit this information (Fig. 26). The molecules are not close packed since the diffraction pattern is only of a single order. The paraffin side chains will be packing to give an orthorhombic structure as with long chain hydrocarbons. Another type of packing would be to have the chains in a semi molten state with large amounts of rotation in which they would each occupy cylindrical volumes, but this would give a hexagonal pattern which was not observed. In β-copper phthalocyanines the copper is able to coordinate to the nitrogens in adjacent molecules giving a distorted octahedral geometry. This is the reason for the tilted packing in β-phthalocyanine. This stabilisation may account for the presence of the small areas of 1.7 nm lattices. It may be that in an uncompressed monolayer this molecule will lie parallel to the water surface but when compressed, as in a Langmuir Blodgett film, the molecules will stand on end allowing the copper an octahedral coordination. It

is also possible that a monolayer of molecules parallel to the water surface acts as a substrate for the tilted stacking.

Dihydroxy-silicon-octadodecyloxy-phthalocyanine would appear to be a very disordered film since the diffraction pattern is composed of rings. The spacings of 2.83 nm and 0.33 nm would suggest that there is some face to face stacking of the molecules. The hydroxyls above and below the plane of the ring which will hydrogen bond to each other will also interact with the water surface disrupting the formation of stacks.

Octadodecyloxy-phthalocyanine-polysiloxane is a special case since the molecules are already stacked face to face. On the water surface the molecules do aggregate and areas of lattices are seen. The lattices are short in the polymer chain direction, probably because of the hydroxyl end groups interacting with the water substrate. The lattice size is small 2.5 and 2.0 nm suggesting that there is some interleaving or overlapping. The phthalocyanines will be standing upright on the water surface. Diffraction showed the expected reflections at 2.6, 0.43 and 0.33 nm. However there is also a diffuse ring at 1.23 nm this may be due to a periodic "kink" in the molecular stack to accomadate the disruption caused by the overlapping chains (Fig. 27).

Films of all the materials were heated in situ in the

FIG. 27

Periodic Kink in Polysiloxane Chains

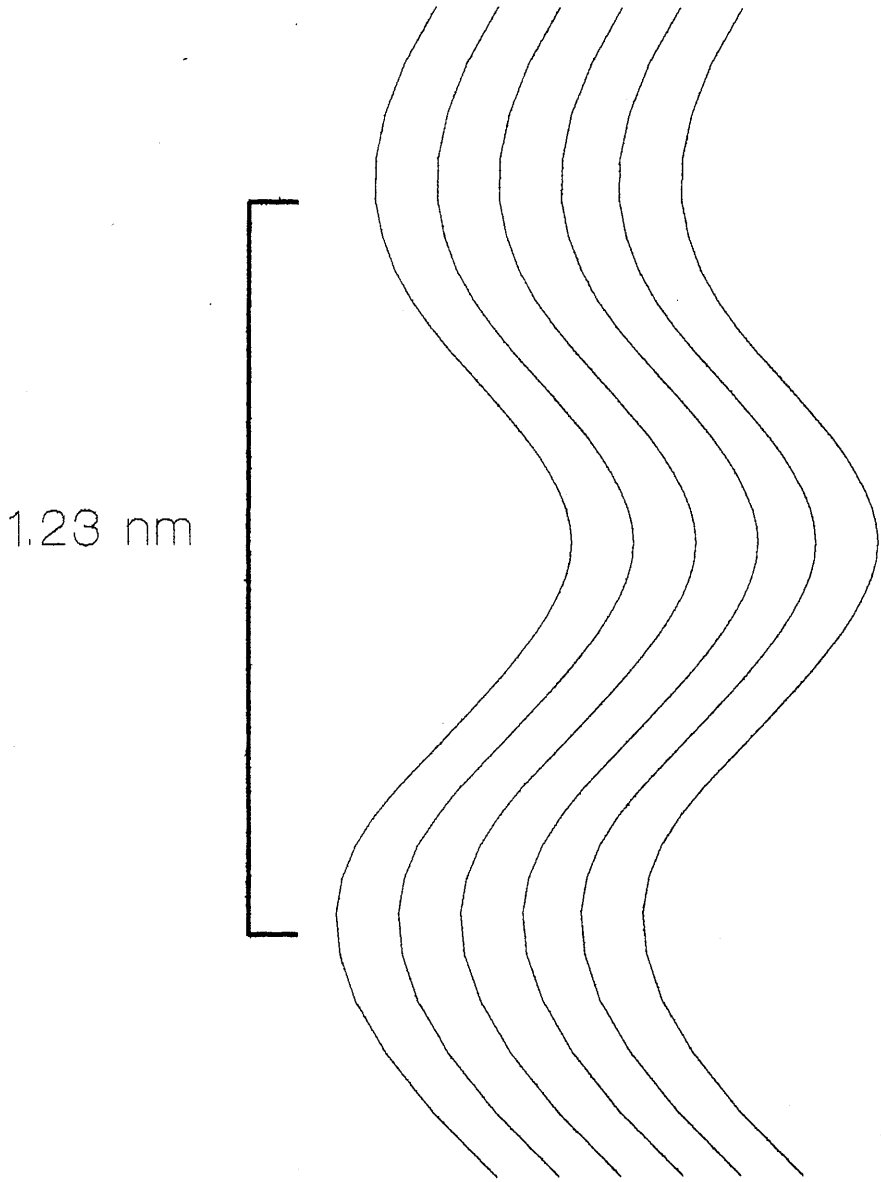

FIG. 28

Effect of Heating

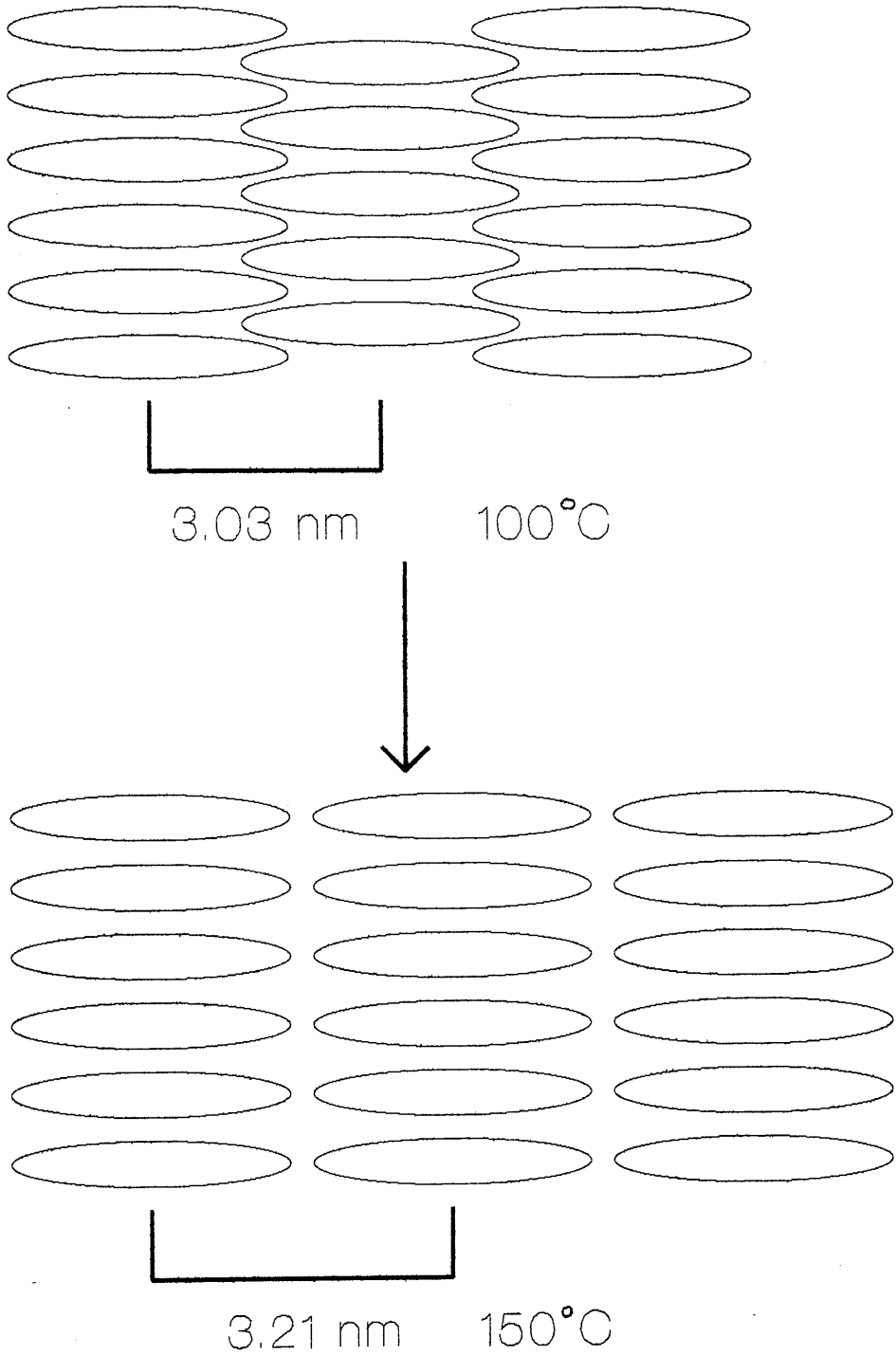

microscope whilst being examined by electron diffraction. Only the octadodecyloxy-phthalocyanine gave reflections that were observable at elevated temperatures. On heating a water cast film to 100° and then 150°C the largest spacing increased to 3.03 and 3.21 nm respectively (Fig. 28). Here we are witnessing the film originally formed on a water surface reorganising to the discotic mesophase. The water surface obviously exerts a strong influence on the film forcing the paraffin chains to overlap to minimise the hydrophobic water-hydrocarbon interactions. When this inflence is removed this compound will behave as a bulk solid and will self organise into the discotic phase above 90°C.

Chapter 9 CONCLUSIONS

9.1 Evaporated Thin Films

The physical vapour deposition of perylene was investigated by Transmission Electron Microscopy. Many parameters affect the formation of an evaporated film but in this study substrate temperature (T_S) in particular was investigated. The other variables which include type of substrate, quality of vacuum and rate of evaporation were held constant. T_S was shown to cause large changes in crystal morphology and crystallinity over a relatively narrow temperature range. The increase in T_S changes the way the film grows by several mechanisms. Increasing T_S lowers the number of nucleation sites thus raising the average crystal size. It decreases the adhesive force between the substrate and the adsorbed molecules allowing greater migration and thus the growth of larger better ordered crystals. This also allows epitaxial interactions to order the film to a greater extent. At higher T_S epitaxial interactions would appear to become less important and the film appears as if it had been annealed. Re-evaporation becomes an important factor at high T_S. The 1/3 boiling point rule (Vincett et al 1977) for ordering is generally supported by these findings. Though higher temperatures are required for crystallinity with large crystallite size.

Quaterrylene films also show a large T_S dependence, though as expected over a greater temperature range.

The behaviour of both perylene and quaterrylene indicates the preferred contact face of the evaporant is that with the molecules perpendicular to the ionic substrate, in this case the ab face. With other less ionic substrates molecules have been shown to stack with their aromatic faces parallel to the substrate (Wittman and Lotz 1990).

9.2 Octa-Substituted Phthalocyanines

Preparation of thin films of the octa-substituted phthalocyanines that were synthesised, was best achieved by on a water surface. This also facilitated examination by Transmission Electron Microscopy since the films could be easily transferred to a grid. The metal free and both silicon derivatives all arranged themselves in a "face to face" stack with the molecular axes parallel to the water surface. This is a similar packing to that observed in the discotic mesophase with these materials. The hydrophobic side chains appear to minimise their interaction with the water surface by overlapping with each other thus decreasing the area of interaction with the water. At higher temperatures in the microscope hot-stage the inter-columnar distance increases since the hydrophobic interaction is no longer present, and the film on carbon behaves more like in the solid state.

The polysiloxane phthalocyanine oligomer, which was the most stable compound in the electron beam, showed the

expected undulations. It also appeared to be forming a nematic mesophase since all the molecules were pointing in a similar direction over quite large areas of the film. The long narrow shape of this molecule would certainly favour the formation of a nematic mesophase.

Only the copper phthalocyanine derivative lay flat on the water surface. This is probably due to the more ionic nature of the Cu^{II} in the centre of the phthalocyanine. The aliphatic side chains are in this case able to minimise their interaction with water surface by pointing away from the water.

In conclusion the importance of the water surface has been demonstrated in all these films, and has forced the phthalocyanines to adopt several new packing arrangements, with the "face to face" and side chain interactions playing the most important roles.

Ahmed H. (1971), Proc. 25th Anniv Meeting of EMAG, Inst. Phys. Conference Series No. 30.

Akamatu H., Inokuchi H. and Matsunaya Y.(1954), Nature, 173, 168.

Andrews K.W., Dyson D.J. and Keown S.R. (1967), "Interpretation of Electron Diffraction Patterns", Adam Hilger Ltd.

Ashida M. (1966), Bull. Chem. Soc. Japan, 39, 2632.

Ashida M., Hamada A. and Watanabe T. (1972), Bull. Chem. Soc. Japan 45, 2312.

A.S.T.M., "Index to the Powder Diffraction File",(1971).

Ballauf M. (1987), Liq. Cryst., 2, 519.

Baumeister W. and Hahn M. (1973), Cytobiologie, 7, 244.

Baumeister W., Lembecke G., Durr R. and Phipps B. (1991), "Electron Crystallography of Organic Molecules",Ed. J.R. Fryer and D. Dorset, pp 283, NATO ASI Series Vol. 328.

Blodgett K.B. (1935), J. Am. Chem. Soc., 57, 1007.

Brown G. and Wolken J. (1979), "Liquid Crystals and Biological Structures", Academic Press.

Boerchia A. and Bonhomme P. (1974), Optik, 39, 437.

Bull R.A. and Bulkowski J.E. (1983), J. Colloid Interface Sci., 92, 1.

Buseck P., Cowley J. and Eyring L., Eds., "High Resolution Transmission Electron Microscopy" (1988), Oxford University Press.

Carter F.C. (1982), "Molecular Electronic Devices", Marcel Dekker, New York.

Chandrasekhar S., Sadashiva B.K. and Suresh K.A.(1977), Pramana., 9, 471.

Chemla D. and Zyss J. (1988), "Nonlinear Optical Properties of Organic Molecules and Crystals", New York Academic.

Cho I. and Lim Y. (1988), Mol. Cryst. Liq. Cryst., 154, 9.

Clar E., Kelly W. and Laird R.M., (1956), Mh. Chem., 87, 391.

Cook M.J., Daniel M.F., Harrison K.J., McKeown N.B. and Thomson A.J., (1987), J. Chem. Soc. Chem. Comm., 1148.

Cook M. McKeown N. and Thomson A.J., (1989), Chem. of Materials, 1, No. 3, 287.

Cosslett V.E. (1978), J. Microsc., 113, 113.

Cowley J.M. and Moodie A.F. (1957), Acta. Cryst., 10, 606.

Craig A., B.Sc. Thesis, Glasgow University, (1988).

Dawson I.M. and Watson D.H. (1959), J. Mol. Biol., 1, 30.

Debe M.K. (1982), J. Vac. Sci. Technol., 21, 74.

Dorset D. (1990), "Electron Crystallography of Organic Molecules",Ed. J.R. Fryer and D. Dorset, pp 1, NATO ASI Series Vol. 328.

Drauglis E., Gretz R. and Jaffee R. (1969) "Molecular Proceeses on Solid Surfaces" McGraw Hill

Emsley J.W. (1990), "Nuclear Magnetic Resonance of Liquid Crystals", NATO ASI Series, Vol. 141.

Fan P.L., Larson D.C. and Labes M.M. (1972), Thin Solid Films, 12, S3.

Ferraris J., Cowan D.O., Walatka V.V. and Perlstein J.H. (1973), J. Am. Chem. Soc., 95, 948.

Friedel G. (1922), Ann. Phys., 18, 273.

Friedlander G. and Kennedy K.W. (1962), "Nuclear and Radiochemistry", Wiley, New York.

Fryer J.R. (1978), Acta Cryst., A34, 603.

Fryer J.R. (1979), Acta Cryst., A35, 327.

Fryer J.R. (1979b), "The Chemical Applications of the Transmission Electron Microscope", Academic Press.

Fryer J.R. and Smith D.J. (1981), Nature, 291, 481.

Fryer J.R. and Holland F.M. (1983), Ultramicroscopy, 11, 67.

Fryer J.R., Hann R.A. and Eyres B.L. (1985), Nature, 313, 382.

Fryer J.R. and Dorset D.D., J. Micros., 145, (1987), 61,

de Gennes P.G. (1984), J. Phys. Lettr., 44, L567.

Glaeser R.M. (1971), J. Ultrastructure Res., 36, 466.

Goodman J.F. and Clunie J.S. (1974), "Liquid Crystals and Plastic Crystals", Vol. 2, pp1, Wiley.

Gray G. and Windsor P. (1974), "Liquid Crystals and Plastic Crystals", Vol. 2, Wiley.

Green M. (ed) (1973), "Solid State Surface Science" Vol. 2, Marcel Dekker New York.

Grinton G.R. and Cowley J.M. (1971), Optik, 34, 221.

Grubb D.T. (1974), J. Mats. Sci., 9, 1715.

Grundy P.J. and Jones G.A. (1976), "Electron Microscopy in the Study of Materials", Arnold.

Herrmann-Schonherr O., Wendorff J., Kreuder W. and Ringsdorf H. (1986), Makromol. Chem., Rapid Commun., 7, 97.

Howells E.R. (1984), "Technology of Chemicals and Materials for Electronics", Ellis Horwood Ltd.

Hui S.W., Cheng M., Ho J.T. and Pindak R. (1990), "Electron Crystallography of Organic Molecules",Ed. J.R. Fryer and D. Dorset, pp 11, NATO ASI Series Vol. 328.

Inokuchi H, Kuroda H, Akamatu H, Bull. Chem. Soc. Japan 34, (1961), 749.

Inoue T., Yase K., Okada M., Okada S., Matsuda H., Nakanishi H. and Kato M. (1989), Thin Solid Films, 180, 199.

Issacson M., Johnson D. and Crewe A.W. (1976), Rad. Res., 55, 205.

Kitaigorodskii A.I., "Molecular Crystals and Molecules", Academic Press, (1973).

Knoll M. and Ruska E. (1932), Ann. der Physik, 12, 607.

Kohne B. and Praefcke K. (1984), Angew. Chem. Int. Eng., 23, 82.

Kuhn H. and Mobius D. (1971), Angew. Chem. Int. Ed. Eng., 10, 620.

Langmuir I. (1917), J. Am. Chem. Soc., 39, 1848.

Luckhurst G. and Gray G. (1979), "The Molecular Physics of Liquid Crystals", Academic Press.

Lynch D.F. and O'Keefe M.A. (1972), Acta. Cryst., A28, 536.

Mathews J.W. (1975) (ed) "Epitaxial Growth" part B, Academic Press

McArdle C.B. (1989) "Side Chain Liquid Crystal Polymers", Blackie.

McConnell C. and Fryer J.R. (1991), Submitted for publication.

Menter J.W. (1956), Proc. Roy. Soc (Lond.), A236, 119.

Misell D.L. (1978) "Practical Methods in Electron Microscopy", Vol. 7, North Holland.

Mulvey T. (1991), Microscopy and Analysis, 22, March, 1991.

Murata Y., Fryer J.R. and Baird T. (1976), J. Microsc., 108, 261.

Murata Y., Fryer J.R., Baird T. and Murata H. (1977), Acta Cryst., A33, 198.

Pashley D.W. (1965), Adv. Phys. 14, 327.

Pawlowski G. and Hanack M. (1980) Synthesis, 287.

Peterson I.R. and Russell G.J. (1984), Phil. Mag. A., 49, 463.

Piechocki C., Simon J., Skoulios A., Gullion D. and Weber P. (1982), J. Am. Chem. Soc., 104, 5245.

Pugh D. and Sherwood J.N. (1988), Chem. in Brit., pp544.

Reinitzer F. (1888), Monatsh. Chem., 9, 421.

Ringsdorf H., Wustefeld R., Zerta E., Ebert M. and Wendorff J., (1989) Angew. Chem. Int. Ed. Eng., 28, 914.

Roberts G.G., Baker S., Petty M.C. and Twigg M.V. (1983), Thin Solid Films, 99, 53.

Roberts G.G. (1984) in "Technology of Chemicals and Materials for the Electronics Industry", Ed. Horwells E.R., Ellis Horwood Ltd.

Robertson J.M. (1935), J. Chem. Soc., 615.

Sauer T. and Wegner G. (1988). Mol. Cryst. Liq. Cryst., 162B, 97.

Scherzer O. (1949), J. Appl. Phys., 20, 20.

Sirlin C., Bosio L. and Simon J. (1988), J. Chem. Soc. Chem. Comm., 236.

Sluyters J.H., Baars A., Van Der Pol J.F. and Drenth W. (1989), J. Electroanal. Chem., 271, 41.

Spence J.H.R. (1981), "Experimental High Resolution Electron Microscopy", Clarendon Press.

Steinstrasser R. and Pohl L. (1973), Angew. Chem. Int. Ed. Eng., 12, 617.

Thomas S.J., Williams J.O. and Jones W. (1972), Proc. 7th Int.

Symp. React. Solids, 515.

Ueda R, and Mullin J.B., Eds. "Crystal Growth and Characterisation", (1974), North Holland Publishing.

Urayama H., Yamochi H., Saio G., Nozawa K., Sugano T., Kinoshita M., Sato S., Oshima K., Kawamoto A. and Tanaka J. (1988), Chem. Lett., 55.

Uyeda N., Kobayashi T., Suito E., Harada Y., and Watanabe M. (1972) J. Appl. Phys., 43, 5181.

Uyeda N., Kobayashi T. and Siajo H. (1977), J. Cryst. Growth 40, 118.

Uyeda N. and Murata Y. (1982), J. Cryst. Growth. 57, 551.

Uyeda N., Takenaka, T., Aoyama K., Matsumoto M. and Fujiyoshi Y. (1987), Nature, 327, 319.

Uyeda N. (1990), "Electron Crystallography of Organic Molecules",Ed. J.R. Fryer and D. Dorset, pp 147, NATO ASI Series Vol. 328.

Vincett P.S., Barlow W.A. and Roberts G.G., (1977), J. Appl. Phys., 48, 3900.

Voigt-Martin I. (1990), "Electron Crystallography of Organic Molecules",Ed. J.R. Fryer and D. Dorset, pp 197, NATO ASI Series Vol. 328.

Voigt-Martin I., Krug H. and Van Dyck D., (1990), J. Phys. France, 51, 2347.

Voigt-Martin I., Durst H., Brzezinski V., Krug H., Kreuder W. and Ringsdorff H. (1989), Angew. Chem. Int. Ed. Engl., 28, No3, 323.

Wittman J.C., Hodge A.M. and Lotz B. (1983), J. Polym. Sci. (Polym. Phys.), 21, 2495.

Wittman J.C. and Lotz B., (1990) in "Electron Crystallography of Organic Molecules",Ed. J.R. Fryer and D. Dorset, NATO ASI Series Vol. 328.

Wudl F. (1984), Acc. Chem. Res., 17, 227.

Young M. and Levine E. (1974), Optik 38, 257.

Contrast Transfer Functions for the Jeol 1200 EX at diferent defocus values. a) 0 nm b) 10 nm c) 100 nm d) 1000 nm

C_s = 1.9 mm, 120 kV